

Facilitating Long Term Out-Back Water Solutions (G-FLOWS)
Task 6: Groundwater recharge characteristics
across key priority areas

Leaney, FW, Taylor, AR, Jolly, ID and Davies PJ



Goyder Institute for Water Research
Technical Report Series No. 13/6



www.goyderinstitute.org



Goyder Institute for Water Research Technical Report Series ISSN: 1839-2725

The Goyder Institute for Water Research is a partnership between the South Australian Government through the Department for Environment, Water and Natural Resources, CSIRO, Flinders University, the University of Adelaide and the University of South Australia. The Institute will enhance the South Australian Government's capacity to develop and deliver science-based policy solutions in water management. It brings together the best scientists and researchers across Australia to provide expert and independent scientific advice to inform good government water policy and identify future threats and opportunities to water security.



Department of Environment,
Water and Natural Resources



Enquires should be addressed to: Goyder Institute for Water Research
Level 1, Torrens Building
220 Victoria Square, Adelaide, SA, 5000
tel: 08-8303 8952
e-mail: enquiries@goyderinstitute.org

Citation

Leaney, FW, Taylor, AR, Jolly, ID, and Davies PJ, 2013, *Facilitating Long Term Out-Back Water Solutions (G-FLOWS) Task 6: Groundwater recharge characteristics across key priority areas*, Goyder Institute for Water Research Technical Report Series No. 13/6, Adelaide, South Australia

Copyright

© 2013 CSIRO To the extent permitted by law, all rights are reserved and no part of this publication covered by copyright may be reproduced or copied in any form or by any means except with the written permission of CSIRO.

Disclaimer

The Participants advise that the information contained in this publication comprises general statements based on scientific research and does not warrant or represent the completeness of any information or material in this publication.

Table of Contents

TABLE OF CONTENTS	III
EXECUTIVE SUMMARY	VI
ACKNOWLEDGEMENTS	VIII
GLOSSARY	IX
GLOSSARY	IX
INTRODUCTION	13
BACKGROUND.....	13
G-FLOWS PROJECT	14
TASK 6.....	15
<i>Background</i>	15
<i>Objectives</i>	15
SECTION 1 - DESKTOP STUDY	17
OVERVIEW OF STUDY REGION	17
LOCATION	17
CLIMATE	17
GEOLOGY.....	18
HYDROGEOLOGY	20
SURFACE HYDROLOGY	21
LAND USE	21
SOILS	21
METHODS	23
ANALYSIS OF HISTORICAL RAINFALL AND EVAPORATION	23
ESTIMATION OF RECHARGE USING EXISTING INFORMATION	23
<i>Method of Last Resort</i>	23
<i>Groundwater Chloride Mass Balance</i>	26
RESULTS	28
ANALYSIS OF HISTORICAL RAINFALL AND EVAPORATION	28
<i>Ernabella</i>	28
ESTIMATION OF RECHARGE USING EXISTING INFORMATION	34

<i>Method of Last Resort</i>	34
<i>Groundwater Chloride Mass Balance</i>	35
DISCUSSION	38
ANALYSIS OF HISTORICAL RAINFALL AND EVAPORATION	38
ESTIMATION OF RECHARGE USING EXISTING INFORMATION	38
ESTIMATION OF RECHARGE USING THE METHOD OF LAST RESORT AND THE GROUNDWATER CHLORIDE MASS BALANCE METHODS	39
SECTION 2 - FIELD STUDY OF THE MUSGRAVE PROVINCE	41
OVERVIEW OF STUDY AREA	41
PREVIOUS STUDIES IN ARID CENTRAL AUSTRALIA	42
<i>APY Lands (Dodds et al, 2001; Cresswell et al., 2002)</i>	43
<i>Western Water Study, Northern Territory (Cresswell et al., 1999)</i>	47
<i>Ti Tree Basin (Harrington, 1994-2003)</i>	48
<i>Ayres Range South station (Custance, 2012) and De Rose Hill station (Craven, 2012)</i>	48
<i>Finke River Study (Love et al., 2013)</i>	49
COMPARISON OF RAW DATA FROM PREVIOUS STUDIES.....	50
<i>Groundwater salinity and major ion composition</i>	50
<i>Carbon isotopes</i>	51
<i>Stable isotopes of water</i>	52
COMPARISON OF RECHARGE RATES FROM PREVIOUS STUDIES	52
METHODS	54
RESULTS	58
HYDROCHEMISTRY	59
<i>Carbon isotopes</i>	60
<i>Stable isotopes of water</i>	62
ANTHROPOGENIC SF ₆ AND CFC ANALYSES	64
<i>Noble gas analyses</i>	65
SPATIAL DISTRIBUTION IN ENVIRONMENTAL TRACER CONCENTRATIONS	66
CHANGES IN HYDROCHEMISTRY ALONG INFERRED FLOW PATHS (TRANSECTS)	69
DISCUSSION	71

MEAN RESIDENCE TIME OF GROUNDWATER	71
NEW APPROACH TO INTERPRETING STABLE ISOTOPE DATA IN THE ARID REGIONS OF CENTRAL AUSTRALIA	72
TEMPORAL CHANGES IN GROUNDWATER LEVEL AND $\Delta^{18}\text{O}$, $\Delta^{2}\text{H}$ AND ^{14}C COMPOSITION (1997-2012)	75
RECHARGE RATES, MECHANISMS AND GROUNDWATER FLOW	79
CONCLUSIONS.....	80
FURTHER WORK.....	81
REFERENCES.....	82
APPENDIX A – FURTHER ANALYSIS OF HISTORICAL RAINFALL AND EVAPORATION	86
BARTON	86
COOBER PEDY	92
COOK	97
MARALINGA	102
MARLA	107
NULLARBOR.....	112
TARCOOLA.....	117
APPENDIX B - ESTIMATION OF RECHARGE USING THE METHOD OF LAST RESORT	122
APPENDIX C - ESTIMATION OF RECHARGE USING THE GROUNDWATER CHLORIDE MASS BALANCE METHOD	124

Executive Summary

Planned and potential mining and energy development in South Australia's far north is set to have significant consequences for the water resources of the region and will result in a substantial increase in infrastructure requirements, including access to water resources and Aboriginal Lands for exploration and potential mine developments. Knowledge about the character and variability of groundwater resources, the sustainability of this resource and its relationship to environmental and cultural assets remains very limited, particularly in the Musgrave Province, the North East and North West Gawler Craton, and parts of the Frome Embayment. This project, undertaken as a desktop and a field study as part of Stage 1 of the G-FLOWS project, addresses some of these issues.

The desktop study involved detailed analyses of the available historical rainfall and potential evaporation data at 8 stations (Barton, Coober Pedy, Cook, Ernabella, Maralinga, Marla, Nullarbor and Tarcoola) in the Alinytjara-Wilurara/western South Australian Arid Lands Natural Resources Management regions and the production of maps of recharge across the whole of the far north using the Method of Last Resort (MOLR) and Groundwater Chloride Mass Balance (GCMB) methods. The field study involved the use of environmental tracers to estimate recharge rates and determine recharge processes in the Musgrave Province located in the Pitjantjatjara Yankunytjatjara (APY) Lands.

The desktop study showed that the Alinytjara-Wilurara/western South Australian Arid Lands Natural Resources Management regions are extremely arid with a seasonal pattern in rainfall that varies from winter dominant in the south (i.e. Nullarbor) to summer dominant in the north (i.e. Ernabella). This behaviour in rainfall seasonality reflects the fact that most of the far north is influenced by both the winter rainfall patterns of the Southern Ocean and the summer monsoonal patterns from the north. There is a general trend of decreasing rainfalls (with some wetter periods) until around the 1970's, and then increasing rainfalls after that with variable behaviours during the last decade. This general trend is stronger at some sites (i.e. Barton) than others (i.e. Tarcoola).

Recharge rates determined using the MOLR are in general very low ($<1 \text{ mm yr}^{-1}$) across all of the far north and are indicative of the diffuse recharge regimes. Recharge rates determined using the GCMB method are often greater than those determined using the MOLR because the GCMB method is more likely to identify areas where surface run-on leads to localised recharge whereas the MOLR does not. Furthermore GCMB method could also reflect the uncertainty in chloride deposition.

The field based study showed that this is particularly the case for the Musgrave and potentially the Mann and Tomkinson Ranges in the Musgrave Province, where there are high rates of recharge to occur within the fractured regolith of the Precambrian basement rocks. The high recharge in the Ranges results in fresh groundwater reserves in these areas. Groundwater pumped from the wells in the Musgrave Ranges is modern with a mean residence time of less than 50 years, and probably less than 30 years old. The fresh groundwater reserves result from recharge during large episodic rainfall events where the monthly rainfall exceeds 80 mm month^{-1} . The rainfall needs to be sufficient to cause overland flow to the rivers and valleys for significant recharge to occur to sedimentary aquifers. A revised evaluation of the $\delta^2\text{H}$ vs $\delta^{18}\text{O}$ signature of groundwater in central arid Australia

has been developed that may be used to correlate recharge mechanisms for different areas in Central Australia.

Away from the Ranges in the shallow poorly consolidated Tertiary and Quaternary sediments, saline diffuse recharge dominates with recharge rates significantly less than 1 mm yr^{-1} . Progressing south of the Ranges, groundwater has an increasing component of saline diffuse recharge and decreasing component of recharge from the Ranges. There is a large range in the ^4He concentration in groundwater in the area. In general, higher ^4He concentrations are found in the Tertiary and Quaternary sediments to the south of the study area and, as such, are consistent with older groundwater but this is not always the case. While most of the results from the field study have been informative, those from SF_6 analyses have proved difficult to interpret and warrant further investigation.

Acknowledgements

This study was carried out under the auspices of the G- FLOWS Project, with funding through the Goyder Institute of Water Research and CSIRO Water for a Healthy Country Flagship. We would like to acknowledge that the work reported here would not have been possible without the cooperation and resources of the Anangu Pitjantjatjara Yankunytjatjara (APY) Lands Council, in particular the time and advice provided by Gary McWilliams. We would also like to acknowledge the involvement of the local indigenous communities, in particular the number of key elders that guided us to groundwater wells on various homelands. We would also like to thank staff from various State government agencies. To Adrian Costar from the Department for Environment, Water and Natural Resources (DEWNR) for liaison with the APY Lands Council and advice specific to the DEWNR groundwater database. To David Catley from DEWNR for advice and information specific to the location and operation of various community groundwater production wells. To Simon Wurst from SA Water for providing access to the groundwater well network operated by SA Water. To Jane Murphy from the Department for Communities and Social Inclusion (DCSI) for organising accommodation at various locations in the APY Lands for CSIRO and DEWNR staff during the field sampling campaign. To Colin Kyte for arranging accommodation, arranging access to nearby homelands and extending exceptional hospitality in the community of Wataru.

Glossary

Abstraction	The withdrawal of water from any water resource
AHD	Australian Height Datum; equivalent to: Mean Sea Level (MSL) + 0.026 m; Low Water Mark Fremantle (LWMF) + 0.756 m
Alluvium	Unconsolidated sediments transported by streams and rivers and deposited
Anticline	Sedimentary strata folded in the usually of inverted U-shape
Anoxic	An environment that is depleted of dissolved oxygen
Aquifer	A geological formation or group of formations able to receive, store and transmit significant quantities of water
Archaean	Period containing the oldest rocks of the Earth's crust – older than 2.4 billion years
Baseflow	Portion of river and stream flow coming from groundwater discharge
Basement	Competent rock formations beneath which sedimentary rocks are not found
Bore	A narrow, normally vertical hole drilled into a geological formation to monitor or withdraw groundwater from an aquifer. see Well
Colluvium	Material transported by gravity downhill of slopes
Confined	A permeable bed saturated with water and lying between an upper and a lower confining layer of low permeability, the hydraulic head being higher than the upper surface of the aquifer
Confining bed	Sedimentary bed of very low hydraulic conductivity
Conformably	Sediments deposited in a continuous sequence without a break
Cretaceous	Final period of Mesozoic era; 65-144 million years ago
Dewatering	Short-term abstraction of groundwater to lower the water table and permit the excavation of 'dry' sediment
Ecologically sustainable yield	The amount of water that can be abstracted over time from a water resource while maintaining the ecological values (including assets, functions and processes)

Ecological water requirement	The water regime needed to maintain the ecological values (including assets, functions and processes) of water dependent ecosystems at a low level of risk
Electrical Conductivity	A measure of the salt content of water (the ions in solution determine the capacity of the water to conduct an electric current over a short distance). Measured as microSiemens per centimetre ($\mu\text{S cm}^{-1}$) at a standard temperature of 25°C. Often simply called 'EC' in South Australia. Sea water is about 54,000 $\mu\text{S cm}^{-1}$, or 54,000 EC
Environmental water provision	The water regimes that are provided as a result of the water allocation decision-making process taking into account ecological, social, cultural and economic impacts. They may meet in part or in full the ecological water requirements
Evapotranspiration	A collective term for evaporation and transpiration. It includes water evaporated from the soil surface and water transpired by plants
Fault	A fracture in rocks or sediments along which there has been an observable displacement
Flux	Flow
Formation	A group of rocks or sediments which have certain characteristics in common, were deposited about the same geological period, and which constitute a convenient unit for description
Groundwater dependent ecosystem	An ecosystem that is dependent on groundwater for its existence and health
Hydraulic Conductivity	The flow through a unit cross-sectional area of an aquifer under a unit hydraulic gradient
Gradient	The rate of change of total head per unit distance of flow at a given point and in a given direction
Head	The height of the free surface of a body of water above a given subsurface point
Interburden	Material that lies between two or more bedded zone such as coal seams
Lacustrine	Pertaining to, produced by, or formed in a lake

Leach	Remove soluble matter by percolation of water
Permian	An era of geological time; 225–280 years ago
Petrographic	An analysis, description and classification of rocks such as by means of a microscope
Porosity	The ratio of the volume of void spaces, to the total volume of a rock matrix
Potentiometric surface	An imaginary surface representing the total head of groundwater and defined by the level to which water will rise in a well
Quaternary	Relating to the most recent period in the Cainozoic era, from 2 million years to present
Salinity	A measure of the concentration of total dissolved solids in water 0–500 mg L ⁻¹ , fresh 500–1500 mg L ⁻¹ , fresh to marginal 1500–3000 mg L ⁻¹ , brackish >3000 mg L ⁻¹ , saline
Scarp	A line of cliffs (steep slopes) produced by faulting or by erosion
Semi-confined	A semi-confined or a leaky aquifer that is saturated and bounded above by a semi-permeable layer and below by a layer that is either impermeable or semi-permeable
Semi-unconfined	Intermediate between semi-confined and unconfined, when the upper semi-permeable layer easily transmits water
Specific yield	The volume of water that an unconfined aquifer releases from storage per unit surface area of the aquifer per unit decline in the watertable
Storage coefficient	The volume of water that a confined aquifer releases from storage, per unit surface area of the aquifer, per unit decline in the component of hydraulic head normal to that surface
Sustainable yield	The level of water extraction from a particular system that, if exceeded, would compromise key environmental assets, or ecosystem functions and the productive base of resource
Syncline	A U-shaped fold in sedimentary strata

Tectonic	Pertaining to forces that produce structures or features in rocks
Tertiary	The first period of the Cainozoic era; 2–65 million years ago
Transmissivity	The rate at which water is transmitted through a unit width of an aquifer under a unit hydraulic gradient
Transpiration	The loss of water vapour from a plant, mainly through the leaves
Unconfined	A permeable bed only partially filled with water and overlying a relatively impermeable layer. Its upper boundary is formed by a free watertable or phreatic level under atmospheric pressure
Watertable	The surface of a body of unconfined groundwater at which the pressure is equal to that of the atmosphere
Well	An opening in the ground made or used to obtain access to underground water. This includes soaks, wells, wells and excavations

Introduction

Background

Planned and potential mining and energy development in South Australia's far north is set to have significant consequences for the water resources of the region. These sectors generate significant economic value to the State and their support remains a priority for the Government. The scale of the planned developments and the potential from current exploration programs facilitated by the South Australian Government through the Plan for Accelerated Exploration 2020 (PACE2020) Program (<http://www.pir.sa.gov.au/minerals/pace2020>) will result in a substantial increase in infrastructure requirements, including access to water resources and Aboriginal Lands for exploration and potential mine developments. Presently, knowledge about the character and variability of groundwater resources, the sustainability of this resource and its relationship to environmental and cultural assets remains very limited, particularly in the Musgrave Province, the North East and North West Gawler Craton, and parts of the Frome Embayment. Access to water is a key infrastructure need for mining and energy industry development in these regions. The priority areas for resource development in the far north, as defined by the Department for Manufacturing, Innovation, Trade, Resources and Energy (DMITRE), are shown in Figure 1.

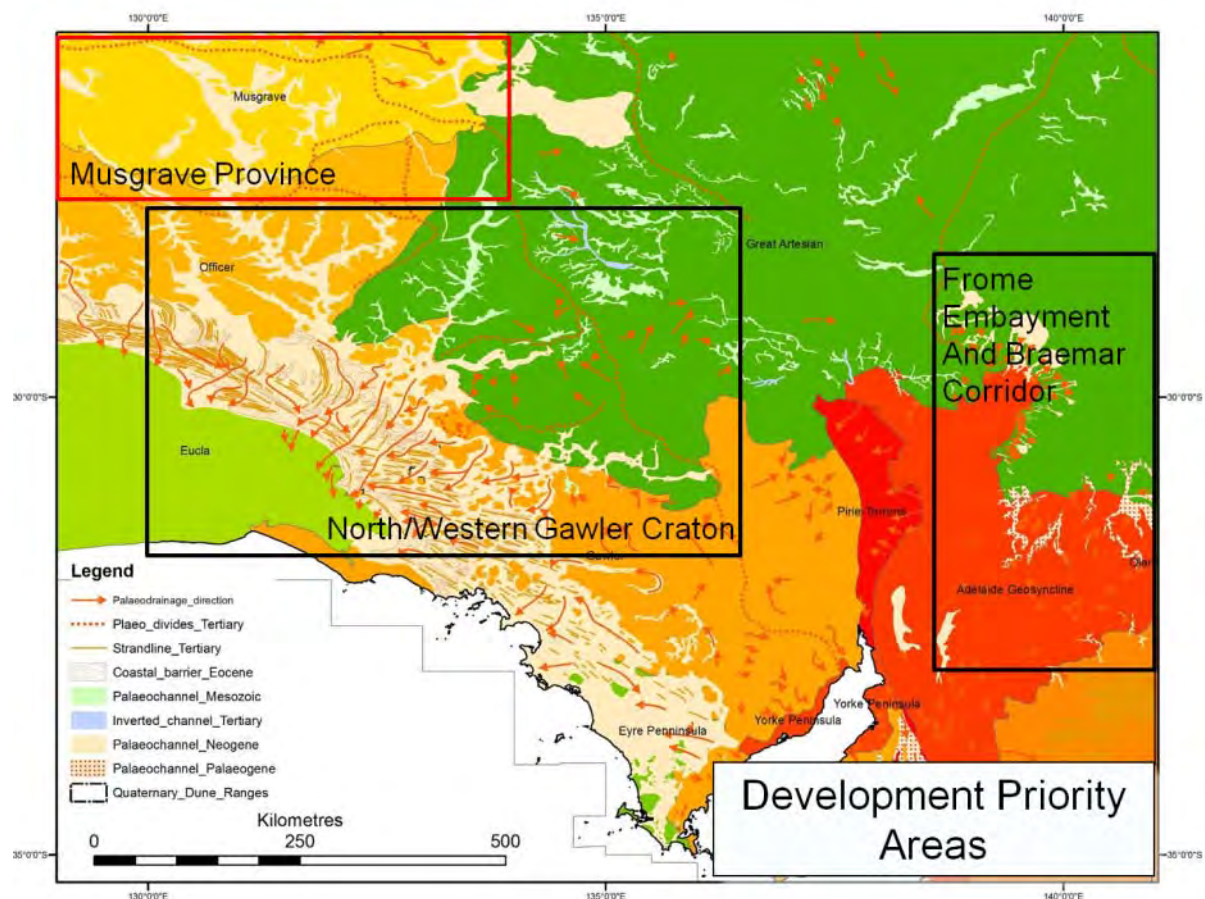


Figure 1. Priority areas for Industry development in the far north of South Australia.

G-FLOWS Project

The G-FLOWS project, through a staged program of research, aims to invest in the development of an integrated water resource management strategy, thereby facilitating the economic growth potential of these priority regions. Stage 1 of the G-FLOWS project had the following specific objectives:

1. For select resource development priority areas, identify the location and characteristics of aquifers, their capacity, and the quality and variability of the contained groundwater resources. This will build on available data and, through the development and application of procedures and protocols involving the integrated analysis and interpretation of geological and airborne geophysical data, linked to targeted drilling and hydrogeological investigations, it will provide the foundation for extending the comprehensiveness of the study.
2. Undertake a desk top study and review of cultural, ecological and environmental assets that have groundwater dependencies.
3. Develop an understanding of groundwater recharge across the priority areas.
4. Develop information packages that draw on extant databases and information from new and related projects to provide guidance and advice on potential and viable water resources, including GIS compatible mapping products and models for distribution to industry through the relevant State agencies.
5. Develop an informed strategy and Stage 2 proposal for employing regional geophysical data and targeted ground investigations to extend the understanding of aquifer characteristics and groundwater resources in other priority areas earmarked for development, while taking account of ecological and environmental assets.

Stage 1 is comprised of the following tasks:

1. Project management.
2. Collate extant geological, geophysical and hydrogeological information (including industry data) on groundwater and aquifers in agreed priority areas.
3. Forward modelling study, and review and QaQc of available geophysical data sets in priority areas in consultation with PIRSA, GA and industry.
4. Develop procedures and protocols for processing historical geophysical data and generating maps of groundwater and aquifer characteristics.
5. Case studies on the integration of regional and local scale geoscience data for groundwater and aquifer characterisation in key areas targeted for Industry development.
6. Groundwater recharge characteristics across key priority areas.
7. Desktop study on groundwater dependent/linked cultural flows and ecological and environmental assets in priority areas.
8. Detailed documentation of aquifer systems, their extent and variability, and groundwater characteristics in priority areas.
9. Final report for Stage 1.

Task 6

Background

The primary requirement for management of water resources in any region is an accurate water balance. This, in turn, requires estimation of groundwater recharge and discharge rates and, where possible, knowledge of their spatial distribution. This task will draw on procedures for estimating regional measurement of recharge and discharge in data poor areas that have been developed in other CSIRO Water for a Healthy Country Flagship projects, specifically the NWC funded activity “A Consistent Approach to Groundwater Recharge Determination in Data-Poor Areas”. The G-FLOWS initiative covers areas that are data poor and outcomes from this work, including the issues of regional measurement of recharge in data poor areas and the identification of parameters associated with climate, soils, regolith, near-surface geology, landforms and vegetation that collectively influence recharge and discharge rates, will feed into and inform the development of appropriate information packages to be developed in the first stage of this project. The groundwater systems in the non-prescribed wells areas of northern South Australia are only sampled sporadically by often widely separated wells. In addition knowledge of aquifer hydraulics are poorly understood, and consequently a combination of approaches that link hydrochemistry and isotopic studies may allow for a better understanding of recharge.

A regional groundwater-sampling and analysis program has been undertaken across priority areas, building on work being undertaken by DMITRE with particular emphasis on some of the deeper aquifer systems which may represent significant resources. The program aim was to investigate the spatial distribution of groundwater ages around the priority areas defined for detailed investigation, but also more generally across the northern part of the State. The significance of contemporary recharge processes through ephemeral river systems will be examined against the likelihood of palaeo-recharge within targeted aquifer systems. The ionic and isotopic composition of groundwater will be used to indicate potential flow paths and investigate groundwater evolution.

Objectives

Task 6 has the following specific objectives:

1. A review of accessible groundwater wells in key areas in order to establish reliable sampling points (i.e. wells with known construction and geology logs). This process will also assist in identifying regions of data paucity that may be targeted in the drilling program.
2. Collection and analysis of groundwater samples for physical parameters, major ion chemistry and selected environmental tracers.
3. Sampling of key wells for regional estimation of groundwater age relationships.
4. Conduct isotope analysis of selected water samples to define groundwater residence times and hydraulic properties.
5. Definition of key groundwater recharge and discharge processes and rates across key priority areas for industrial development in the arid regions of northern South Australia. This task will also involve the identification of parameters associated with climate, soils, regolith, near-surface geology, landforms and vegetation that collectively influence recharge and discharge rates across the priority areas.
6. Develop a spatial understanding of groundwater ages across targeted aquifers in the priority areas and more generally across the arid north of the State.

More specifically, Task 6 has been divided into two sections. In the first section of the report, a desktop evaluation has been undertaken to address objectives 5 and 6 above. In section 2, a field study addresses objectives 1-4 above for the Pitjantjatjara Yankunytjatjara (APY) Lands in the far North-West of South Australia. In so doing, the study provides estimates of recharge rates and evaluates recharge mechanisms for that area.

Section 1 - Desktop Study

Overview of study region

Location

The study area in Stage 1 of G-FLOWS is the Alinytjara-Wilurara/western South Australian Arid Lands Natural Resources Management regions. The desktop studies in this report cover this region. The field studies in this report concentrate on the APY Lands in the Musgrave Province priority area (shown in Figure 1).

Climate

According to the Koppen-Geiger climate classification (Koppen, 1936) the study area is dominated by the Arid, desert, hot (BWh) zone (Figure 2). There are also smaller areas of Arid, steppe, hot (BSh) and Arid, steppe, cold (BSk) in both the north and in the south, and Arid, desert, cold (BWk) in the south. The mean annual rainfall in the study area ranges from $\sim 240 \text{ mm yr}^{-1}$ in the south and the north-west down to $< 150 \text{ mm yr}^{-1}$ in the centre (Figure 3).

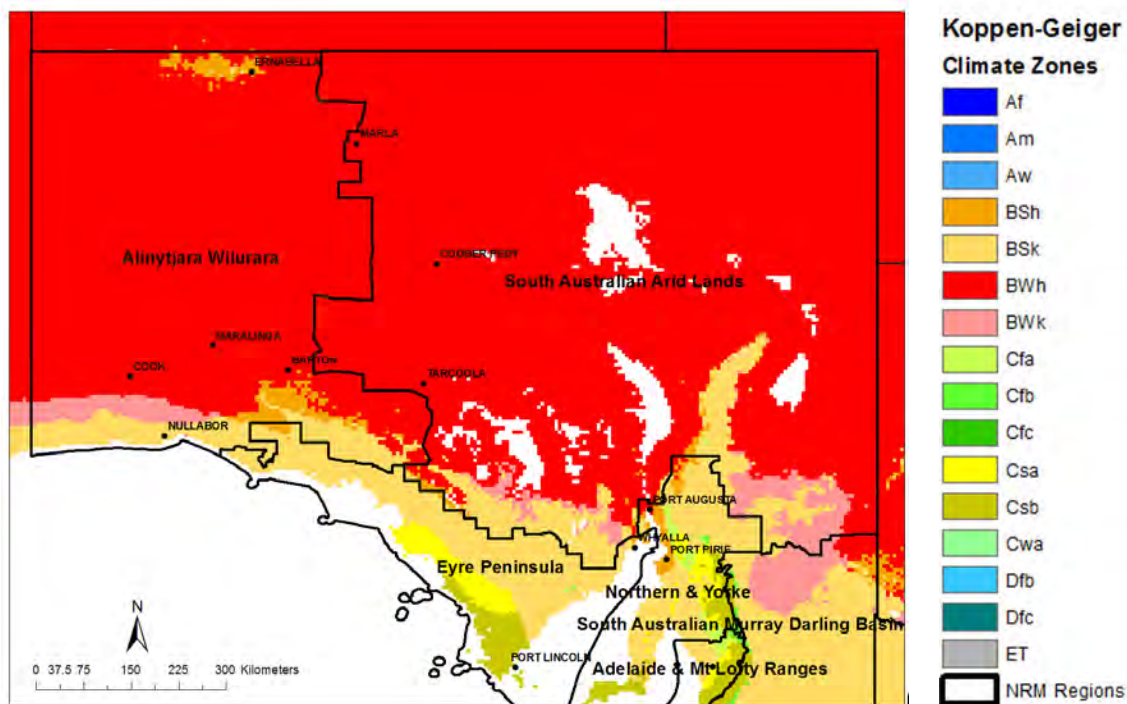


Figure 2. Koppen-Geiger climate classification map (Crosbie et al., 2012). Also shown are the locations of the eight sites in the study area where historical rainfall and pan evaporation data from the SILO climate database (Jeffrey et al., 2001) were analysed.

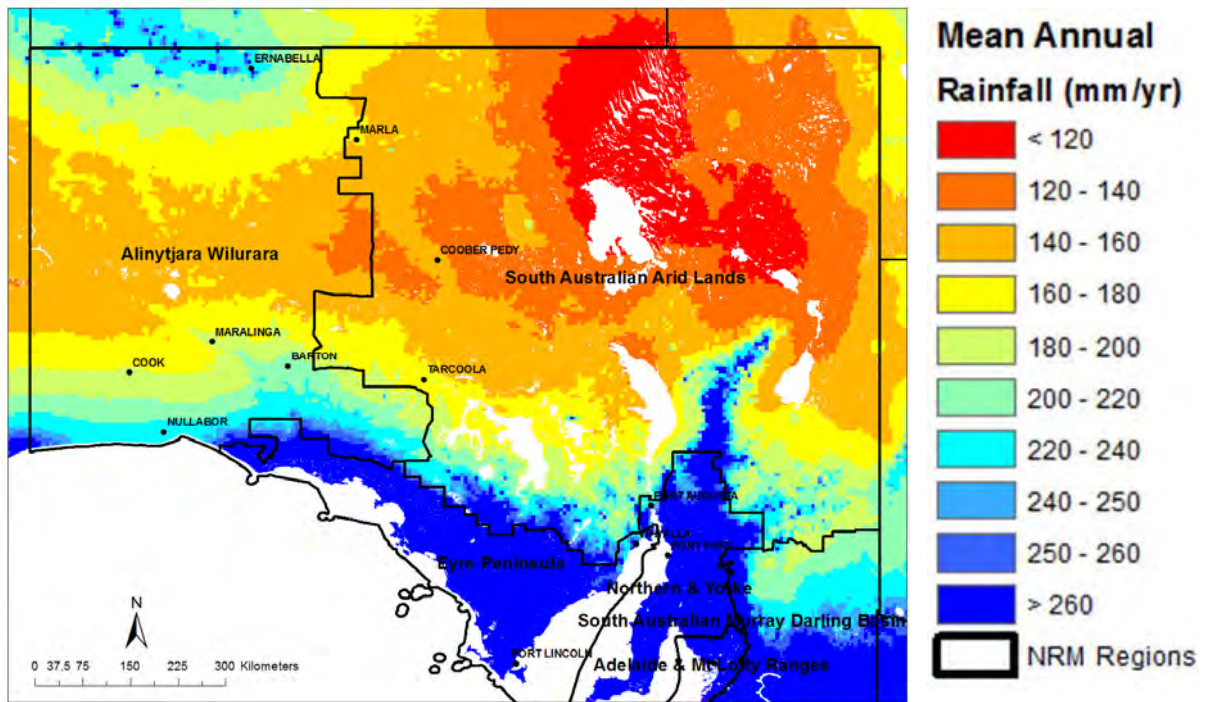


Figure 3. Mean annual rainfall map derived from the SILO climate database for the period 1889-2010 (Jeffrey et al., 2001). Also shown are the locations of the eight sites in the study area where historical rainfall and pan evaporation data from the SILO climate database were analysed.

Geology

The geology of the Alinytjara-Wilurara Natural Resources Management region has been reviewed by GHD (2009) and summarised in Watt and Berens (2011). They described five major geological provinces (Figure 4):

- Gawler Craton – Precambrian crystalline basement craton comprised of gneiss, schist, granite and banded iron formations overlain by Palaeozoic, Mesozoic and Tertiary sedimentary rock
- Musgrave Province – Precambrian crystalline basement craton comprised of volcanic, granite and metamorphic complexes
- Officer Basin – Late Proterozoic and early Palaeozoic sedimentary basin comprised of sandstone, siltstone and shale formations
- Great Artesian Basin – Mesozoic sediments of the Eromanga Basin which overly the Cambrian sediments of the Arckaringa Basin
- Eucla Basin – Tertiary limestone and siliclastic sediments overlying the sandstone formations of the Bight Basin. Cainozoic palaeovalleys draining the Musgrave Province and Gawler Craton extend into the Eucla Basin

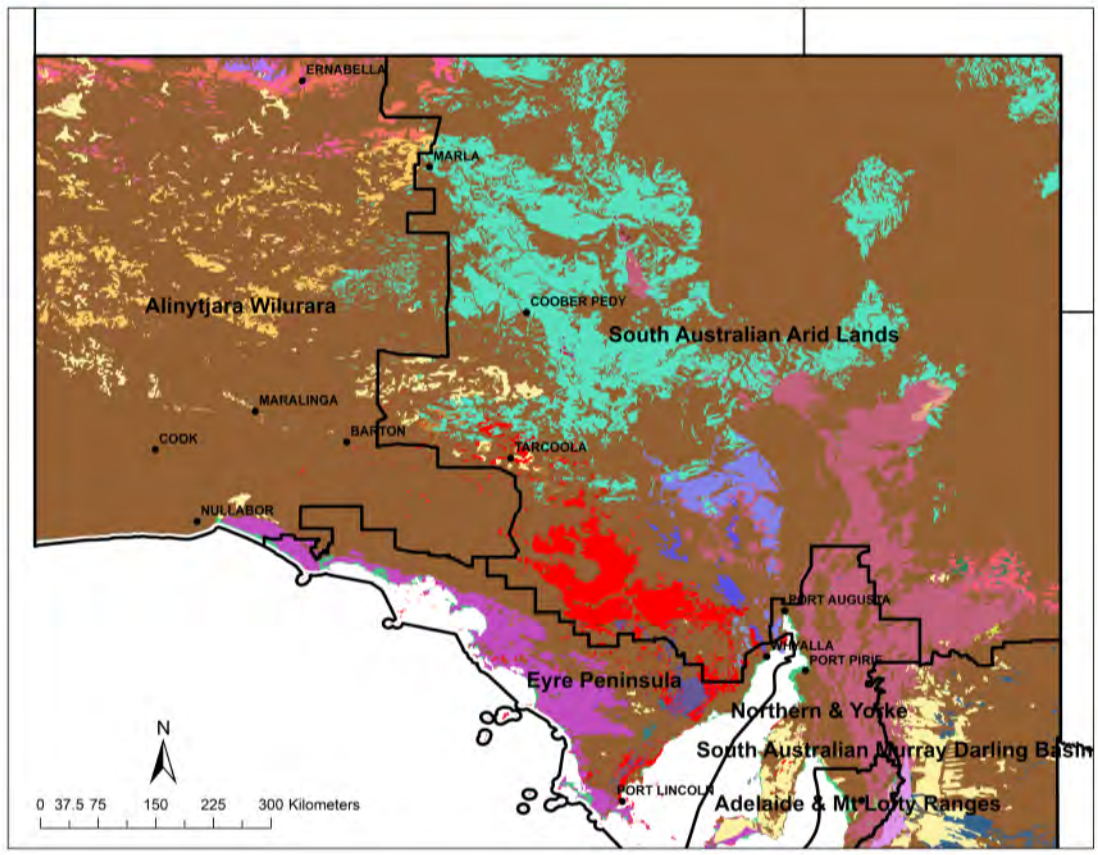


Figure 4. Geological Provinces of South Australia (from 1:2 million Surface Geology map of South Australia obtained from the South Australian Resources Information Geoserver - <https://sarig.pir.sa.gov.au/Map>). Also shown are the locations of the eight sites in the study area where historical rainfall and pan evaporation data from the SILO climate database were analysed.

In the South Australian Arid Lands Natural Resources Management region there are four major geological provinces (Figure 4):

- Gawler Craton – Precambrian crystalline basement craton comprised of gneiss, schist, granite and banded iron formations overlain by Palaeozoic, Mesozoic and Tertiary sedimentary rock
- Great Artesian Basin – Mesozoic sediments of the Eromanga Basin which overly the Cambrian sediments of the Arkaringa Basin

- Adelaide Geosyncline and Stuart Shelf – Neoproterozoic to Cambrian age sequences of sedimentary rocks and minor volcanic rocks
- Cariewerloo Basin - Intracratonic basin comprised of Palaeo-Mesoproterozoic, unmetamorphosed and largely undeformed, quartz dominated, fluvial sedimentary rocks

In addition to these geological provinces, there are very large areas of undifferentiated Quaternary alluvial/fluvial sediments that form the surficial cover in both Natural Resources Management regions.

Hydrogeology

GHD (2009) and Watt and Berens (2011) also reviewed and summarised the hydrogeology of the Alinytjara-Wilurara Natural Resources Management region and found that the regional aquifers are closely linked to the geological provinces thus:

- Gawler Craton - igneous and metamorphic rocks form the regional fractured rock aquifer overlain locally by unconsolidated granular aquifers associated with palaeovalley deposits
- Musgrave Province - the igneous and metamorphic rocks of the Musgrave Ranges form a regional fractured rock aquifer of highly variable yield and generally limited resource potential. The Mann, Tomkinson and Musgrave Ranges are located in the Musgrave Province.
- Officer Basin - groundwater within the Officer Basin is associated with the sandstone rocks as well as Tertiary palaeovalley deposits
- Great Artesian Basin - compared with other areas of the GAB, the sedimentary sequence of the Arkaringa and Eromanga Basins comprise fractured rock aquifers of relatively limited potential and are beyond the limit of artesian conditions
- Eucla Basin - Tertiary limestones and sandstones comprise regional fractured rock/karstic aquifers throughout the Eucla Basin with an underlying confined aquifer associated with the sandstones of the Bight Basin
- Palaeovalleys - Tertiary deposits are typically several metres to 50 m thick, but can reach up to 80 m (Hou et al. 2003) and have the potential to contain significant volumes of water

Information on the hydrogeology of the far north was also reviewed by AGT (2010) and for the South Australian Arid Lands Natural Resources Management region can be summarised as follows:

- Great Artesian Basin - The western portion is as described above. In the eastern portion the Mesozoic sediments comprise an extensive highly transmissive aquifer system with artesian flows
- Arkaringa Basin – Permian sediments underlying the Great Artesian Basin have some permeable sand aquifer units
- Lake Eyre Basin - Overlies the Great Artesian Basin and the Tertiary sand units can comprise transmissive aquifers

- Torrens Basin - Infill depression between the Gawler Craton and the Adelaide Geosyncline that contains Tertiary sands and overlying Quaternary alluvium which comprise a regional aquifer
- Adelaide Geosyncline – Fractured sedimentary rocks in the Flinders Ranges contain groundwater

Surface hydrology

As described in SAALNRMB (2010), there are three major surface drainage divisions covering the study area, namely the Lake Eyre Drainage Division, the Western Plateau Drainage Division and the South Australian Gulf Drainage Division (see http://www.bom.gov.au/hydro/wr/basins/basin-hi_grid.jpg).

Drainage in the Lake Eyre Drainage Division terminates at Lake Eyre. Major rivers that drain the Lake Eyre Basin from the west are the Macumba River, Arckaringa Creek and the Neales River. These are normally ephemeral but can flow significantly in times of flood. Semi-permanent waterholes are supplied from flood events. There are two major rivers to the east that drain a very large area extending to the highlands of central Queensland; the Warburton River and Cooper Creek. Annual run-off from the Great Dividing Range and the Barkley Tablelands of Queensland into the river systems fills some waterholes close to the borders, which are considered permanent.

The Western Plateau Drainage Division has the Gairdner, Nullabor and Warburton Basins within the study area. There are no major river systems within the any of these basins, resulting in many large salt lakes, the most notable being Lake Gairdner.

The South Australian Gulf Drainage Division has the Mambray Coast and Torrens Basins within the study area. Drainage in the Torrens Basin is directed towards Lake Torrens mostly from the western flank of the northern Flinders Ranges.

Land use

Land use is dominated by pasture grazing (sheep for meat and wool, cattle), land administered by the Department for Defence (Maralinga Restricted Area and Woomera Prohibited Area), and Aboriginal Lands (Anangu Pitjantjatjara Yankunytjatjara Lands and Maralinga Tjarutja Lands). Other important land uses are Commonwealth, State and private conservation areas, mineral exploration and mining, tourism activities, and residential townships. SAALNRMB (2010) and AWRMB (2011) have good information on land use and tenure in the study area.

Soils

The soils present in the study area are shown in Figure 5. The main soil orders represented are Calcarosols (i.e. soils that are calcareous throughout the profile), Rudosols (i.e. soils lacking pedological development, with little or no texture or colour change with depth), Kandosols (i.e. soils lacking a clear and abrupt textural contrast B horizon), Sodosols (i.e. soils with a clear or abrupt textural B horizon in which is the upper 0.2 m of the B2 horizon is sodic) and Tenosols (i.e. soils with weak pedological development except for the A horizon). All of these soil orders are typical for the arid central/southern regions of Australia.

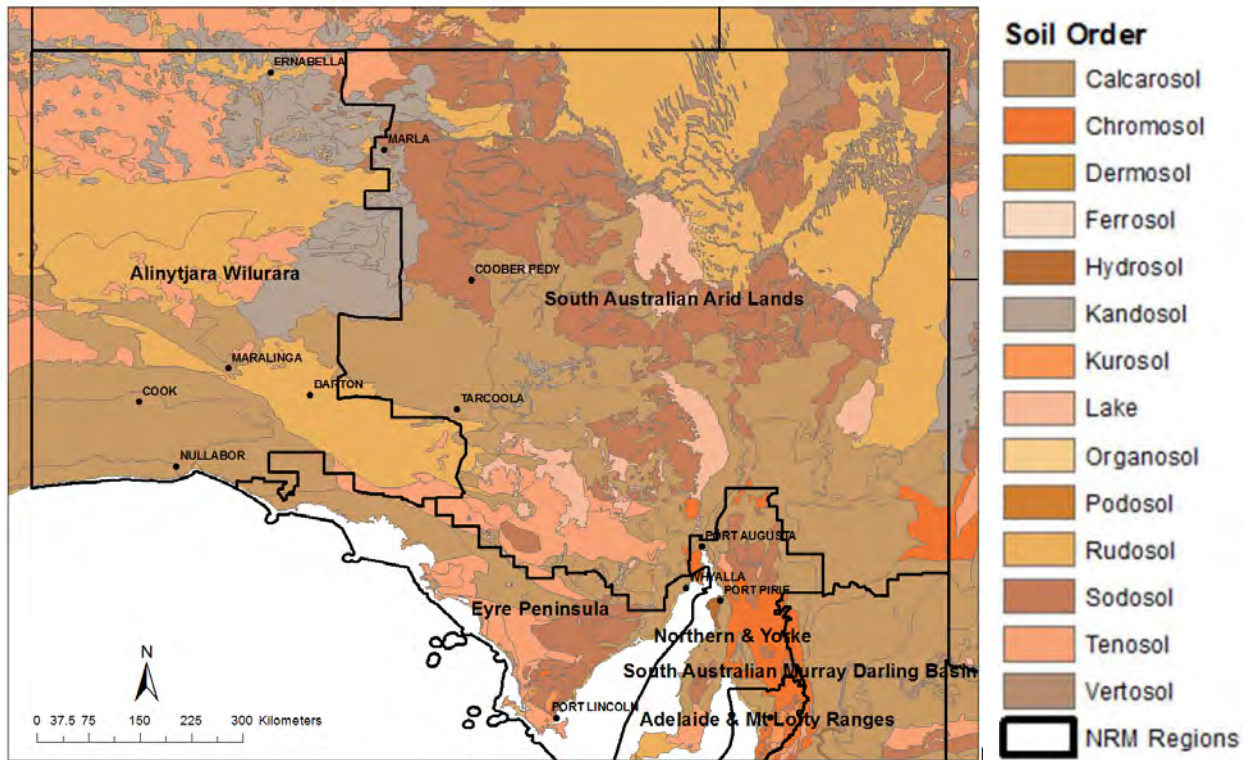


Figure 5. Australian Soil Classification soil order map (from the Atlas of Australian Soils, <http://www.asris.csiro.au/themes/Atlas.html>). Also shown are the locations of the eight sites in the study area where historical rainfall and pan evaporation data from the SILO climate database (Jeffrey et al., 2001) were analysed.

Methods

Analysis of historical rainfall and evaporation

Because recharge and discharge is closely related to rainfall and potential evaporation we carried out a detailed analysis of the historical data available for the study area. Eight sites (Barton, Coober Pedy, Cook, Ernabella, Maralinga, Marla, Nullarbor and Tarcoola; Figure 2) had historical Patch Point meteorological data available in the SILO climate database

(<http://www.longpaddock.qld.gov.au/silo/>). The Patch Point Dataset uses original Bureau of Meteorology measurements for a particular meteorological station, but missing data are filled (“patched”) with interpolated values (Jeffrey et al., 2001). In the case of the eight sites presented here all of the data is interpolated. Daily rainfall data for the period 1889 – 2010, and daily pan evaporation data for the period 1970 – 2010 was utilised.

The daily, monthly and annual rainfall and pan evaporation data were graphed and analysed using the ‘hydroTSM’ package (Zambrano-Bigiarini, 2011) in the R programming environment (Venables et al., 2011). The annual rainfall data were further analysed in Microsoft Excel for long-term trends by plotting the cumulative deviation from the mean annual rainfall.

Estimation of recharge using existing information

With the exception of the Dodds et al. (2001) and Creswell et al. (2002) studies in the Musgrave Province, the recharge regime in the the Alinytjara-Wilurara/western South Australian Arid Lands Natural Resources Management regions is largely unknown. What little is known about recharge in this region has been summarised in the recent report by GHD (2009).

In order to provide a spatial understanding of possible recharge in the study area new estimates of diffuse recharge were made using the Method of Last Resort developed in the recent National Water Commission Project “A Consistent Approach to Groundwater Recharge Determination in Data Poor Areas” (see <http://www.csiro.au/en/Outcomes/Water/Water-information-systems/Recharge-Discharge-Estimation-Suite.aspx>). Information on chloride deposition in rainfall developed in this project was also used to make new estimates of recharge using an established method, Groundwater Chloride Mass Balance, and these were used to assess the likelihood of localised recharge in the study area.

Method of Last Resort

The Method of Last Resort (MOLR) developed by Crosbie et al. (2010b) was applied to the whole of South Australia. The method used a sub-set of ~4400 recharge and/or deep drainage estimates from 172 studies in Australia compiled by Crosbie et al. (2010a) to develop simple empirical relationships between recharge and average annual rainfall, vegetation and soil order that can be applied to nationally available datasets. Leaney et al. (2011) and Jolly et al. (2011) further simplified the MOLR relationships developed by Crosbie et al. (2010b) by combining the perennial and tree vegetation types due to a lack of data under these vegetation types. The soils groupings used by Crosbie et al. (2010b) that were retained for this final version of the MOLR were:

- Vertosols (VE)
- Calcarosols (CA), Chromosols (CH), Kurosols (KU) and Sodosols (SO)
- Podosols (PO)
- Rudosols (RU), Kandasols (KA) and Tenosols (TE)
- Ferrosols (FE), Dermosols (DE), Hydrosols (HY) and Organosols (OR)

No estimate of recharge is possible using the MOLR from the last soils group (FE, DE, HY, OR) due to a lack of field studies required to develop the relationships.

The relationships that were developed between recharge and mean annual rainfall, soil order and vegetation type used a two parameter regression model are shown in Equation 1.

Equation 1 $R = 10^{aP+b}$

where a and b are the fitting parameters from a least squares regression between annual average rainfall (P) and the logarithm of annual average recharge (R). Figure 6 shows the relationships observed between average annual rainfall and average annual recharge for the combination of soil and vegetation groups. The annual vegetation class is displayed in red, and the perennials and the trees are displayed in green. In black is all the recharge estimates irrespective of vegetation type. The line of best fit is the bold colour line while the thin black line is the 95% prediction interval about the line of best fit. A line of best fit is only presented on Figure 6 when that line is statistically significant ($p < 0.05$). Table 1 shows the regression parameters used in the MOLR and the rainfall ranges that they apply to (from Figure 6). Note that the number of significant figures in the table does not indicate the degree of accuracy (confidence) in the relationships. Also note that some locations in the study area had mean annual rainfalls slightly lower than the minimum rainfall limit of the regressions but they were used nonetheless as it was considered that the relationships probably also held at these slightly lower rainfalls.

Table 1. Regression parameters used in the MOLR and the rainfall ranges that they apply to (from Figure 6). (A is annual vegetation; P & T is perennial and trees vegetation type).

	best		upper		lower		Rainfall (mm/yr)	
	a	b	a	b	a	b	min	max
VE - A	2.78E-03	-3.02E-01	2.79E-03	8.05E-01	2.77E-03	-1.41E+00	255	805
VE - P & T	2.83E-03	-1.51E+00	2.88E-03	-2.44E-01	2.79E-03	-2.77E+00	255	1070
CA,CH,KU,SO - A	1.58E-03	3.57E-01	1.63E-03	1.50E+00	1.52E-03	-7.85E-01	250	901
CA,CH,KU,SO - P & T	1.67E-03	-1.09E+00	1.69E-03	5.69E-01	1.64E-03	-2.75E+00	250	976
PO - A	4.10E-03	-8.05E-01	3.94E-03	5.27E-03	4.25E-03	-1.62E+00	550	803
PO - P & T	1.32E-03	1.08E+00	1.37E-03	1.71E+00	1.28E-03	4.43E-01	550	1265
RU,KA,TE - A	4.14E-03	-1.26E+00	5.54E-03	1.37E-03	2.73E-03	-2.53E+00	390	650
RU,KA,TE - P & T	1.75E-03	-7.10E-01	1.97E-03	3.53E-01	1.53E-03	-1.77E+00	100	1585

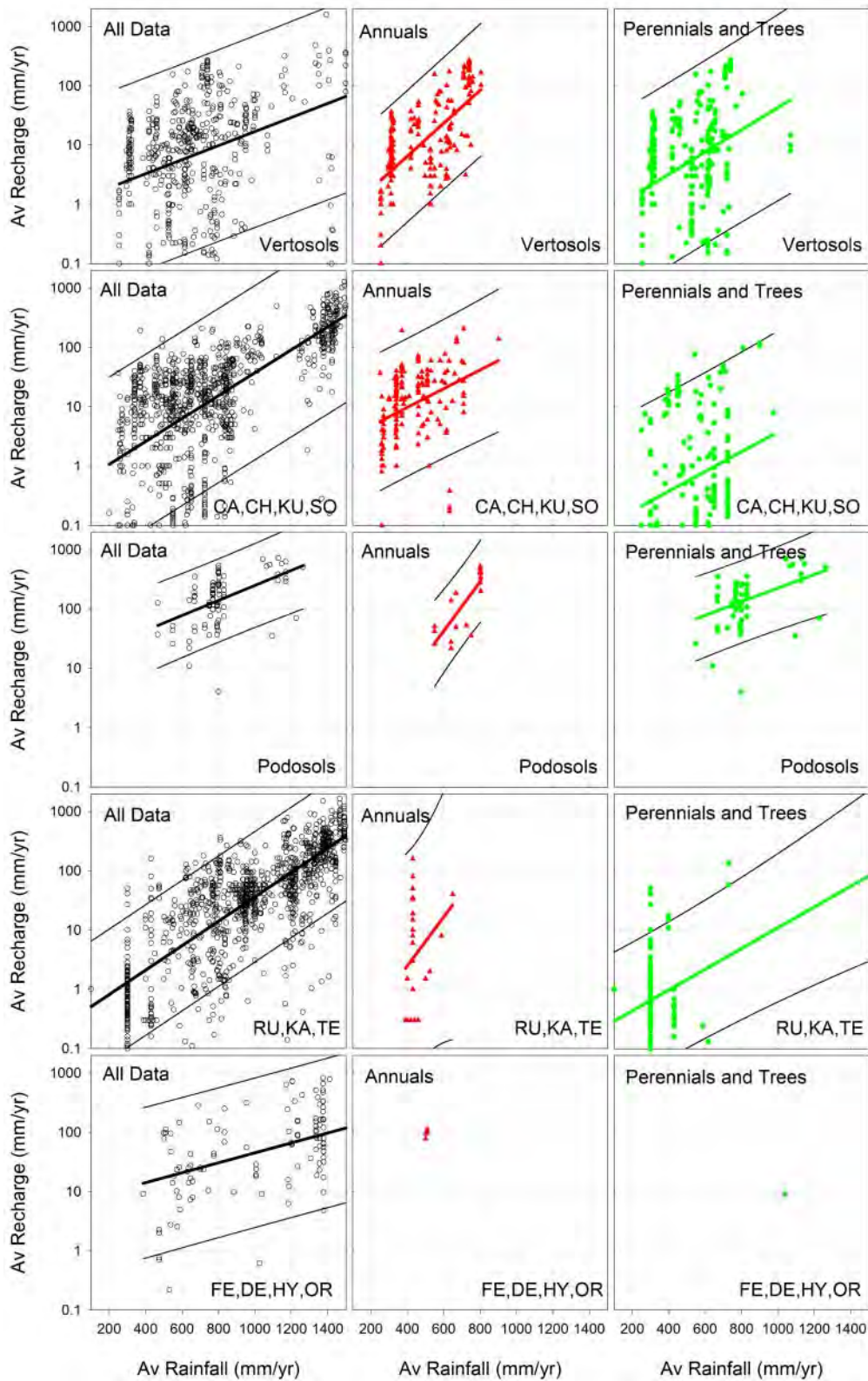


Figure 6. Relationships developed for estimating recharge using the MOLR based upon soil order, vegetation type and rainfall (from Leaney et al., 2011).

Groundwater Chloride Mass Balance

The Groundwater Chloride Mass Balance (GCMB) method is based on the assumption chloride in pore water is excluded by evaporation and transpiration leaving it to concentrate in the unsaturated zone, and eventually reach the groundwater via advection. It is a method for estimating net groundwater recharge because chloride can continue to be concentrated in the saturated zone if vegetation is exploiting this source of water. However, the GCMB method can only be used when the groundwater at the depth of the screen is at steady-state as it is based on the assumption that the rainfall chloride deposition rate is at steady state with the chloride flux of the recharge to the groundwater (see Equation 2). Hence, if there has been vegetation clearing at the site, no estimate of recharge (or deep drainage) is possible until the hydrological water balance has reached a new steady state at the depth of the point where the groundwater sample has been sampled. In the north of South Australia it is not unreasonable to assume that most sites have not experienced vegetation clearing.

The only unknowns in the GCMB method are an estimate of the chloride deposition rate at the ground surface and the chloride concentration of the groundwater as shown in Equation 2.

Equation 2 $R = D / C_{gw}$

where R is recharge rate, D is chloride deposition rate and C_{gw} is the concentration of chloride in the groundwater.

The assumptions inherent in the method are that:

1. The chloride in the groundwater originates from precipitation (not rock weathering or halite dissolution).
2. The chloride imported or exported via runoff or runoff can be accounted for.
3. The chloride is conservative in the system.
4. The chloride deposition rate has not changed over time.

The chloride deposition rate (with 95% prediction intervals) was derived from the maps developed in the National water Commission Project "A Consistent Approach to Groundwater Recharge Determination in Data Poor Areas" (Figure 7).

Data on chloride concentration in groundwater was obtained from the South Australian Department for Water and consisted of data from: (i) fractured rock wells to 100 m depth; and (ii) Quaternary and Tertiary wells to 50 m. It was considered that these two categories of wells are the ones most suitable for using the GCMB method.

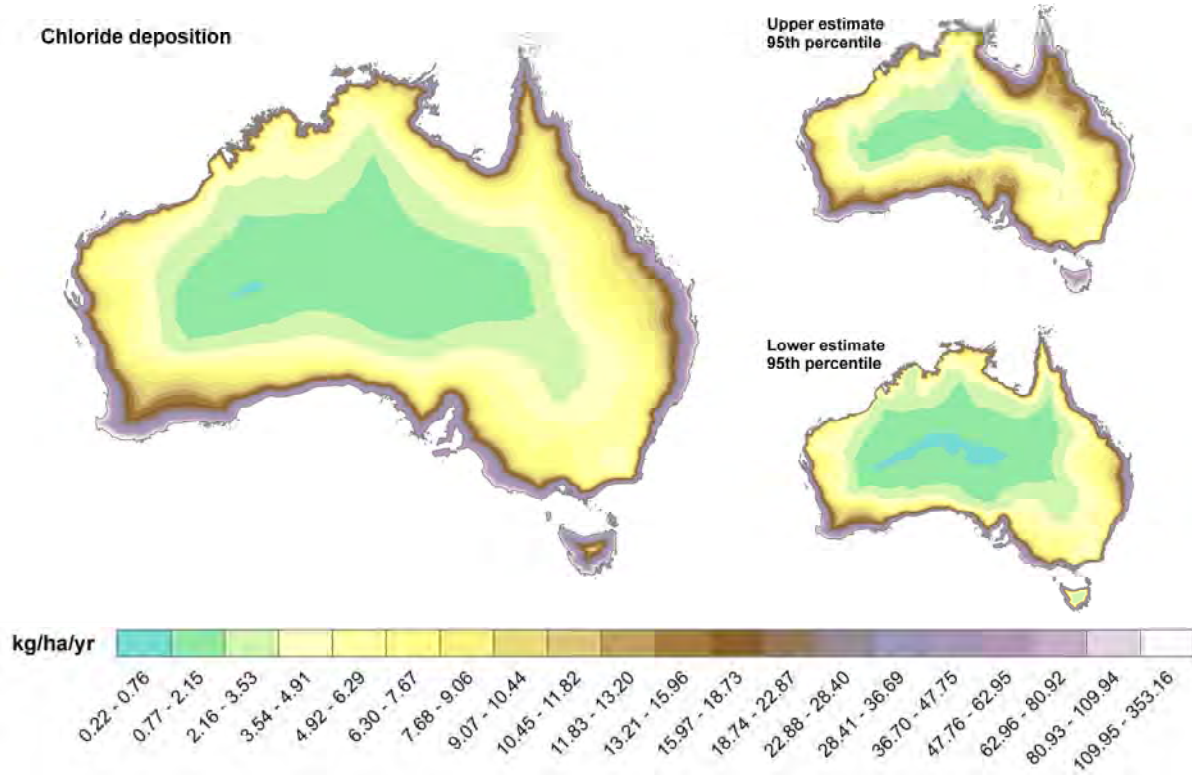


Figure 7. Maps of interpolated rainfall chloride deposition for Australia (largest) and the upper and lower 95% percentiles of interpolated estimates (from Leaney et al., 2011).

Results

In this section, rainfall and pan evaporation data (daily, monthly, annual, monthly mean and standard deviation) are shown for the township of Ernabella, located within the APY Lands. The analysis of these data highlights that rainfall in the Musgrave Province is extremely variable (particularly on a daily basis) but has a clear summer dominance. It also illustrates that there have been long periods where the annual rainfall has either been lower or higher than the annual average, suggesting a pattern of long-term variability. The analysis also highlights the very high rates of evaporation (which are also highly variable, but less so than the rainfall), which combined with the highly variable rainfall, suggests that recharge is likely to be very episodic in nature.

Similar treatment of rainfall and pan evaporation data is given for a further 7 townships outside of the APY Lands but within the Alinytjara-Wilurara/western South Australian Arid Lands Natural Resources Management regions (Appendix A). It is worth noting that Ernabella is in a higher elevation and higher rainfall area compared to the other townships in Appendix A.

Analysis of historical rainfall and evaporation

Ernabella

Time series of daily, monthly and annual rainfall, with one and three year moving averages are shown in Figure 8. A boxplot of the monthly rainfall is shown in Figure 9. A plot of the cumulative annual deviation from the mean annual rainfall is shown in Figure 10. A summary of the daily, monthly and annual rainfall statistics is given in Table 2.

Ernabella is located in the north-central part of the study area and is the only site in a BSh climate zone. It has mean daily, monthly and annual rainfalls of 0.7, 20.4 and 244.7 mm respectively. The highly variable rainfall regime is illustrated by the high standard deviations of the daily, month and annual rainfalls. The variability is most extreme in the daily rainfall, followed by the monthly rainfall and then the annual rainfall, as illustrated by the coefficients of variation of each. The boxplot suggests that there is a summer dominance in the rainfall. The cumulative deviation from the mean plot shows that the annual rainfalls generally declined relative to the mean until the early 1970's (with some wetter years in the early 1920's and the 1940's and 1950's), then increased until the late 1980's, and have had no clear trends since then.

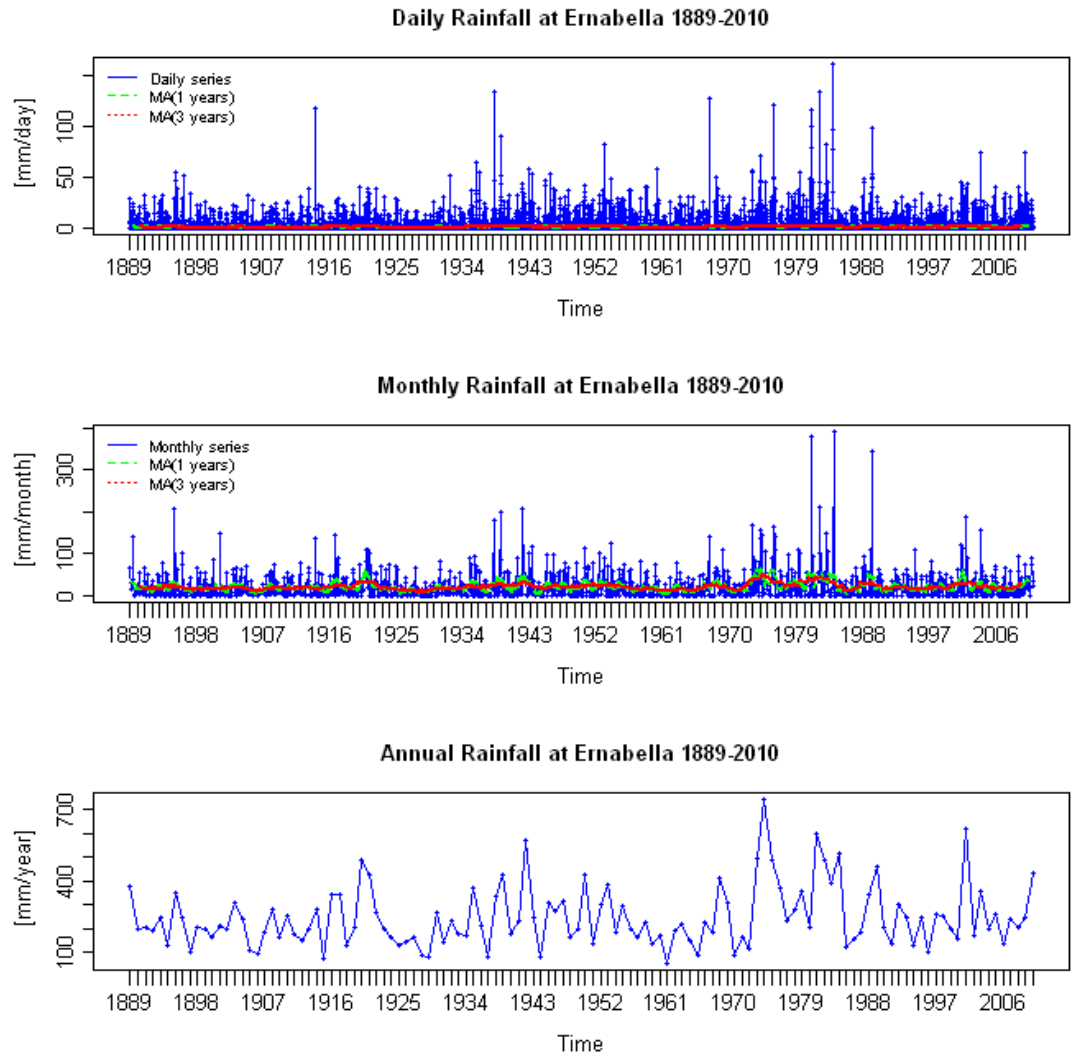


Figure 8. Time series of daily, monthly and annual rainfall at Ernabella. One year and three year moving averages are shown in green and red respectively.

Monthly Rainfall at Ernabella 1889-2010

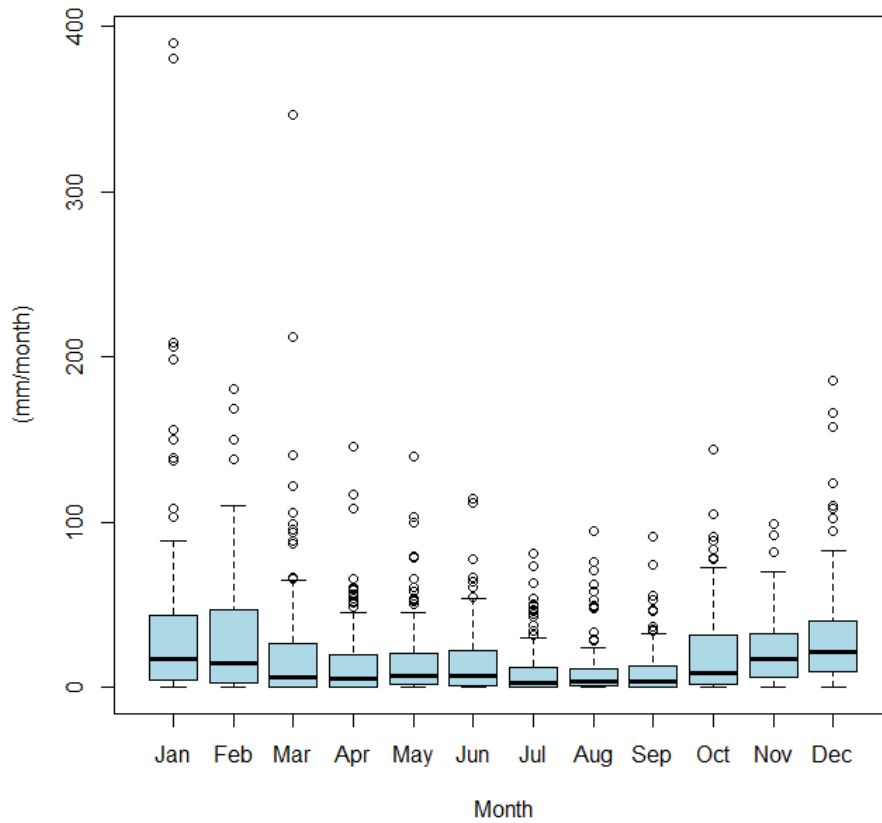


Figure 9. Boxplot of the monthly rainfall at Ernabella. The bottom and top of each box are the first and third quartiles, the band inside each box is the second quartile (the median), the ends of each of the whiskers are 1.5 times the interquartile range of the lower and upper quartiles, and the circles are outliers.

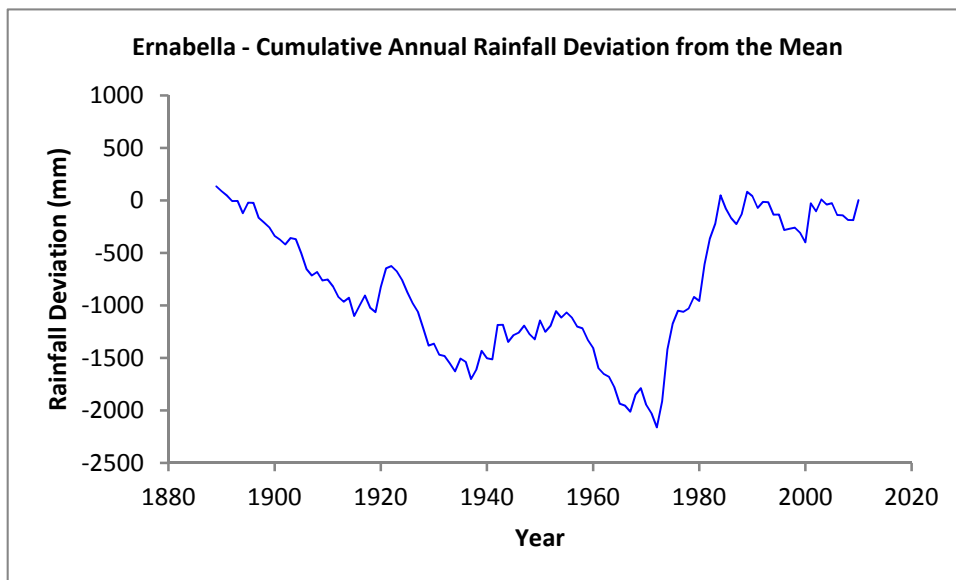


Figure 10. Plot of the cumulative annual deviation from the mean annual rainfall at Ernabella.

Table 2. Summary of the daily, monthly and annual rainfall statistics at Ernabella.

Statistic	Daily	Monthly	Annual
Minimum (mm)	0.0	0.0	52.5
First quartile (mm)	0.0	1.5	162.7
Median (mm)	0.0	8.2	204.7
Mean (mm)	0.7	20.4	244.7
Third quartile (mm)	0.0	26.6	304.6
Maximum (mm)	159.8	390.1	739.2
Interquartile range (mm)	0.0	25.1	141.8
Standard deviation (mm)	3.7	32.7	127.1
Coefficient of variation	5.6	1.6	0.5
Number of points	44599	1464	122

Time series of daily, monthly and annual pan evaporation, with one and three year moving averages are shown in Figure 11. A boxplot of the monthly pan evaporation is shown in Figure 12. A summary of the daily, monthly and annual pan evaporation statistics is given in Table 3.

The pan evaporation at Ernabella is extremely high, with the mean daily, monthly and annual values of 8.0, 242.8 and 2914.0 mm respectively far exceeding those of the rainfall. The monthly boxplot shows that there is a strong seasonal pattern with lowest values in winter and highest values in summer. Whilst the evaporation is highly variable, the coefficients of variation are all much lower than those for rainfall.

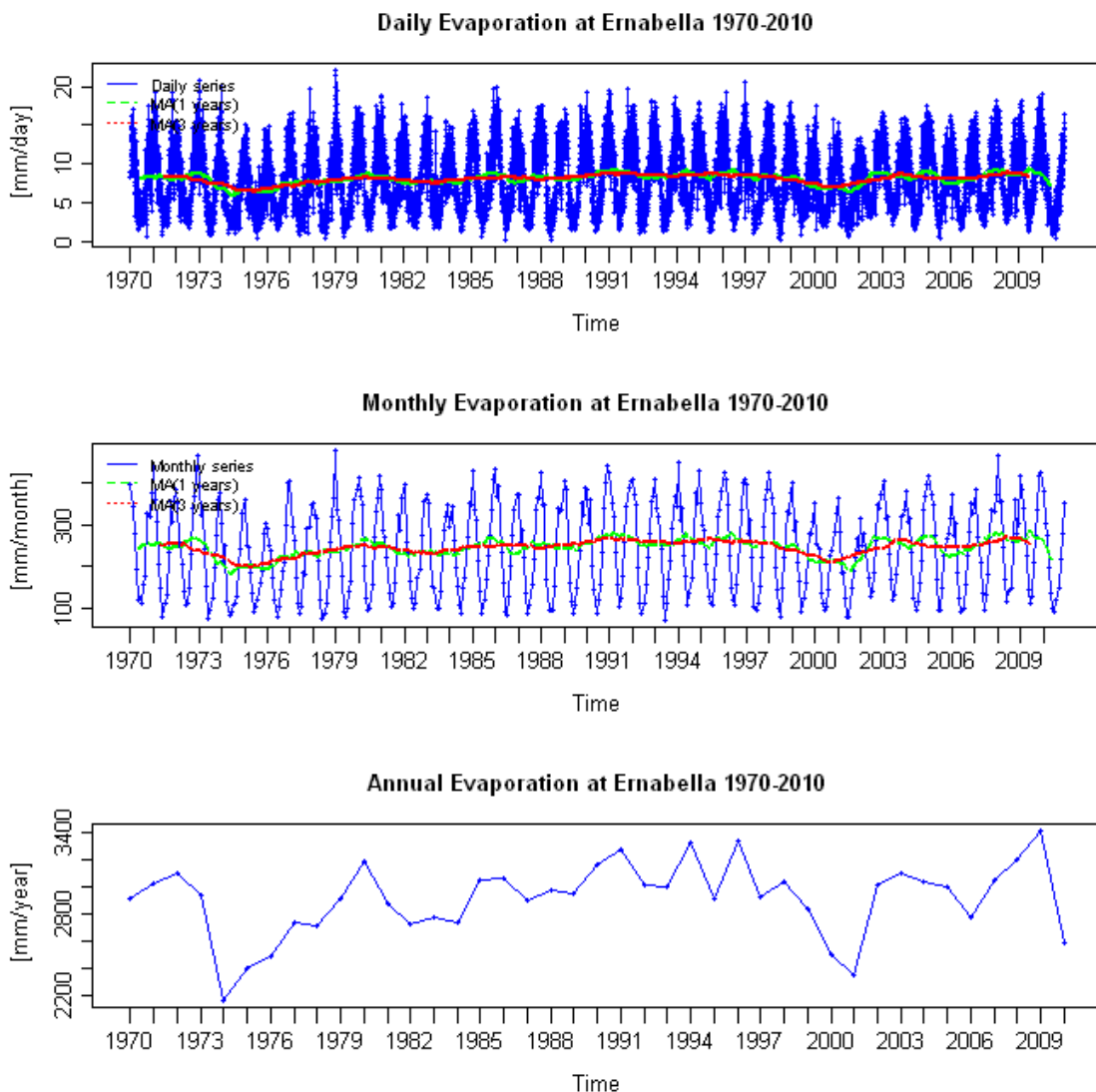


Figure 11. Time series of daily, monthly and annual pan evaporation at Ernabella. One year and three year moving averages are shown in green and red respectively.

Monthly Evaporation at Ernabella 1970-2010

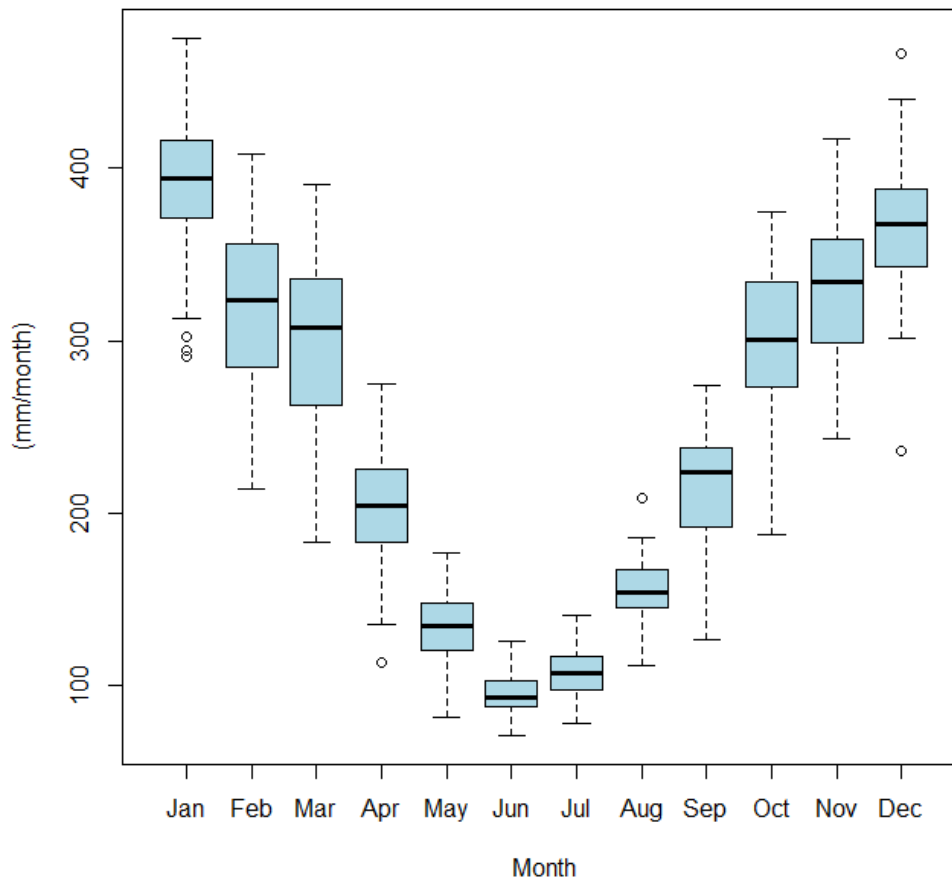


Figure 12. Boxplot of the monthly pan evaporation at Ernabella. The bottom and top of each box are the first and third quartiles, the band inside each box is the second quartile (the median), the ends of each of the whiskers are 1.5 times the interquartile range of the lower and upper quartiles, and the circles are outliers.

Table 3. Summary of the daily, monthly and annual pan evaporation statistics at Ernabella.

Statistic	Daily	Monthly	Annual
Minimum (mm)	0.2	70.8	2170.0
First quartile (mm)	4.4	144.5	2777.0
Median (mm)	7.6	241.6	2945.0
Mean (mm)	8.0	242.8	2914.0
Third quartile (mm)	11.2	336.7	3053.0
Maximum (mm)	22.0	475.6	3402.0
Interquartile range (mm)	6.8	192.2	276.6
Standard deviation (mm)	4.0	105.6	268.6
Coefficient of variation	0.5	0.4	0.1
Number of points	14975	492	41

Estimation of recharge using existing information

Method of Last Resort

In the Method of Last Resort regressions (Figure 6) the prediction intervals around the line of best fit were very wide. As such we present maps of these mean annual recharge estimates that have been made using the line of best fit (

Figure 13) as well as the lower 95% prediction interval and the upper 95% prediction interval (as shown in Appendix B, Figure 82, Figure 83).

The estimates made using the line of best fit are all very low in the Alinytjara-Wilurara/western South Australian Arid Lands Natural Resources Management regions with values all less than 0.5 mm yr⁻¹. The estimates made using the lower 95% prediction interval are extremely low in the study area with no values exceeding 0.1 mm yr⁻¹. The estimates made using the upper 95% prediction interval are mostly less than 10 mm yr⁻¹.

Despite the inherent uncertainties in the Method of Last Resort, the overall interpretation is that this method estimates diffuse recharge to be uniformly low in the Alinytjara-Wilurara/western South Australian Arid Lands Natural Resources Management regions.

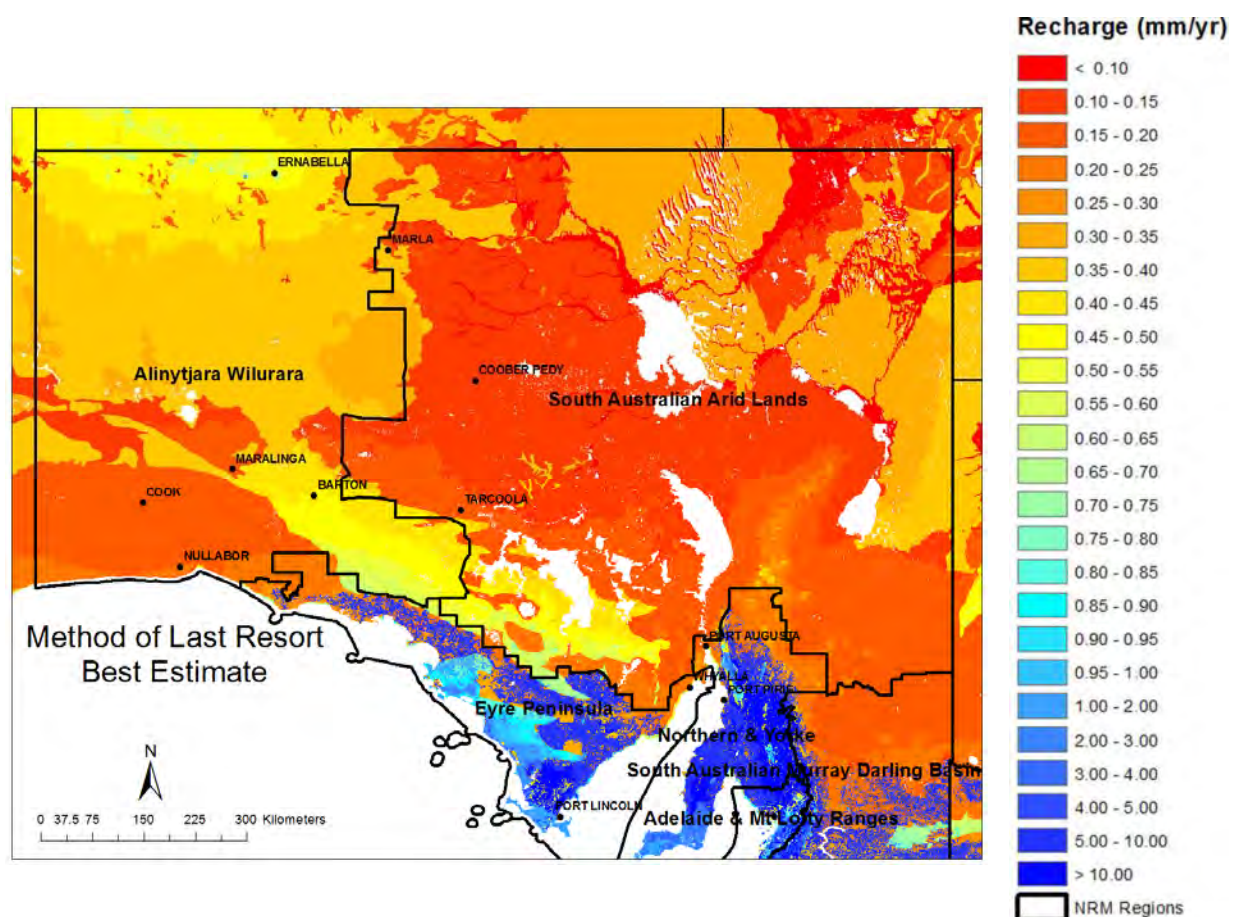


Figure 13. Map of mean annual recharge estimates made with the Method of Last Resort using the line of best fit. Also shown are the locations of the eight sites in the study area where historical rainfall and pan evaporation data from the SILO climate database were analysed.

Groundwater Chloride Mass Balance

The interpolated rainfall chloride deposition maps (Figure 7) also had prediction intervals around the best estimates which were very wide. As such we present maps of Groundwater Chloride Mass balance mean annual recharge estimates that have been made using the best estimate and the lower 95% prediction interval and the upper 95% prediction interval. The recharge estimates for the fractured rock wells are shown in Figure 14, with 95% predictions in Appendix C (Figure 84, Figure 85). The recharge estimates for the Quaternary and Tertiary wells are shown in Figure 15 with 95% predictions in Appendix C (Figure 86, Figure 87).

The best estimates made using this approach range from <0.1 to 33 mm yr^{-1} for the fractured rock wells with a mean of 1 mm yr^{-1} . Similarly the best estimates made using this approach range from <0.1 to 93 mm yr^{-1} for the Quaternary and Tertiary wells with a mean of 1 mm yr^{-1} . The estimates made using the lower 95% prediction interval range from $<0.1 \text{ mm yr}^{-1}$ to 29 mm yr^{-1} , and from $<0.1 \text{ mm yr}^{-1}$ to 52 mm yr^{-1} , for the fractured rock and Quaternary and Tertiary wells respectively. The estimates made using the upper 95% prediction interval range from $<0.1 \text{ mm yr}^{-1}$ to 53 mm yr^{-1} , and from $<0.1 \text{ mm yr}^{-1}$ to 237 mm yr^{-1} , for the fractured rock and Quaternary and Tertiary wells respectively.

While there are inherent assumptions in the Groundwater Chloride Mass Balance method (most notably that there has been no land use change at the site or the site has reached a new hydrologic steady-state at the screen depth) and uncertainties in the rainfall chloride deposition rates that affect its validity in any given situation, the general consensus is that its estimates are likely to be less uncertain than those of the Method of Last Resort (Leaney et al., 2011). The results show that there are often very low recharge rates in the Alinytjara-Wilurara/western South Australian Arid Lands Natural Resources Management regions that are consistent with the diffuse recharge estimates of the Method of Last Resort. However there are a significant number of wells that exhibit much higher values using the Groundwater Chloride Mass Balance method, which suggests that there may be some locations in the study areas where localised recharge is occurring. This is discussed in more detail below.

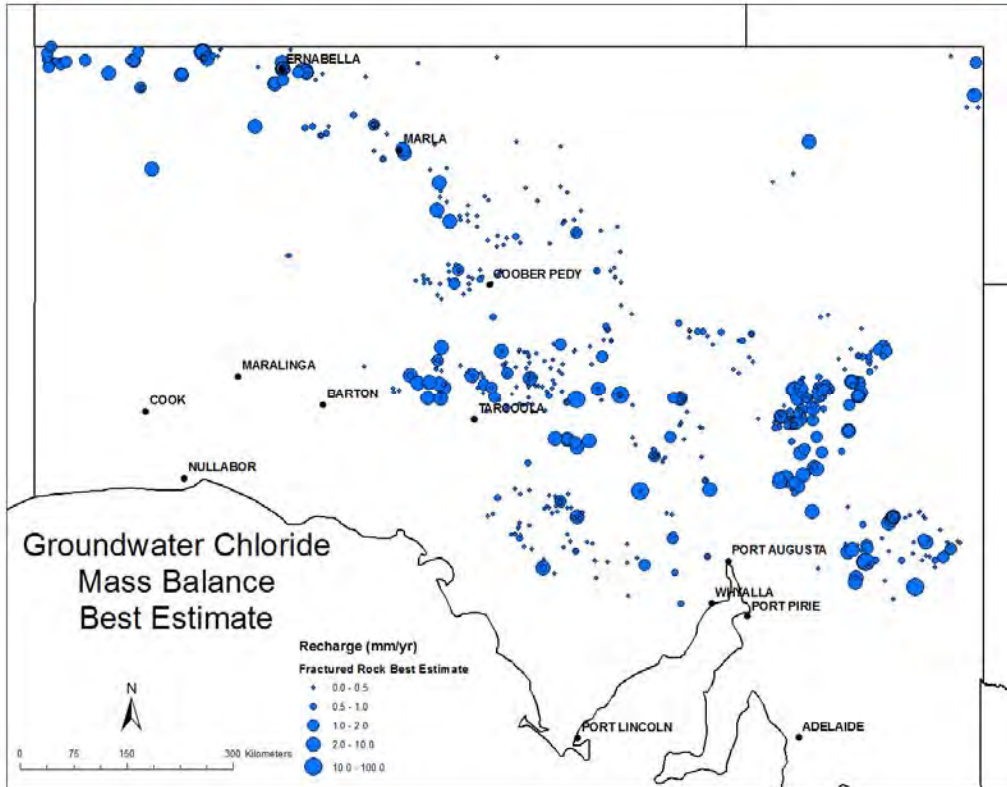


Figure 14. Map of mean annual recharge estimates for fractured rock wells made with the Groundwater Chloride Mass Balance method using the best estimates for the rainfall chloride deposition rate. Also shown are the locations of the eight sites in the study area where historical rainfall and pan evaporation data from the SILO climate database were analysed.

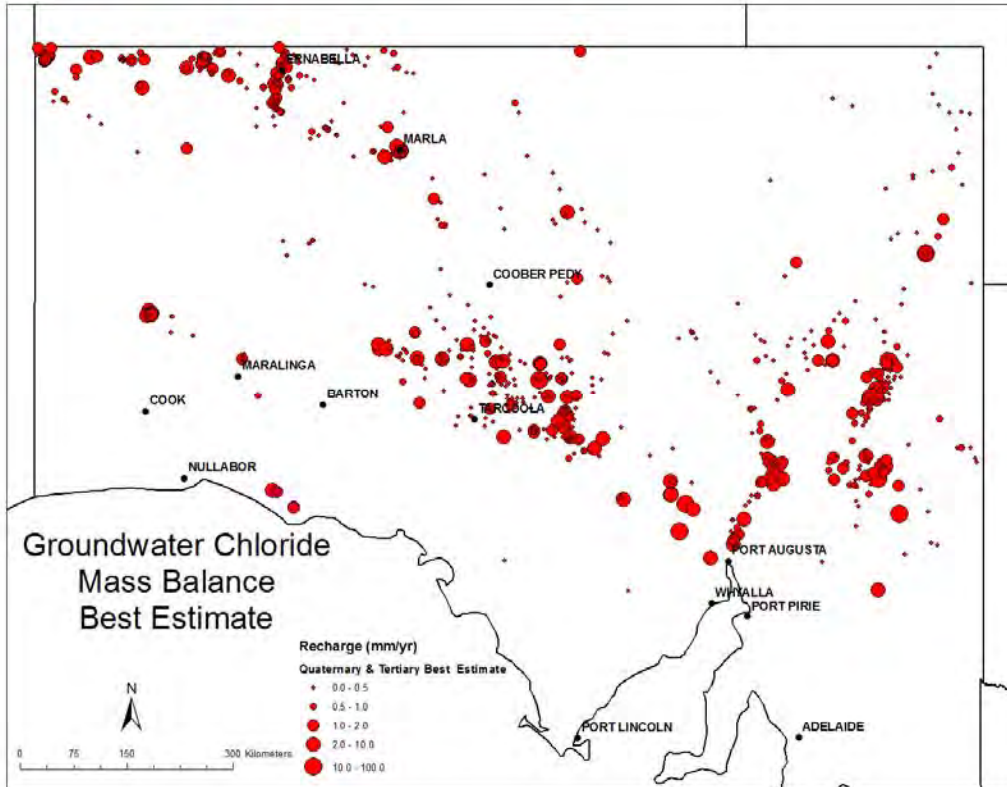


Figure 15. Map of mean annual recharge estimates for Quaternary and Tertiary wells made with the Groundwater Chloride Mass Balance method using the best estimates for the rainfall chloride deposition rate. Also shown are the locations of the eight sites in the study area where historical rainfall and pan evaporation data from the SILO climate database were analysed.

Discussion

Analysis of historical rainfall and evaporation

The study area is extremely arid with low rainfall and high evaporation, as reflected in the Koppen-Geiger climate classifications (Figure 2).

There is a general trend of decreasing rainfall and increasing evaporation from south to north. The exception to this is the BSh and BSk climate zones in the vicinity of Ernabella which are due to the influence of the Musgrave Ranges (e.g. the rainfall at Ernabella is similar to that at Nullarbor, the most southerly site in the study area).

The seasonal pattern in rainfall varies across the study area; in the far south (i.e. Nullarbor) it is winter dominant, in the far north it is summer dominant (i.e. Ernabella), and in most of the rest there is no clear seasonal trend. This behaviour in rainfall seasonality reflects the fact that most of the study area is influenced by both the winter rainfall patterns of the Southern Ocean and the summer monsoonal patterns from the north. There is a clear seasonal pattern in evaporation across the entire study area, with the lowest evaporation in winter and highest evaporation in summer.

There is some evidence of consistent patterns in the long-term mean annual rainfalls. There is a general trend of decreasing rainfalls (with some wetter periods) until around the 1970's, and then increasing rainfalls after that with variable behaviours during the last decade. This general trend is stronger at some sites (i.e. Barton) than others (i.e. Tarcoola). The patterns in the long-term mean annual pan evaporation rates were not analysed due to the relatively short available record (41 years) compared to that of the rainfall (122 years).

Estimation of recharge using existing information

Throughout the entire study area pan evaporation exceeds rainfall for all periods of the year, except during intermittent high rainfall events. This suggests that there is only very limited opportunity for drainage of water below the root zone, and so diffuse recharge rates are likely to be low throughout the study area. Other studies in southern Northern Territory have also found low diffuse recharge rates (e.g. Creswell et al., 1999) and determined that the dominant recharge mechanism is localised infiltration of flood waters following heavy, sustained rainfall events which only occur every 5 to 10 years (Harrington et al., 1999; 2002). The episodic nature of recharge in the Alinytjara-Wilurara Natural Resources Management region was discussed in Dodds and Sampson (2000) who speculated that months with rainfalls exceeding 100 mm may be more significant for recharge than annual rainfall totals. More recently, the study of AGT (2008) reported that some of the community wells in the Alinytjara-Wilurara Natural Resources Management region experience groundwater level increases following significant rainfall, suggesting the possibility of localised recharge. It is therefore not unreasonable to postulate that episodic localised recharge may be the dominant recharge mechanism in the study area.

Estimation of recharge using the Method of Last Resort and the Groundwater Chloride Mass Balance methods

As discussed in the Results section, some of the mean annual recharge estimates made using the Groundwater Chloride Mass Balance method were much higher than those made using the Method of last Resort. This is shown graphically in Figure 16 and Figure 17. There appears to be a mean annual recharge threshold of between 0.1 and 0.5 mm yr⁻¹ (i.e. log(recharge) between -1.1 and -0.3) whereby the Groundwater Chloride Mass Balance estimates begin to exceed those of the Method of Last Resort. This suggests that recharge estimates greater than 0.5 mm yr⁻¹ may be due to localised rather than diffuse processes. The possibility of localised recharge is further demonstrated by Figure 18. This clearly shows that in the high elevation fractured rocks and along the Quaternary and Tertiary valley streamlines of the Musgrave Province recharge is estimated to be much higher using the Groundwater Chloride Mass Balance method.

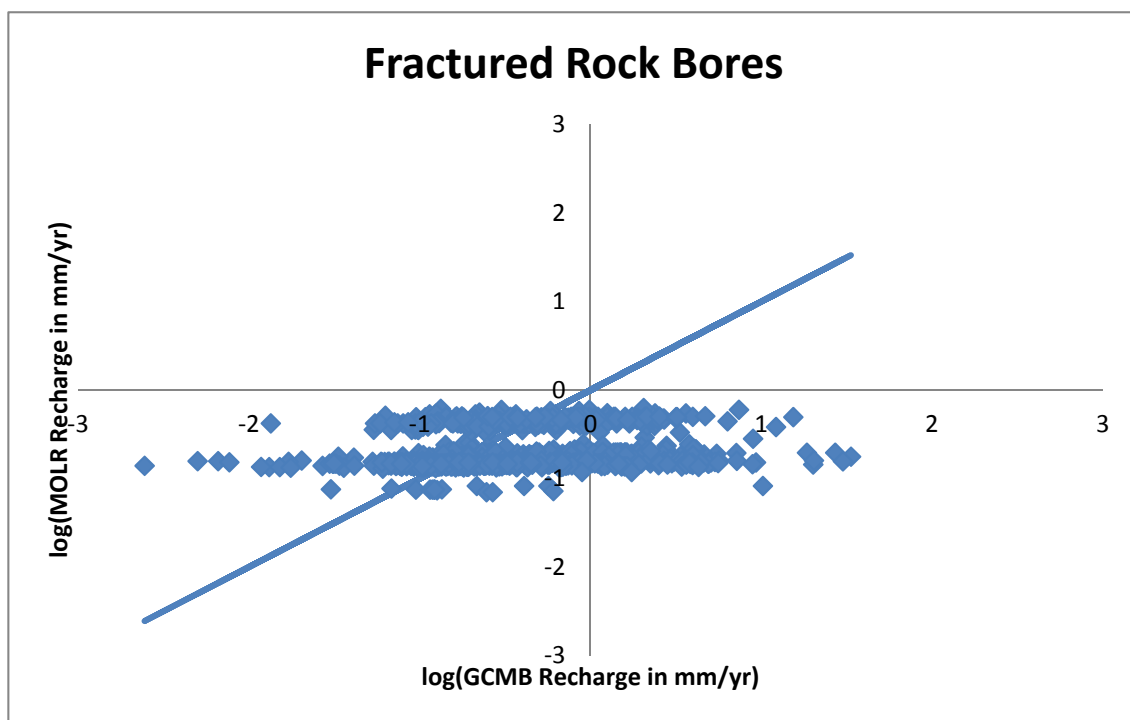


Figure 16. Plot of mean annual recharge estimates for the fractured rock wells made using the Method of Last Resort (MOLR) versus the estimates made using the Groundwater Chloride Mass Balance (GCMB). The plot is on a logarithmic scale with the solid line being the 1:1 line.

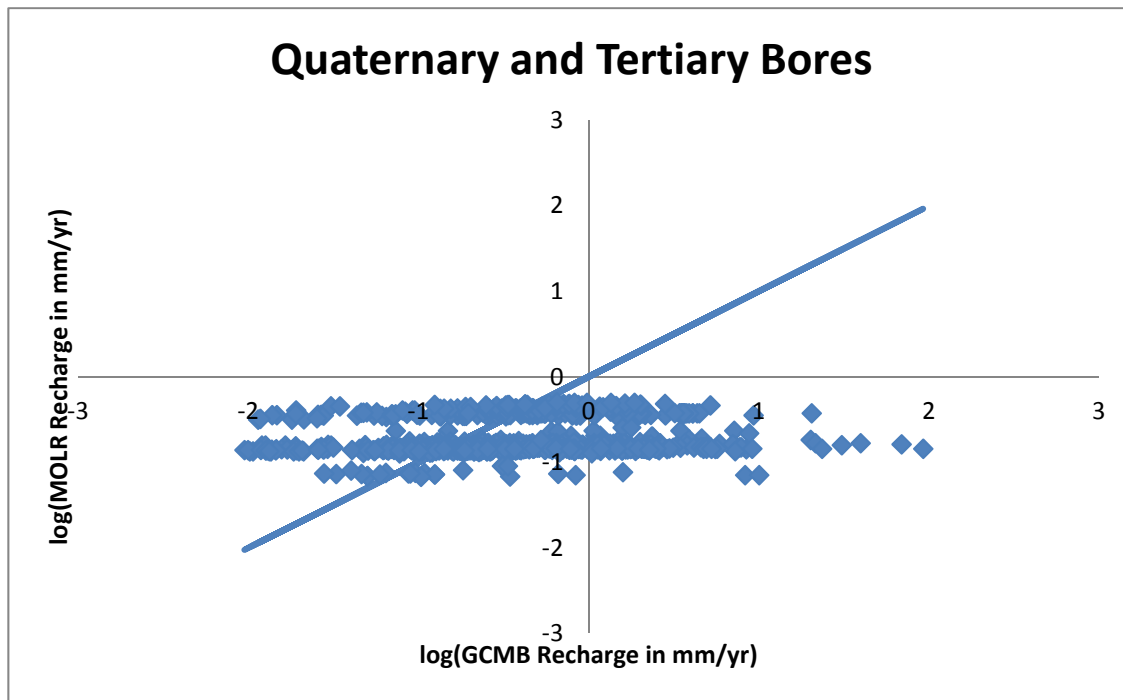


Figure 17. Plot of mean annual recharge estimates for the Quaternary and Tertiary wells made using the Method of Last Resort (MOLR) versus the estimates made using the Groundwater Chloride Mass Balance (GCMB). The plot is on a logarithmic scale with the solid line being the 1:1 line.

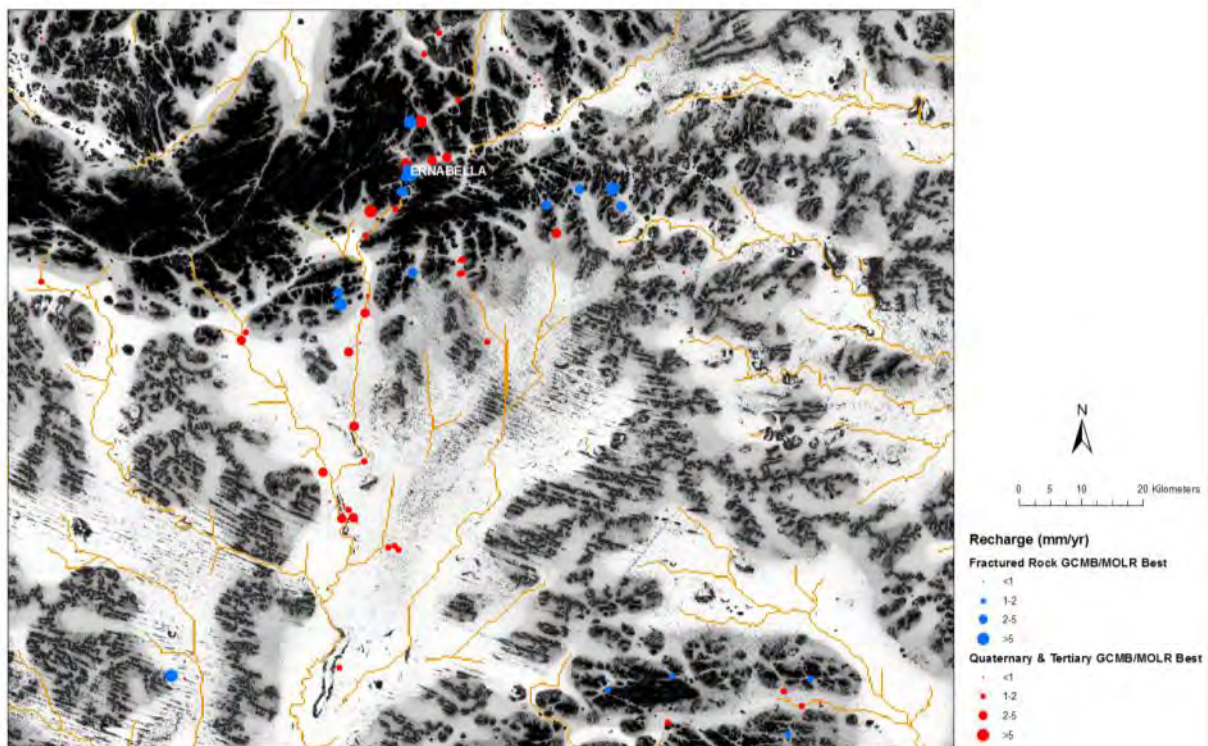


Figure 18. Ratio of the recharge estimates made using the Groundwater Chloride Mass Balance methods and the Method of Last Resort in a sub-area of the Musgrave Province. The background shading is predictions of the high elevation areas (black) and valley bottoms (white) made using the Multi Resolution Valley Bottom Flatness Index Level 6 (Gallant and Dowling, 2003) carried out by Lewis et al. (2010). The orange lines are predicted stream lines derived from the 9 second DEM of Australia.

Section 2 - Field Study of the Musgrave Province

Overview of study area

The field study area for this project is the South Australian portion of the Musgrave Province (Figure 19), a 60,000 km² geologically diverse area in the northwest of South Australia and is part of the APY Lands (Figure 22) (Tewkesbury and Dodds, 1997). The Musgrave Province is a Mesoproterozoic crystalline basement that is bound to the North by the Amadeus Basin, to the east by the Eromanga Basin and to the south and west by the Officer Basin (Major and Connor 1993). Extensive outcrop of basement rock occurs in the north as the Musgrave and Mann Ranges with smaller outcrops in the north-west as the Tomkinson Range, the south-west as the Birksgate Range and the south-east as the Everard Ranges. Where basement outcrop does not occur, Quaternary sand dunes of the Great Victoria Desert cover the region, along with other sediments including Pleistocene calcrete and Holocene alluvial, fluvial and aeolian deposits (Lewis et al. 2010). A general summary of the climate, geology, hydrogeology, soils and vegetation for the Alinytjara-Wilurara/Western South Australian Arid Lands Natural Resources Management Regions, which includes the Musgrave Province, is given in Section 1 of this report.

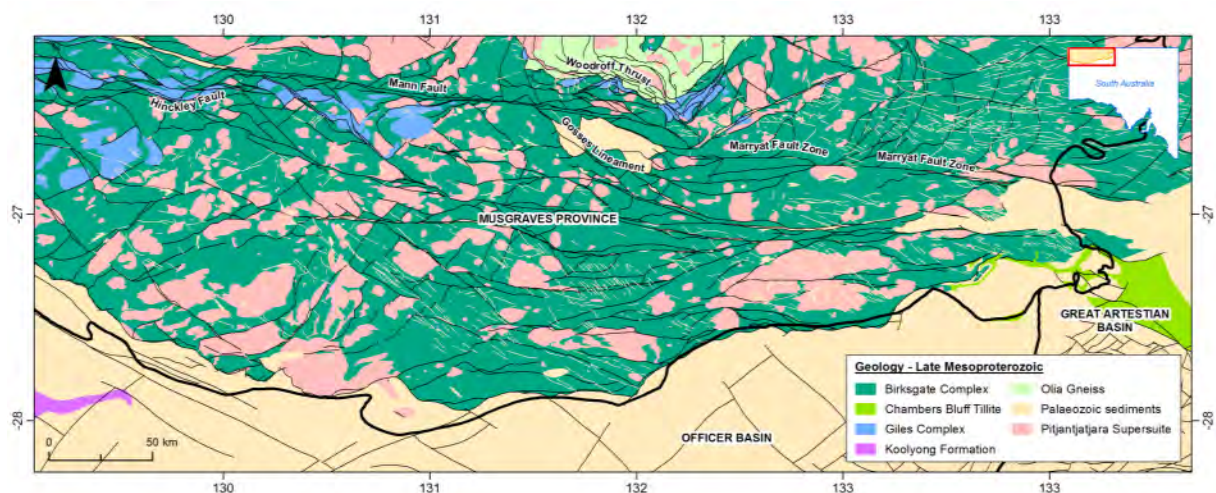


Figure 19. Basement geological map of the Musgrave Province (1 to 2 million).

The Musgrave Province is, in general, higher in elevation and has a higher rainfall than the other Natural Resource Management Regions described in Section 1. The northern part of the study area is located in the east-west trending Mann and Musgrave Ranges (Figure 20) (~1000 m to 1400 m AHD respectively and mean annual rainfall ~ 260 mm yr⁻¹) while the middle and southern part of the study area is described as rolling dune country of the Officer Basin (~500 m AHD and rainfall ~180 mm yr⁻¹). Groundwater wells within the Musgrave Province occurs within the fractured regolith of the Precambrian basement rocks, the shallow poorly consolidated Tertiary palaeovalley sediments, and the localised Quaternary alluvial deposits (GHD 2009; Magee 2009).

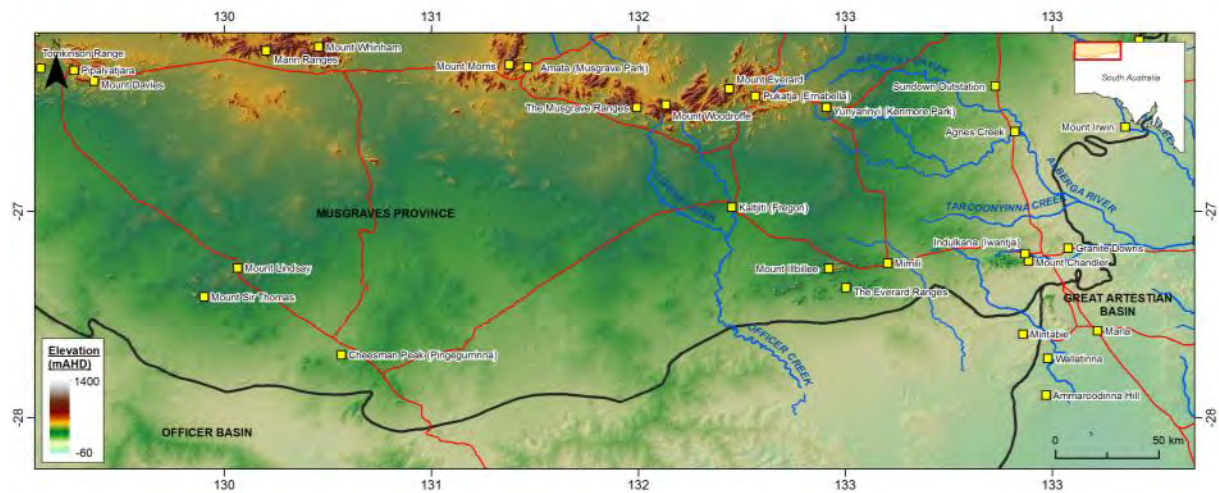


Figure 20. Location map of the Musgrave Province including ground surface elevation, towns and mountain ranges.

A number of palaeovalleys consisting predominantly of unconsolidated sediments, silts, sands and gravels are incised into the crystalline basement rock of the Musgrave Province (Watt and Berens 2011). These palaeovalleys (Figure 21) extend from the foot of the Mann and Musgrave Ranges southwards across the Officer Basin, obscured by the surficial cover of the Great Victorian Desert (Magee 2009). The Lindsay palaeovalley is the most prominent palaeovalley in the Musgrave Province, beginning south of the Musgrave Ranges and following the 131° longitude line as it continues due south into the Officer Basin.

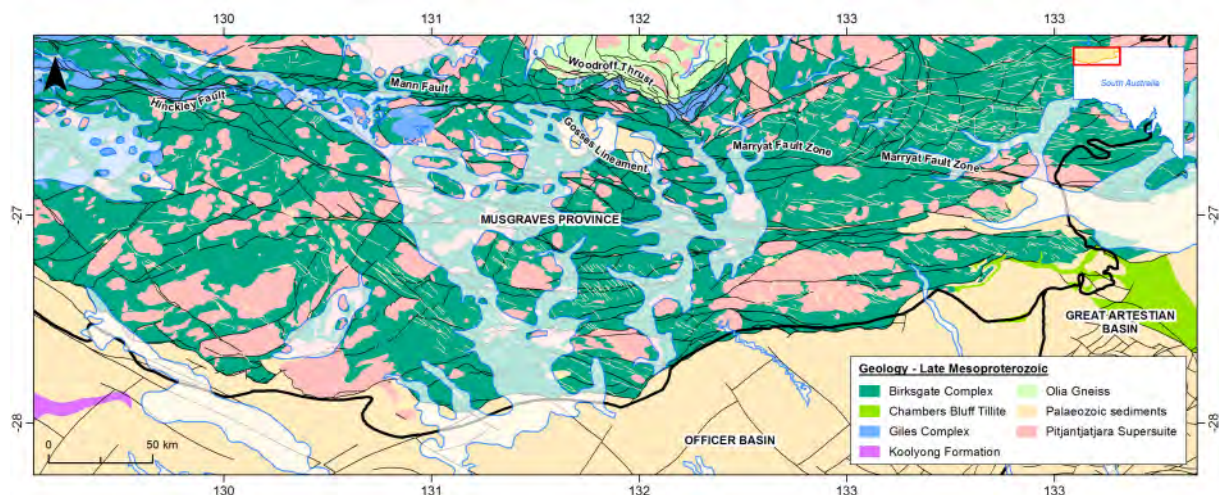


Figure 21. Location of palaeovalleys (light blue shading) throughout the Musgrave Province (1 to 2 million).

Previous studies in arid central Australia

There have been surprisingly numerous studies involving the use of environmental tracers to estimate recharge rates and determine recharge processes in Central Australia. In this section, we limit our summary to field-based studies that are within ~500 km of the Musgrave Province and also have made use of environmental isotopes in their work (Figure 22).

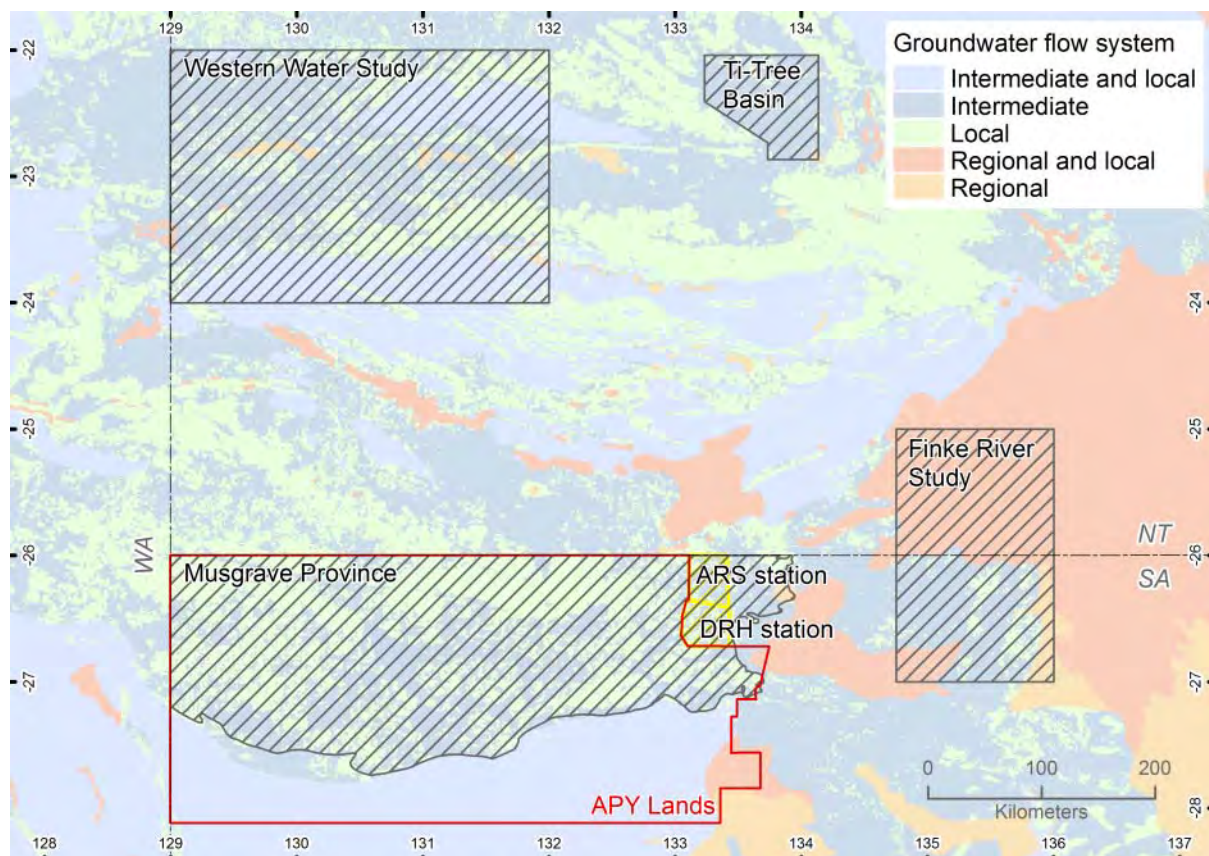


Figure 22. Location of previous groundwater studies in central Australia overlaying national groundwater flow systems (Coram et al. 2000).

APY Lands (Dodds et al, 2001; Cresswell et al., 2002)

Dodds (1996) made the first attempt at evaluating the APY Lands community water supplies in the area and found that water supplies are derived from localised shallow aquifers in fractured rock. Because of the long-term aridity of this region, recharge to the aquifers is believed to be low and sporadic, with long groundwater residence times resulting in evaporation of the groundwater and subsequent increased salinities (Fitzgerald et al. 2000).

In early 1997, the Nganampa Health Council, concerned about increasing salinity levels and potential associated Health problems, commissioned a comprehensive assessment of groundwater quality in the APY Lands. This study included analyses to determine the concentrations of naturally occurring chemicals, heavy metals, radiological parameters, coliforms (total and e-coli) and by-products of chlorine disinfection or alum flocculation used in the water treatment. Results of the Nganampa Health Council initiated study were reported in Fitzgerald et al. (2000).

The Nganampa Health Council also initiated work on the sustainability of the water resources in the APY Lands and this was reported in Dodds et al. (2001) and in Cresswell et al. (2002). These publications described the results for a suite of analyses for isotopic and hydrochemical tracers that have contributed to the assessment of the groundwater resources in the area and a conceptual model(s) for recharge. The report also provided a brief summary of salinity levels and sustainability of the groundwater supplies for the 8 main communities in the area; Indulkana (Iwantja), Mimili, Kaltjiti (Fregon), Umuwa, Pukatja (Ernabella) , Yunyarinyi (Kenmore Park), Amata, Pipalyatjara and

Kalka. In terms of the field sampling, from 1997 to 1999 groundwater samples were collected by the Bureau of Rural Sciences (BRS) from 30 wells in the APY Lands and analyses undertaken for Carbon-14 (^{14}C) (28 wells), Chlorine-36 (^{36}Cl) (29 wells) and tritium (^3H) (5 wells). A single sample of surface water was also collected and analysed for ^{36}Cl . The locations of the wells sampled are shown in (Figure 23) and the results along with aquifer type, standing water level (SWL) and screen depth are shown in Table 4. Stable isotope analyses deuterium ($\delta^2\text{H}$) and oxygen-18 ($\delta^{18}\text{O}$) were also undertaken on the water samples but these were not reported.

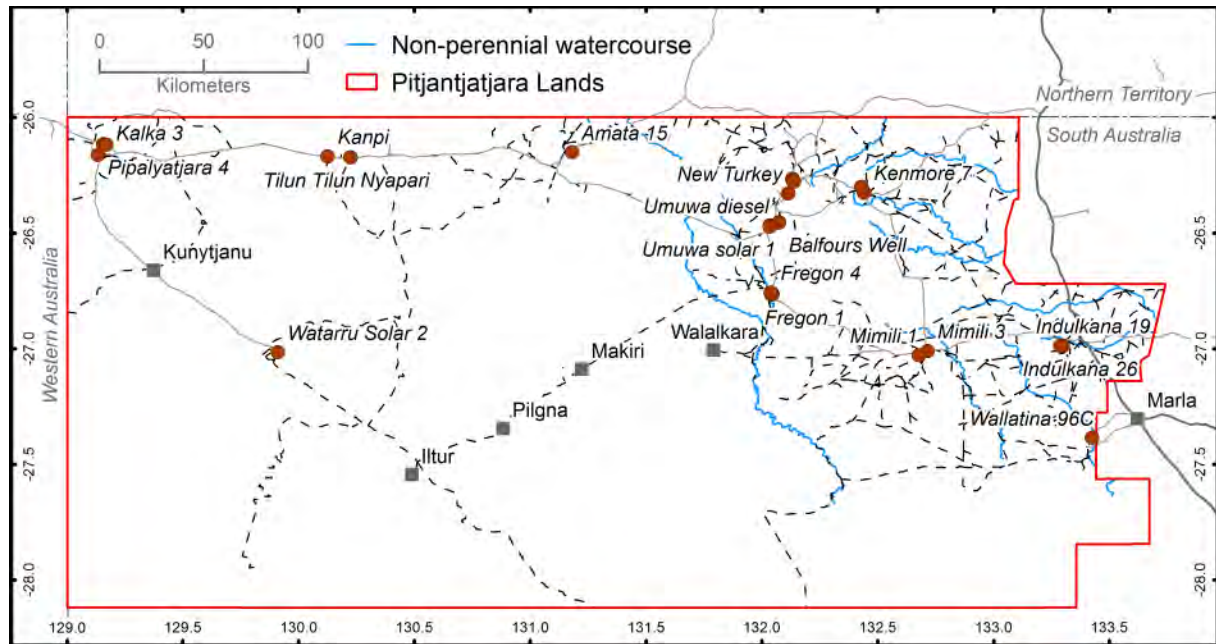


Figure 23. Location map of the APY Lands and wells (red circles) sampled (Figure 1 of Dodds et al. 2001).

Table 4. Groundwater wells and a surface water feature sampled in the APY Lands by Dodds et al. 2001 (Table 1 of Dodds et al., 2001).

Sample no	Cl	³⁶ Cl/Cl	³⁶ Cl	³ H	¹⁴ C	SWL	Well depth	Aquifer depth	Aquifer type	Name
AP#	(mg/L)	(x 10 ⁻¹⁵)	(x 10 ⁶ atoms/L)	T.U.	(pMC)	(m)	(m)	(m)		
124	388	118	778	–	56	8.3	37	8.3–35.7	Granulite	Kanpi
13	322	138	755	–	77	11	60	40–54	Granite	Mimili 3
4	366	141	877	–	30	15.6	68	55–60	Sandstone	Indulkana 19
99/3	283	151	727	–	n.d.	33	63	54–60	Gneiss	Watarru Solar 2
122	125	152	323	–	86	21.7	41.3	30–34	Granulite	Nyapari
99/1	31	159	83	–	n.d.	–	–	–	–	Pond (surface water)
132	95	161	260	<0.3	82	28–31	60	29–60	Gabbro	Kalka 2
38	483	161	982	–	67	11.6	21.5	11.6–20	Calcrete	Fregon 1
133	142	163	393	<0.3	63	17.4	60	–	Gabbro	Pipalyatjara 10
3	282	167	800	–	24	35	79	74	Sandstone	Indulkana 19A
126	99	177	298	–	82	15–19	40	24–30	Gabbro	Kalka 3
5	324	177	974	–	15	0	48	9–42	Sandstone	Indulkana 26
39	435	180	1330	–	63	12	48	39–45	Granulite	Fregon 7
44	462	181	1420	–	91	4.3	8	4.5–8	TQ Sediments	Umuwa Campgr.
73	209	192	682	–	59	9.5	19.2	19.2	TQ Sediments	Wallatina 96C
35	359	192	1171	–	n.d.	9	36	18–30	Granulite	Fregon 14
32	625	195	2070	–	58	11.5	35	20	Wthd schist	Fregon 4
7	311	218	1152	–	74	15.7	34.3	26	Gneiss	Mimili 1
145	184	229	716	–	69	17–21	36.8	22–36	Gabbro	Pipalyatjara 4
114	185	374	1175	–	100	8.6	36	30–36	Granulite	Amata 15
43	180	415	1269	–	100	5.9	6–12	12.6	Granulite	Balfours Well
50	190	609	1965	–	104	9.4	39.3	30–39	Ademalite	New Turkey
107	55	796	744	–	103	9.2	36	26	Granulite	Kenmore 7
49	76	880	1136	2.2	113	9.2	29.1	9.2–24	Ademalite	Ernabella 45
111	54	941	863	–	109	7.2	30	17.5	Granulite	Kenmore 94B
53	56	947	901	1.7	101	6.9	45	27–39	Granulite	Umuwa diesel
56	102	967	1675	–	111	9	21	12–18	Ademalite	Ernabella 42
55	36.2	n.d.	–	–	114	9	18	11–18	Ademalite	Ernabella 1
29	29	1512	745	–	109	6.5	24	21–21	Granulite	Umawa solar 1
99/2	82	1564	2171	–	n.d.	25.3	42.3	32–39	Granulite	Tilun Tilun

The ¹⁴C data showed that 10 of the 13 groundwater samples collected from wells screened in the Granulite or Ademalite aquifer type have post modern ¹⁴C concentrations (>100 percent modern carbon, pMC). These wells also had ³⁶Cl/³⁵Cl ratios in the range 609 – 1512 x 10⁻¹⁵ and ³H concentrations of 1.1 – 2.2 TU. All of these isotopic indicators suggested that the water being sampled in these wells recharged the aquifer since the mid 1950's. Cresswell et al. (2002) refined these suggested groundwater ages for these samples by normalizing the ³⁶Cl ratios to peak values and values recorded at Maralinga during the nuclear testing. The revised groundwater recharge dates range from 1958-1968. It is worth noting that the chloride concentration of the groundwater in these aquifers was low (29-190 mg L⁻¹), which was also indicative of high rates of recharge in these areas.

Cresswell et al. (2002) also showed that the mean depth of the bomb spike in $^{36}\text{Cl}/^{35}\text{Cl}$ ratios for some of the groundwater samples was ~9 metres below the surface. Cresswell et al. (2002) estimated the amount of water present in the unsaturated zone from the ground surface to that depth (i.e. the depth of the main $^{36}\text{Cl}/^{35}\text{Cl}$ bomb spike). Using this data and assuming the age of the water to be of 45 years, Cresswell et al. (2002) estimated a recharge rate of 10 mm yr^{-1} in these areas of the Musgrave Ranges. Cresswell et al. (2002) also noted that one well (Tilun Tilun) had deeper penetration (~25 m) of the bomb spike and estimated that recharge in this area of the Mann Ranges, where fractured rocks occur adjacent to sandy flats, was up to 30 mm yr^{-1} .

For groundwater samples collected from the deeper aquifers (aquifer type: sandstone, gneiss, gabbro, calcrete, Tertiary/Quaternary sediments and weathered schist), the ^{14}C ranged from 24 to 95 pMC. This was interpreted by Cresswell et al. (2002) as groundwater that had recharged within the last 5000 years.

Although the $\delta^2\text{H}$ and $\delta^{18}\text{O}$ analyses were never reported they were presented in a subsequent conference talk (Stephen Hostetler, pers. comm.). The $\delta^{18}\text{O}$ and $\delta^2\text{H}$ compositions for the groundwater samples ranged from approximately -9.2 to -5.8 ‰ Vienna Standard Mean Ocean Water (VSMOW) and -44 to -67 ‰ VSMOW respectively (Figure 24). Also plotted on Figure 24 is the local meteoric water line (MWL) for Alice Springs and the $\delta^{18}\text{O}$ and $\delta^2\text{H}$ compositions of rainfall for months with 0-50 mm, 50-100 mm, 100-150 mm, 150-200 mm and >200 mm of rain. The $\delta^{18}\text{O}$ and $\delta^2\text{H}$ composition of the groundwater plots quite close to the Alice Springs MWL indicating relatively rapid recharge and minimal evaporation at many of the sites. There is a suggestion of greater evaporation for wells where the $\delta^{18}\text{O}$ and $\delta^2\text{H}$ compositions are enriched ($\delta^{18}\text{O} > -8$ ‰ VSMOW). Using this approach, one would conclude that the groundwater $\delta^{18}\text{O}$ and $\delta^2\text{H}$ signature for the modern wells is associated with monthly rainfall totals of 100-150 mm.

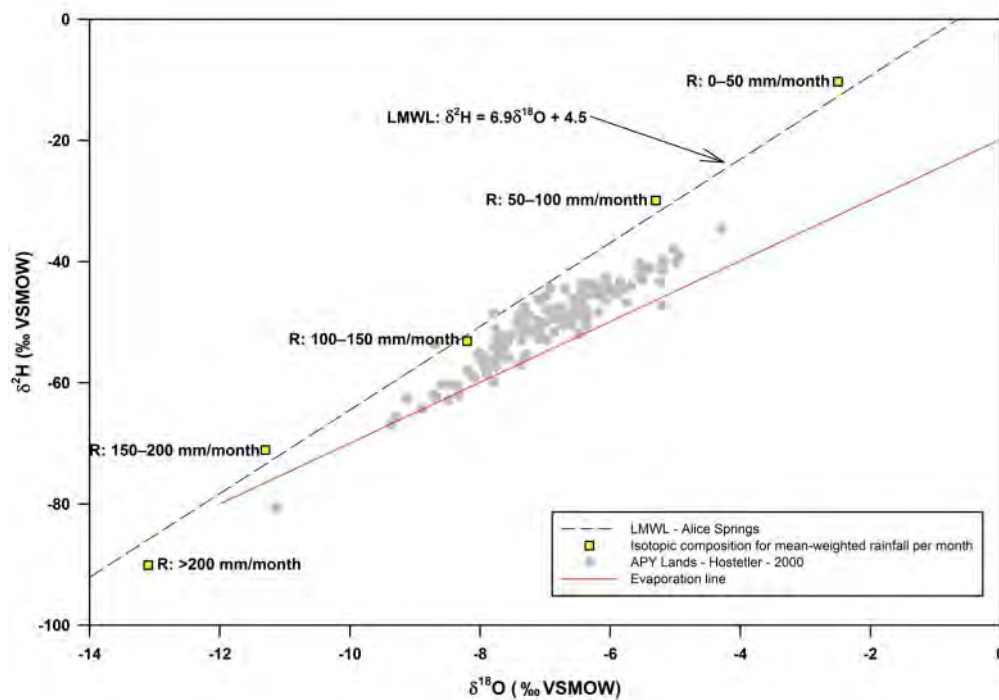


Figure 24. Stable hydrogen versus oxygen isotope composition for groundwater samples in the APY Lands. Also shown is the Local Meteoric Water Line (LMWL) for Alice Springs rainfall, an evaporation line for an open water body (slope 5 shown in red) and the isotopic composition of monthly rainfall intervals (Stephen Hostetler, pers. comm.).

Western Water Study, Northern Territory (Cresswell et al., 1999)

In the late 1990s, an assessment was undertaken by the Australian Geological Survey Organisation (AGSO) and Australian National University (ANU) on recharge to the groundwater systems in an arid south-western part of the Northern Territory (Western Water Study). The Western Water study area is about 300 km north of the APY Lands and has a similar arid climate and vegetation cover.

Cresswell et al. (1999) analysed groundwater samples for stable isotopes of water, $\delta^2\text{H}$ and $\delta^{18}\text{O}$, ^{14}C and ^{36}Cl to estimate recharge rates and determine recharge mechanisms for the sands and calcretes of the Cainozoic aquifers and the fractured rock Ngalia aquifers in the area. The authors concluded from the ^{14}C data for shallow groundwaters that recharge rates were low ($<1 \text{ mm yr}^{-1}$). They also suggested that there were likely to be two periods of recharge, current post-glacial and a period more than 80,000 years ago (Cresswell et al., 1999).

A summary of some of the raw data is presented at the end of this section. This data is combined and compared with that from the following previous studies in the arid regions of central Australia area showing the similarities and differences in the data, recharge rates and recharge mechanisms observed.

Ti Tree Basin (Harrington, 1994-2003)

Harrington undertook a comprehensive study on recharge mechanisms and chemical evolution of groundwater in the Ti Tree Basin for his PhD thesis (Harrington, 1999, Harrington et al., 2002, Harrington and Herczeg, 2003). The Ti Tree Basin is located ~500 km north-east of the APY Lands and, despite the distance, experiences an arid climate similar to the APY Lands. In addition, the methods used by Harrington to estimate recharge rates and determine recharge mechanisms in the Ti Tree Basin are similar to those used in the APY Lands. With these similarities, the Ti Tree Basin study provides an interesting background and comparison to the APY Lands study and is summarised here.

The Ti Tree Basin is a 5500 km² sedimentary basin with several Tertiary sandstone and carbonate aquifers containing large volumes of high quality groundwater. Harrington's PhD study measured the hydrochemistry, stable isotopes of water, $\delta^2\text{H}$ and $\delta^{18}\text{O}$, ^{14}C , Carbon-13 ($\delta^{13}\text{C}$) and strontium isotopes $^{87}\text{Sr}/^{86}\text{Sr}$ from 42 wells in the Basin along with a range of measurements and analyses on unsaturated zone samples. He estimated recharge rates using the GCMB method and a modified version of the ^{14}C method developed by Vogel (1967) and later by Walker and Cook (1991) as discussed in Harrington et al. (2002). Recharge rate estimates ranged from between 0.1 and ~2 mm yr⁻¹ at most sites for both methods, although several ^{14}C derived recharge rates were much higher (between 5 and 50 mm yr⁻¹). They concluded flood-out recharge to the freshest groundwater (TDS < 1000 mg L⁻¹) is 1.9 mm yr⁻¹ compared with a mean recharge rate of ~0.2 mm yr⁻¹ for the rest of the basin.

Harrington et al. (2002) were the first to use the comparison of $\delta^2\text{H}$ and $\delta^{18}\text{O}$ compositions of groundwater with that of the Alice Springs Local Meteoric Water Line to suggest that recharge resulted from larger rainfall events. In the case of the Ti Tree Basin, they suggested that intense rainfall events whereby at least 150-200 mm of rain fell in a month was required to produce substantial recharge. When presenting ^2H and ^{18}O in the following summary, data for wells near the Hanson and Woodforde Rivers where river recharge is clearly the dominant recharge mechanism, are presented separately from the rest of the data (as per Harrington, 1999; Figure 6.8).

Ayres Range South station (Custance, 2012) and De Rose Hill station (Craven, 2012)

The Ayres Range South (ARS) and De Rose Hill (DRH) studies were undertaken by Custance (2012) and Craven (2012) as part of their Honours theses. Both studies have contributed and complimented components of Task 6 of the G-FLOWS project. The ARS and DRH study sites cover an area approximately 80 km x 50 km, located immediately to the east of the APY Lands on the eastern flank of the Musgrave Province. The De Rose Hill station is situated to the south of the Ayres Range South station. The climate for the ARS and DRH studies is arid, hot desert (Koppen-Geiger classification BWh), similar to that for the Ti Tree Basin and APY Lands. Terrain is generally flat (average elevation ~460 m AHD) with vegetation dominated by arid grasses and shrublands with eucalyptus trees in the riparian zones. This is similar to the southern half of the APY Lands.

Custance (2012) also estimated recharge rates using the GCMB and the Harrington et al. (2002) ^{14}C methods. Estimates of recharge rate at 11 well sites in the ARS study ranged from less than 0.1 to ~0.6 mm yr⁻¹ with a similar range of values from 16 estimates at the DRH sites. Recharge rate estimates using the ^{14}C method are dependent on the value used for aquifer thickness with higher recharge rates estimated when using a thinner aquifer. However, even when using a relatively thin

estimate for aquifer thickness (20 m), the recharge rates were still up to an order of magnitude less than the GCMB estimates (Table 5, Custance, 2012).

Table 5. Recharge rates determined in the ARS study using both ¹⁴C and GCMB methods.

ID	Well Name	¹⁴ C (H=40 m) (mm yr ⁻¹)	¹⁴ C (H=30 m) (mm yr ⁻¹)	¹⁴ C (H=20 m) (mm yr ⁻¹)	GCMB (mm yr ⁻¹)
A	Sundown Well	–	–	–	0.18
B	Independance well	–0.04	0.02	0.10	0.31
C	Holywater Well	–	–	–	0.08
D	Ian's Well	–0.07	–0.005	0.06	0.58
E	Doug's Well	–	–	–	0.58
F	Coultly's Hole	0.005	0.10	–	0.26
G	East Well	–	–	–	0.29
H	Branson's Well	–	–	–	0.11
I	Giveaway Well	–0.02	0.06	–	0.61
J	Hawke's Well	–0.06	0.01	0.09	0.05
K	Guy Fawkes Well	–0.003	0.06	–	0.08

Finke River Study (Love et al., 2013)

The Finke River Study was part of an NWC funded project on “Allocating water and maintaining springs in the Great Artesian Basin”. The study site is the Finke River recharge zone located on the western margin of the Great Artesian Basin approximately 200 km south-east of Alice Springs (~300 km north-east of the APY Lands). Recharge occurs when surface water from episodic flow events in the Finke River drain directly into the GAB J aquifer where it outcrops on the banks of the river or sub-crops underneath the river channel. The river bed material consists predominantly of very well sorted medium-grained quartz sand with a thin clay drape (<1 cm) that is unlikely to act as an effective clogging layer (Love et al., 2013).

Love et al. (2013) reported the hydrochemistry, stable isotopes of water, $\delta^2\text{H}$ and $\delta^{18}\text{O}$, ^{14}C and $\delta^{13}\text{C}$ from ~50 wells in the Basin. The wells were divided into 15 wells designated as unconfined (usually located closer to the river) and 35 wells designated as confined and located further away from the river. The authors estimated recharge rates using a modified version of the ^{14}C method developed by Vogel (1967), modified for estimation of recharge along a river channel (Appelo and Postma, 1993; Cook and Bohlke, 2000). Recharge rate estimates in the river channel ranged from between 380 and 850 mm yr⁻¹ with the recharge zone estimated to cover 13 km². They concluded from the comparison of $\delta^2\text{H}$ and $\delta^{18}\text{O}$ compositions of groundwater in the J aquifer with those of the Alice Springs Local Meteoric Water Line that minimal evaporation occurred during/prior to recharge taking place. They suggested that there was a rapid recharge mechanism, consistent with the conceptual ephemeral river recharge model. They further suggested that recharge is most strongly associated with rainfall events in January to March in the months that exceed 100 mm.

Comparison of raw data from previous studies

As discussed, previous studies investigating recharge rates and processes in several arid regions of central Australia have resulted in a significant data base for environmental tracers. This data is summarised in the following plots.

Groundwater salinity and major ion composition

There is a large range in the salinities of groundwater in the study areas. In the Ti Tree Basin and APY Lands studies, the groundwater salinities range from $\sim 500 \text{ mg L}^{-1}$ to greater than 3000 mg L^{-1} . In the Finke River and the ARS (east of APY Lands), the groundwater salinities are generally less than those for the other study areas. The range in major ion compositions of groundwater for groundwater in the Ti Tree Basin, APY Lands and ARS, as shown in a Piper plot (Figure 25) is also similar.

Each of these studies came to similar conclusions. Groundwater salinities (and [Cl]) inversely reflect recharge rates. Higher salinity and higher [Cl] groundwater results when there are lower rates of recharge, and lower salinity and lower [Cl] groundwaters results when there are higher rates of recharge. However, there is also an increase in groundwater salinity during the evolution of Na-HCO₃ dominated hydrochemical compositions to Na-Cl dominated compositions (as shown in arrows in Figure 25). Harrington and Herczeg (1998 and 2000) established that the mechanisms for these trends included dissolution of gypsum, dissolution or precipitation of Ca-Mg carbonates and weathering of sodium rich silicate minerals. Furthermore, the ionic composition of the more saline, Na-Cl type groundwater are also affected by exchange of Na for Ca on clay mineral surfaces and reverse weathering of silicates.

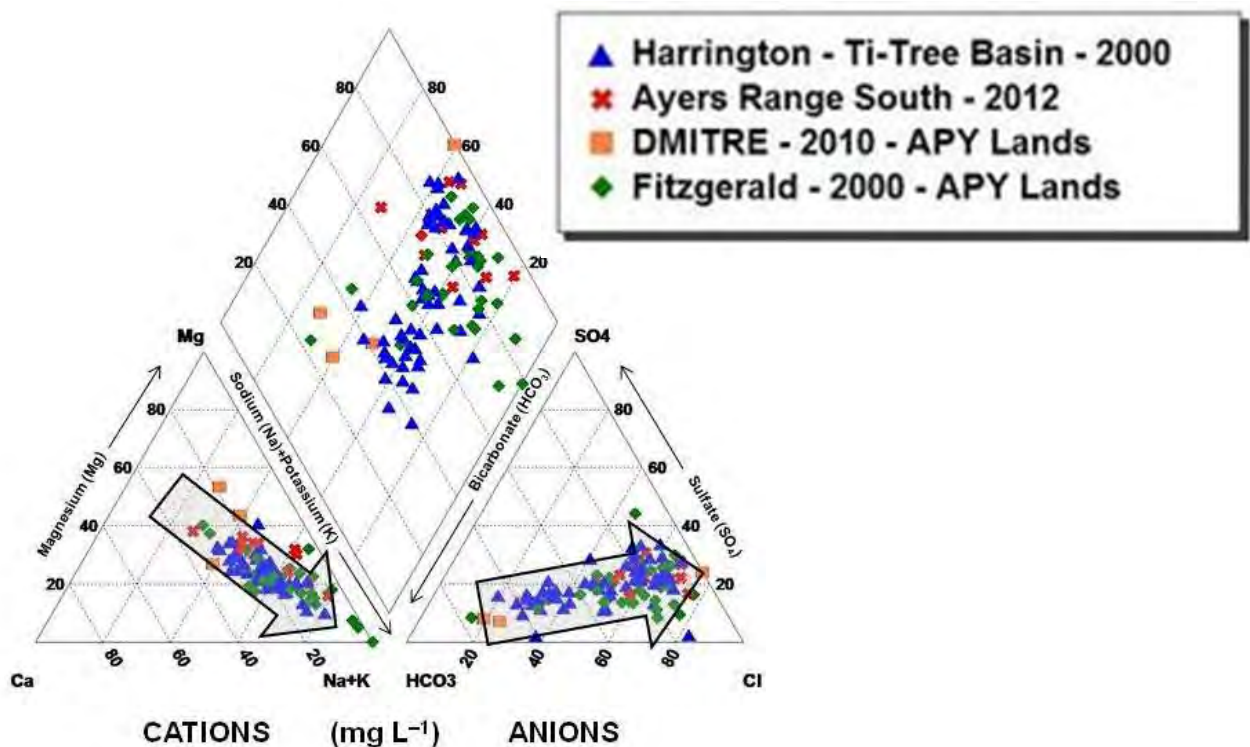


Figure 25. Piper plot illustrating major ion composition of groundwater analysed for previous studies conducted in central Australia.

Carbon isotopes

^{14}C composition is plotted against $\delta^{13}\text{C}$ composition for groundwater from the Ti Tree Basin, ARS, DRH and the Finke River studies (Figure 26). Although ^{14}C data was reported in the earlier APY Lands study, $\delta^{13}\text{C}$ composition was missing and hence has not been plotted. The overall range in $\delta^{13}\text{C}$ composition for the combined study areas is from about -6 to -14 ‰ Pee Dee Belemnite (PDB) (excluding one well from Finke River study) with similar ranges of data for the individual study areas. ^{14}C compositions for the Finke River study are, in general, similar to the range for ARS and DRH and significantly more than those at the Ti Tree Basin. There are many likely reasons for this, including screen and well depths, distance from recharge areas and different recharge rates.

Apparent (maximum) ages of the groundwater can be calculated from the ^{14}C composition assuming radioactive decay of ^{14}C and no water rock interaction. For the data presented in these studies, this would correspond to groundwater ages from close to modern to >30,000 years. There are several methods to correct for water rock interaction and most of the studies have used either a hydrochemical, isotope ($\delta^{13}\text{C}$) or a combined hydrochemical/isotope chemical approach. Some used an approach suggested Harrington et al. (2000) that interpreted Sr-isotopes to determine the extent of carbonate dissolution and silicate weathering. In general, these methods gave “corrected” ages about 1,000-5,000 years younger than apparent ages. However, looking at the range of $\delta^{13}\text{C}$ values for groundwater samples of similar ^{14}C activity, it is not clear that determination of corrected ages is warranted and it may be better to simply consider maximum apparent groundwater ages.

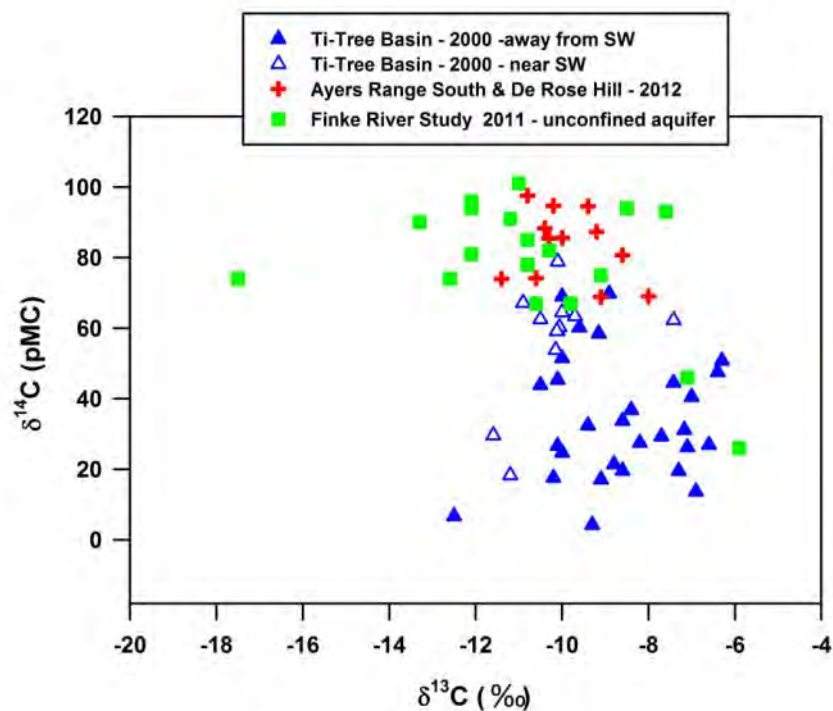


Figure 26. Relationship between measured $\delta^{13}\text{C}$ and ^{14}C for groundwaters analysed from previous studies in central Australia.

Stable isotopes of water

$\delta^2\text{H}$ and $\delta^{18}\text{O}$ compositions of groundwater were measured in all of the previous arid zone studies (Figure 27). The combined isotope data has a large spread, ranging from approximately -4 to -11 ‰ VSMOW in $\delta^{18}\text{O}$ and -34 to -80 ‰ VSMOW in $\delta^2\text{H}$. The range in isotopic composition for most of the studies is also considerable (e.g. $\delta^2\text{H}$ and $\delta^{18}\text{O}$ compositions cover almost the total regional spread for data in the APY Lands). The $\delta^2\text{H}$ and $\delta^{18}\text{O}$ compositions are plotted against the Local Meteoric Water Line (LMWL) for Alice Springs and the mean $\delta^2\text{H}$ and $\delta^{18}\text{O}$ compositions of monthly rainfall intervals. It is worth noting that most of the $\delta^2\text{H}$ and $\delta^{18}\text{O}$ groundwater compositions plot on a straight line parallel to the LMWL with a $\delta^2\text{H}$ displacement of 0-20 ‰ and therefore it is not possible to extrapolate the line of best fit through the well data to a meaningful $\delta^2\text{H}$ and $\delta^{18}\text{O}$ composition on the LMWL, as has been done in many of the previous studies in surrounding areas.

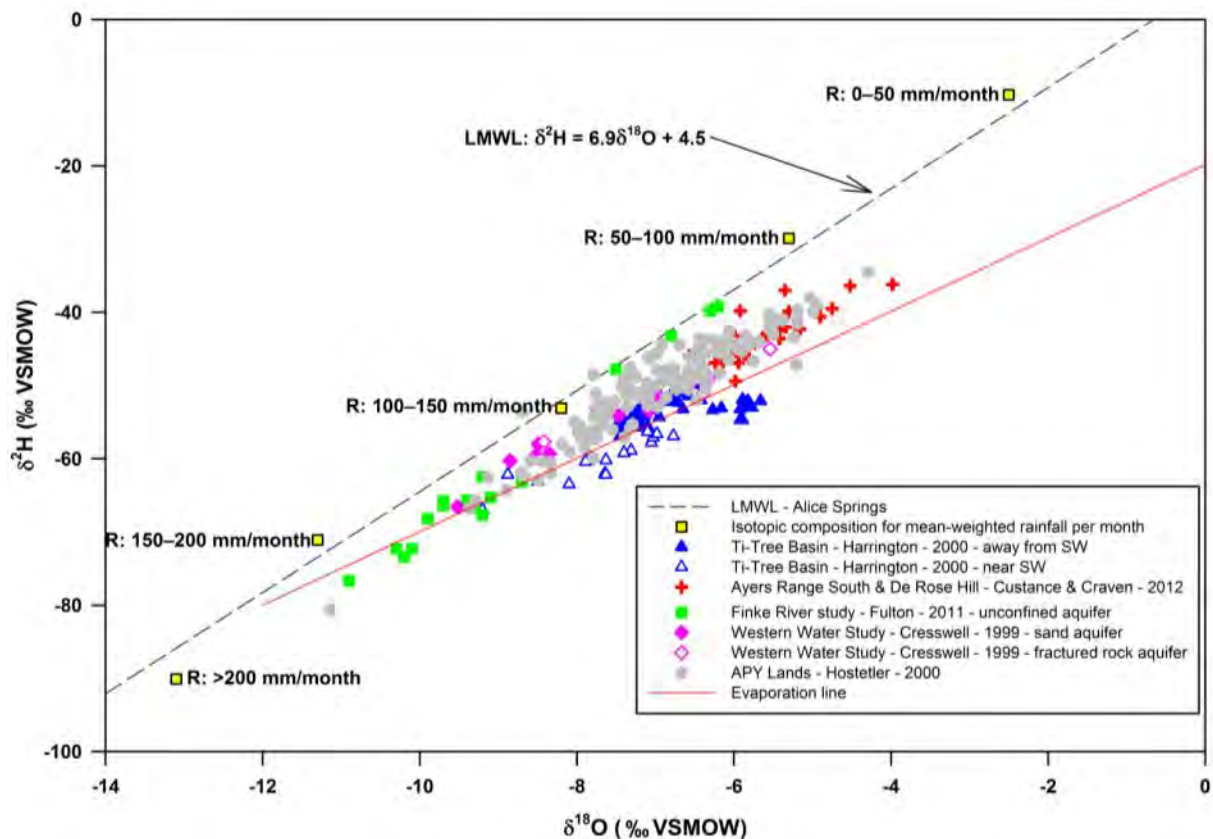


Figure 27. Stable hydrogen versus oxygen isotope composition for groundwater samples analysed for previous studies in central Australia. Also shown is the Local Meteoric Water Line for Alice Springs rainfall and the monthly rainfall totals.

Comparison of recharge rates from previous studies

In addition to the comparison of raw data discussed above, it is also useful to summarise the findings of the individual studies with respect to recharge rates and recharge processes.

For the Musgrave Ranges, Cresswell (2002) suggests recharge rates of 10 mm yr^{-1} in the Ranges and up to 30 mm yr^{-1} where fractured rocks occur adjacent to sandy flats. No estimates were made for areas to the south of the Musgrave Ranges. It was also suggested that monthly rainfall of 150 mm was required for recharge to take place (Hostetler and Cresswell, BRS presentation). For the Ti Tree

Basin, Harrington et al. (2002) suggested flood-out recharge to the freshest groundwater (TDS < 1,000 mg L⁻¹) to be 1.9 mm yr⁻¹ compared with a mean recharge rate of ~0.2 mm yr⁻¹ for the rest of the Basin. They also concluded that monthly rainfall of 150-200 mm was required for recharge to take place.

For the Western Water Study, Cresswell et al. (1999) concluded from the ¹⁴C data for shallow groundwater that recharge rates were low (<1 mm yr⁻¹). They also suggested that there were likely to be two periods of recharge, current post-glacial and a period more than 80,000 years ago. Estimates of recharge rate for the ARS and DRH studies ranged from less than 0.1 to ~0.6 mm y⁻¹ (Custance, 2012) using the GCMB method and up to an order of magnitude less using ¹⁴C data and the approach suggested by Harrington et al. (2002). For the Finke River study, recharge rate estimates in the river channel ranged from between 380 and 850 mm yr⁻¹ with the recharge zone estimated to cover 13 km². They concluded minimal evaporation occurred during/prior to recharge taking place. They further suggested that recharge is most strongly associated with rainfall events in January to March (i.e. when the monthly rainfall totals more commonly exceed 100 mm).

Methods

Initially 41 groundwater wells were identified as potential sample sites throughout the APY Lands (Figure 28), predominantly in the Musgrave Province. The list included some of the wells that had been sampled in 1997/8 that had ^{14}C compositions greater than 100 pMC (Dodds et al., 2001). Also included were numerous wells in the central parts of the APY where no sampling for environmental tracers had previously been undertaken. A number of wells sampled during this study were production wells operated by SA Water to supply water to the local communities on the APY Lands (Figure 29).

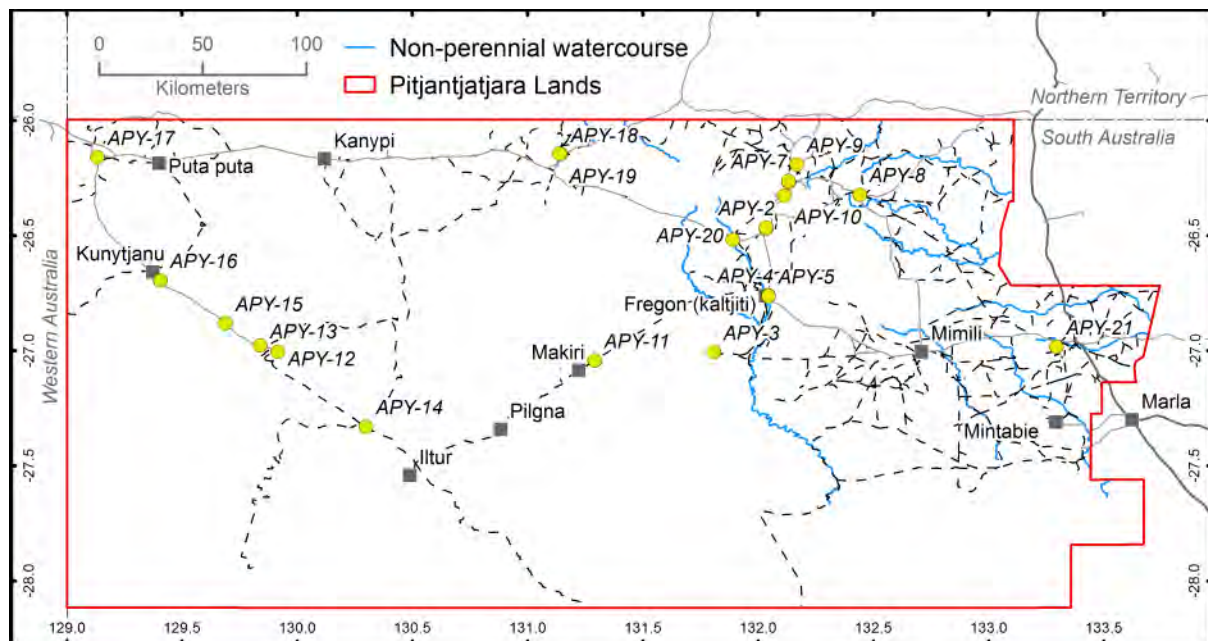


Figure 28. Groundwater wells (yellow circles) sampled for environmental tracers in the APY Lands.

In addition to the production wells a small number of groundwater wells were sampled on traditional homelands that are currently occupied by a very small population or are abandoned. Logistical and time constraints meant that only 21 wells could be sampled. The South Australian well registration details (unit number, well locations, sample ID, ground surface elevations and well depths) are given in Table 6.



Figure 29. Production well supplying groundwater to a local community.

Table 6. Details for groundwater wells sampled in the APY Lands.

Unit Number	Location	Sample ID	Zone	Latitude	Longitude	Ground surface elevation mAHD	Well depth m
534500079	Umawa	APY - 1	53	-26.4710278	132.0352422	589	24.0
534500080	Umawa	APY - 2	53	-26.4666148	132.0351652	591	45.0
524300010	Walalkara	APY - 3	52	-27.0078020	131.8081390	470	39.0
534400031	Fregon	APY - 4	53	-26.7608617	132.0437717	528	48.0
534400047	Fregon	APY - 5	53	-26.7641293	132.0460187	528	30.0
534500033	Ernabella	APY - 6	53	-26.2714785	132.1332642	677	21.0
534500084	Ernabella	APY - 7	53	-26.2644065	132.1319970	681	30.0
534500068	Kenmore Park	APY - 8	53	-26.3240112	132.4417926	620	36.0
534500120	Ernabella	APY - 9	53	-26.1932330	132.1691570	707	33.0
534500024	Ernabella	APY - 10	53	-26.3282737	132.1138533	661	23.9
514300006	Makari	APY - 11	52	-27.0437796	131.2906094	532	36.6
484300012	Wataru	APY - 12	52	-27.0062040	129.9155620	586	71.4
484400002	Wataru	APY - 13	52	-26.9784740	129.8380920	558	30.0
494300007	Wataru/Iltur	APY - 14	52	-27.3307820	130.2979010	461	42.0
484400003	Wataru/Kunytjanu	APY - 15	52	-26.8827970	129.6888690	536	30.0
474400010	Kunytjanu	APY - 16	52	-26.6964780	129.4045810	543	54.0
474500096	Pipalyatjara	APY - 17	52	-26.1626026	129.1325001	637	36.8
514500084	Amata	APY - 18	52	-26.1471067	131.1434956	687	34.5
514500109	Amata	APY - 19	52	-26.1467267	131.1374784	690	55.0
524400021	Watinuma	APY - 20	52	-26.5191550	131.8908468	576	21.0
554400101	Indulkana	APY - 21	53	-26.9843968	133.2954337	438	68.0

Samples from the 21 wells were collected for analyses of $\delta^2\text{H}$ and $\delta^{18}\text{O}$, ^{14}C , $\delta^{13}\text{C}$ and strontium isotopes $^{87}\text{Sr}/^{86}\text{Sr}$. In addition, samples were collected for analyses of tracers of modern recharge, chlorofluorocarbons, CFC11 and CFC12 and sulphur hexafluoride, SF_6 and also for the noble gases helium-4 (^4He), argon-40 (^{40}Ar) and neon-20 (^{20}Ne). At each well, the standing water level was measured and the well was purged for three well volumes, with care taken to ensure that the water level never dropped below the top of the screen. Following purging, groundwater parameters were measured under gentle flow conditions in a vessel using portable probes including EC, pH and redox potential. Dissolved oxygen concentrations were determined by the Winkler titration method. In addition the following water samples were collected.

Groundwater samples were 0.45 μm filtered in the field for stable isotopes of water and major ion chemistry. For the stable isotopes of water, a 30 mL subsample was then stored in a gas-tight collection vessel (McCartney bottle). For major cations, a 50 mL subsample was acidified (to $\text{pH}<2$) and stored in a well-rinsed 125-mL PET bottles. For major anions, total alkalinity, lab EC and lab pH, another 50 mL subsample was stored in a similar manner but without acidification. A field blank for major cations and anions was also prepared by processing a distilled water sample in the same way as the field samples. All samples were analysed at the CSIRO Analytical Chemistry Laboratory (Waite Campus, Adelaide).

A one litre amber coloured bottle of sample water was collected for SF_6 analysis as per instructions from the USGS SF_6 and chlorofluorocarbon (CFC) laboratory (<http://water.usgs.gov/lab/sf6/sampling/>). The SF_6 analyses were undertaken at the CSIRO Isotope Analytical Laboratory on an aliquot of ultra high purity nitrogen that had been equilibrated with ~ 300 ml of the water sample at 25°C and then analysed using a gas chromatograph fitted with an electron capture device.

Three 125 ml bottles of sample water were collected for CFC analysis (Figure 30) as per instructions from the USGS SF_6 and CFC laboratory (<http://water.usgs.gov/lab/sf6/sampling/>). The CFC11 and CFC12 analyses were undertaken at the CSIRO Isotope Analytical Laboratory on an aliquot of gas purged from the water using ultra high purity nitrogen and then analysed using a gas chromatograph fitted with an electron capture device.



Figure 30. CFC sampling on a community production well in the APY Lands.

Samples of groundwater for $\delta^{2}\text{H}$ and $\delta^{18}\text{O}$ analysis were analysed via a GEO 20-20 dual inlet stable isotope gas ratio mass-spectrometer fitted with a 59 port Water Equilibration System (PDZ Europa Ltd. U.K.). Samples of groundwater for ^{14}C analysis were collected in 5 L plastic containers (Figure 31) and the dissolved inorganic carbon precipitated as SrCO_3 under alkaline conditions ($\text{pH} > 11$). Aliquots of CO_2 , prepared via acidification of the precipitate and cryogenic purification, were sent to the AMS laboratory at the Australian National University for ^{14}C analysis. Sub-samples of CO_2 were analysed for $\delta^{13}\text{C}$ via a GEO 20-20 dual inlet stable isotope gas ratio mass-spectrometer.



Figure 31. Carbon-14 sample from a groundwater well at Walalkara in the APY Lands.

Dissolved noble gas samples were collected from all wells using the “copper tube” method (Weiss 1968). This includes flushing a 60 cm length of 3/8” copper tubing with formation water before sealing the sample with pinch-off type clamps, preserving approximately 25 g of water without exposing the sample to the atmosphere where dissolved gases could be gained or lost. Analysis of dissolved noble gases was via cryogenic separation and measured on a quadrupole mass spectrometer.

Results

Field and analytical results for groundwater samples collected during this APY Lands field study are given in Table 7, Table 8, Table 9 and

Table 10. Funding and time constraints meant that no samples were analysed for $^{87}\text{Sr}/^{86}\text{Sr}$ isotope composition and only six samples were analysed for CFC concentration. Results of the current APY Land field study data have been plotted relative to results from previous studies in the APY Lands and surrounding areas where data is available (i.e. for major anion/cation and $\delta^2\text{H}$, $\delta^{18}\text{O}$, ^{14}C and $\delta^{13}\text{C}$ composition).

Table 7. Measured field parameters for groundwater wells in the APY Lands.

Unit Number	Sample ID	Ground surface elevation mAHD	Well depth m	SWL m	RSWL m	SWL date	Field EC uS cm ⁻¹	Field pH	O ₂ (Winkler) mg L ⁻¹	Redox mV
534500079	APY - 1	589	24.0	11.31	577.69	16/04/2010	675	7.5	8	217.4
534500080	APY - 2	591	45.0	11.20	579.60	16/04/2010	750	7.48	6	-
524300010	APY - 3	470	39.0	21.32	448.68	15/05/2003	5320	7.24	8	129
534400031	APY - 4	528	48.0	11.60	516.40	16/04/2010	2300	7.49	7	21
534400047	APY - 5	528	30.0	11.15	516.85	16/04/2010	2076	7.38	7	194
534500033	APY - 6	677	21.0	6.31	670.69	15/04/2010	1152	7.18	3	231.7
534500084	APY - 7	681	30.0	9.51	671.49	15/04/2010	1274	6.94	5	183.1
534500068	APY - 8	620	36.0	11.16	608.84	15/04/2010	771	7.36	7	185
534500120	APY - 9	707	33.0	11.86	695.14	15/04/2010	879	7.43	5	140
534500024	APY - 10	661	23.9	8.12	652.88	18/05/2003	1385	7.06	6	177
514300006	APY - 11	532	36.6	24.90	507.10	5/10/2012	2575	7.08	6	146
484300012	APY - 12	586	71.4	35.46	550.54	16/05/2003	2360	6.91	7	117
484400002	APY - 13	558	30.0	7.41	550.59	7/10/2012	6003	7.32	5	90
494300007	APY - 14	461	42.0	18.41	442.59	7/10/2012	11570	6.7	5	123
484400003	APY - 15	536	30.0	8.10	527.90	8/10/2012	12650	7.12	4	126
474400010	APY - 16	543	54.0	10.80	532.20	8/10/2012	2755	6.9	6	156
474500096	APY - 17	637	36.8	18.52	618.48	18/04/2010	1500	7.3	7	160
514500084	APY - 18	687	34.5	13.86	673.14	17/04/2010	2065	7.06	5	8.7
514500109	APY - 19	690	55.0	14.27	675.73	17/04/2010	1447	7.04	6	86.8
524400021	APY - 20	576	21.0	8.33	567.67	17/05/2003	1690	7.32	5	80
554400101	APY - 21	438	68.0	14.59	423.41	4/05/2008	1825	5.8	5	65

Hydrochemistry

Lower chloride concentrations (26–360 mg L⁻¹) are observed for groundwater in the fractured rock aquifers of the Musgrave and Mann Ranges in the northern part of the APY Lands (Figure 28) compared to those in the central part of the APY Lands where palaeovalleys are covered by the Great Victorian Desert (Table 8). The range in values is similar to that for the earlier APY Lands study and for the relatively fresh near stream samples in the Finke River and Ti Tree Basin areas. The groundwater chloride concentrations for areas south of the Ranges are on average an order of magnitude greater (390–3500 mg L⁻¹) (Table 8)(Figure 28). The spatial distribution and changes in hydrochemistry throughout the APY lands are discussed further on in the report. The values observed in this study are similar to that observed for groundwater away from rivers and creeks in previous studies and are similar to those observed in the Finke River study area where river recharge is thought to occur. The remaining major ion data is plotted in the Piper diagram (Figure 32) showing hydrochemical evolution for data from this project evolving from Calcium, Magnesium, Bicarbonate type waters to Sodium Chloride type waters. This is consistent with previous groundwater studies conducted in central Australia.

Table 8. General chemistry and major ion composition.

Unit Number	Sample ID	Lab pH	Lab E.C. uS cm ⁻¹	Total Alkalinity meq L ⁻¹	Br ⁻ mg L ⁻¹	NO ₃ ⁻ mg L ⁻¹	Cl ⁻ mg L ⁻¹	SO ₄ ⁼ mg L ⁻¹	Ca mg L ⁻¹	K mg L ⁻¹	Mg mg L ⁻¹	Na mg L ⁻¹	Si mg L ⁻¹
534500079	APY - 1	8.0	616	5.2	0.20	21	26	22	44.3	4.76	30.2	40.8	23.5
534500080	APY - 2	8.0	689	5.4	0.31	16	46	27	42.1	3.83	32.8	54	20.7
524300010	APY - 3	7.8	5045	3.8	6.0	140	1200	630	95.7	104	119	676	30.8
534400031	APY - 4	7.9	2207	4.6	3.5	44	490	150	54.2	22.9	49.5	273	30.6
534400047	APY - 5	7.9	1923	4.9	2.7	41	400	130	51.6	16.7	38.8	241	31.1
534500033	APY - 6	7.7	1050	7.4	0.6	2.2	91	74	46	0.849	30.7	131	28.8
534500084	APY - 7	7.8	1166	6.4	0.9	6.7	150	83	59.5	0.934	37.6	123	29.3
534500068	APY - 8	7.9	694	4.9	0.4	30	45	36	38.2	2.9	31.1	59.6	31.7
534500120	APY - 9	7.9	806	6.0	0.43	6.1	60	44	42.6	1.62	28.4	88.5	27.2
534500024	APY - 10	7.8	1260	7.5	0.8	3.2	140	110	53.7	2.1	39.4	153	27.9
514300006	APY - 11	7.5	2365	2.6	3.1	86	550	210	64.7	49.1	53.3	271	28
484300012	APY - 12	7.6	2216	3.9	2.3	56	460	240	53.5	46.3	56.6	248	29.5
484400002	APY - 13	7.8	5590	7.5	6.1	71	1400	680	74.7	124	107	813	29.6
494300007	APY - 14	7.3	11330	5.0	16	71	3300	1500	316	154	350	1280	18.6
484400003	APY - 15	7.7	12640	8.2	17	110	3500	1600	121	384	236	1770	22.1
474400010	APY - 16	7.6	2600	6.0	2.9	99	520	300	105	43.4	71.6	244	33
474500096	APY - 17	8.0	1395	7.4	1.3	41	200	79	20.6	3.91	94.6	104	23.8
514500084	APY - 18	7.6	1928	6.7	2.5	40	360	160	97.9	3.95	62.7	183	21.6
514500109	APY - 19	7.8	1368	6.9	1.4	20	200	94	83.9	2	54.3	112	24.2
524400021	APY - 20	7.7	1567	7.5	1.4	18	220	130	45.7	6.18	33.7	223	24.6
554400101	APY - 21	6.7	1671	1.5	1.9	0.7	390	230	55.7	14.3	46.9	171	5.16

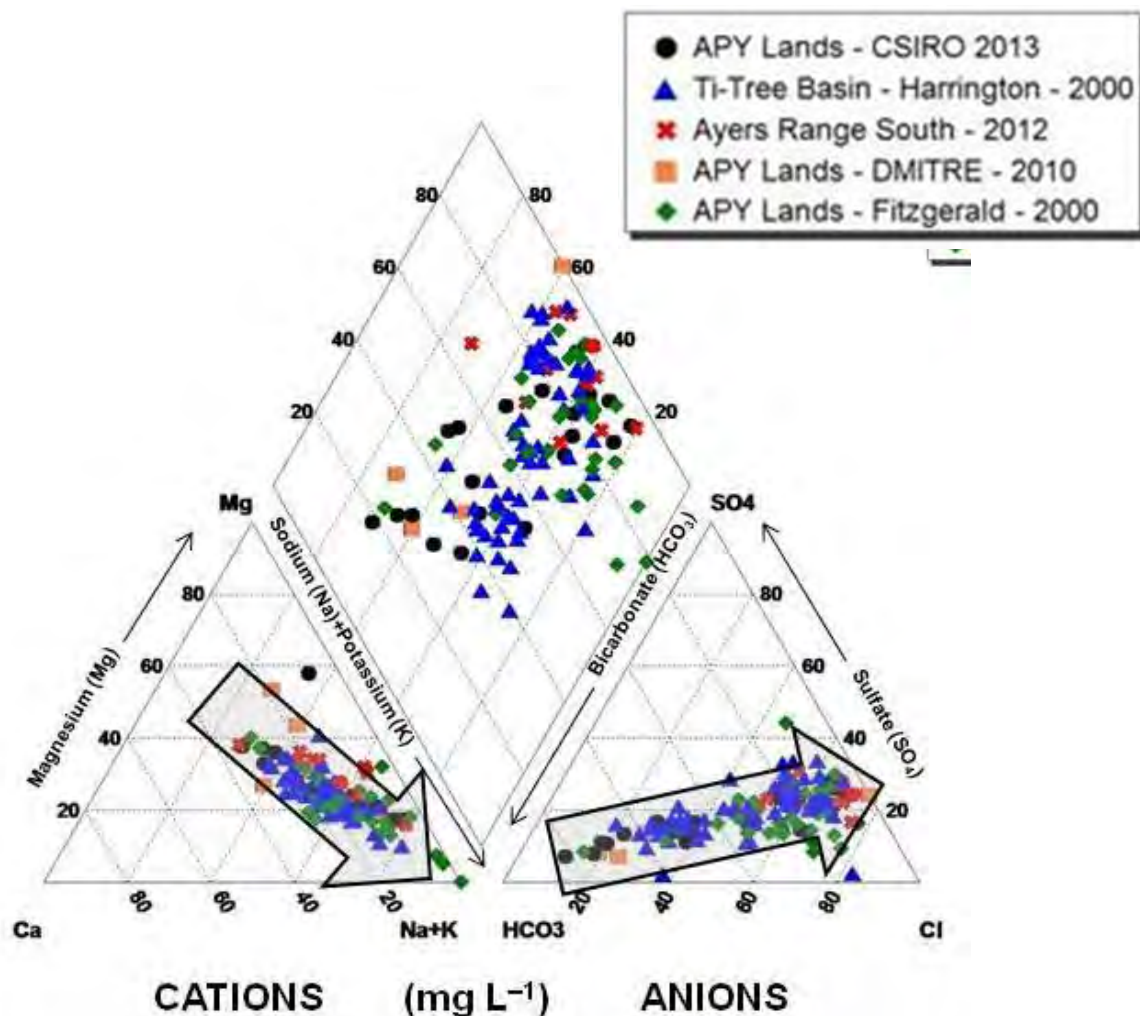


Figure 32. Piper plot illustrating the major ion composition of groundwater analysed for previous studies in central Australia and groundwater samples analysed in this study in the APY Lands.

Carbon isotopes

¹⁴C compositions for groundwater samples collected in this study (Table 9 and Figure 33) ranged from 31.9 to 114.5 pMC. Eight of the eleven groundwater samples from the northern sites were >100 pMC, consistent with post-bomb recharge taking place (i.e. a significant component of recharge has taken place since the above ground atomic bomb testing in the mid 1950s). The remaining three northern sites had ¹⁴C compositions between 76.5 and 93.5 pMC. The southern sites in the arc from Kuytjanu (APY-16) in the west to Amata (APY-18 and 19) in the east have ¹⁴C compositions 42.6 to 67.8 pMC while the eastern most “southern” site at Indulkana (APY-21) has the lowest ¹⁴C composition of 31.9 pMC.

Table 9. Stable isotope and carbon isotope data.

Unit Number	Sample ID	$\delta^{18}\text{O}$ ‰ VSMOW	δD ‰ VSMOW	$\delta^{13}\text{C}$ ‰ PDB	^{14}C pMC	Cl^- mg L^{-1}	TDS mg L^{-1}
534500079	APY - 1	-8.39	-61.2	-9.5	108.3	26	531
534500080	APY - 2	-8.70	-62.5	-10.1	107.7	46	574
524300010	APY - 3	-5.05	-39.4	–	43.4	1200	3235
534400031	APY - 4	-5.74	-43.2	-7.7	61.2	490	1401
534400047	APY - 5	-5.93	-42.2	-7.9	59.7	400	1249
534500033	APY - 6	-8.97	-64.6	-12.9	112.0	91	855
534500084	APY - 7	-8.99	-65.5	-12.8	114.5	150	881
534500068	APY - 8	-8.62	-64.4	-11.5	106.5	45	573
534500120	APY - 9	-8.24	-58.5	-10.9	105.9	60	666
534500024	APY - 10	-8.61	-60.4	-12.3	111.3	140	985
514300006	APY - 11	-5.29	-40.0	-8.4	56.4	550	1475
484300012	APY - 12	-5.12	-37.3	-9.4	57.3	460	1430
484400002	APY - 13	-4.94	-38.2	-9.1	65.3	1400	3763
494300007	APY - 14	-5.29	-40.1	-7.9	42.6	3300	7308
484400003	APY - 15	-5.36	-40.3	–	67.9	3500	8258
474400010	APY - 16	-5.01	-39.2	–	61.8	520	1782
474500096	APY - 17	-6.22	-41.7	–	76.5	200	1018
514500084	APY - 18	-6.40	-47.2	–	93.5	360	1339
514500109	APY - 19	-6.59	-47.2	-10.1	101.9	200	1011
524400021	APY - 20	-7.46	-50.3	-9.8	86.9	220	1159
554400101	APY - 21	-7.02	-45.4	–	31.9	390	1008

Only 15 of the 21 groundwater samples collected produced sufficient CO_2 for an accurate $\delta^{13}\text{C}$ analysis (Table 9 and Figure 33). The range in $\delta^{13}\text{C}$ composition for the groundwater at the northern sites ranges from -9.5 to -12.8 ‰ PDB with that at the southern sites, slightly enriched (-7.7 to -9.4 ‰ PDB). The range in $\delta^{13}\text{C}$ compositions for this current study is similar to that from previous studies with more “modern” groundwater (higher values for ^{14}C) being slightly depleted in $\delta^{13}\text{C}$ composition compared to those of “older” groundwater.

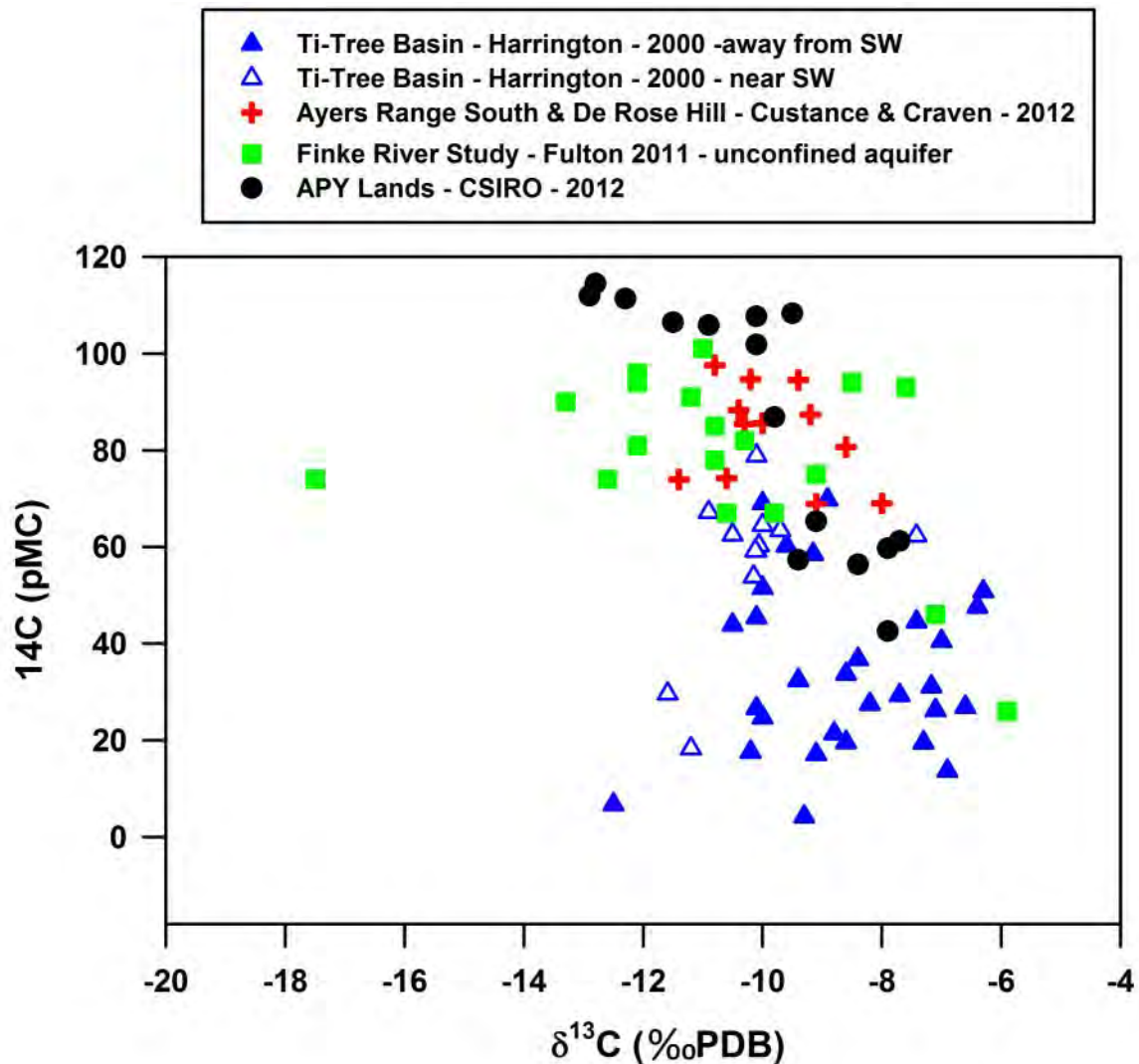


Figure 33. Relationship between measured $\delta^{13}\text{C}$ and ^{14}C for groundwater analysed from previous studies in Central Australia as well as groundwater analysed in this study in the APY Lands.

Stable isotopes of water

The seven groundwater samples with the most modern carbon-14 composition ($^{14}\text{C} > 105.9$ pMC) also have the most depleted $\delta^2\text{H}$ and $\delta^{18}\text{O}$ signature (Figure 34 and Figure 35). Likewise, the groundwater samples with the “oldest” carbon-14 composition also have the most enriched $\delta^2\text{H}$ and $\delta^{18}\text{O}$ signature. Also shown in Figure 35 is the LMWL for Alice Springs and the isotopic composition of different monthly amounts of rainfall at Alice Springs. However, thresholds for monthly amounts of rainfall rather than rainfall amount monthly intervals have been used. This approach, and the reasons for doing so, are described in the Discussion section. The red line indicates an evaporation line of $\delta^2\text{H}$ vs $\delta^{18}\text{O}$ with a slope of 5 extending from the LMWL (at monthly rainfall threshold $R > 80$ mm yr^{-1}).

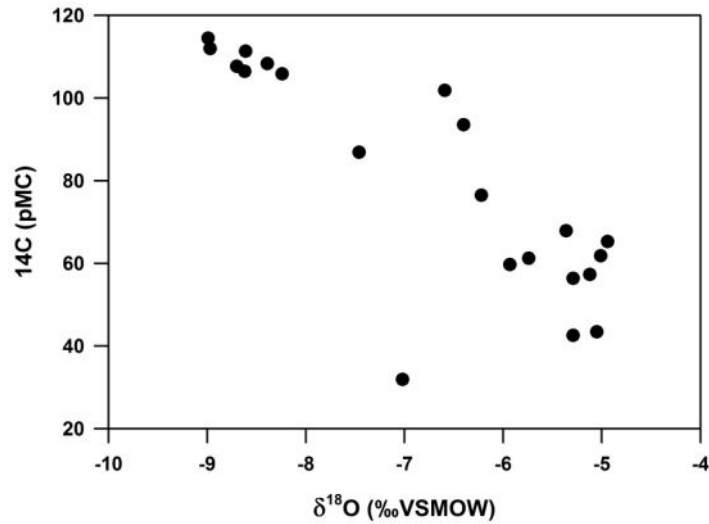


Figure 34. Relationship between measured ^{14}C and $\delta^{18}\text{O}$ for groundwater in this study.

The APY Lands groundwater samples with the most depleted $\delta^2\text{H}$ and $\delta^{18}\text{O}$ signature plot between the Finke River unconfined aquifer and the Ti Tree Basin near river groundwater samples. The APY Lands with the more enriched signature (central area) plot in a range consistent with the previous APY Lands/ARS and DRH groundwater samples.

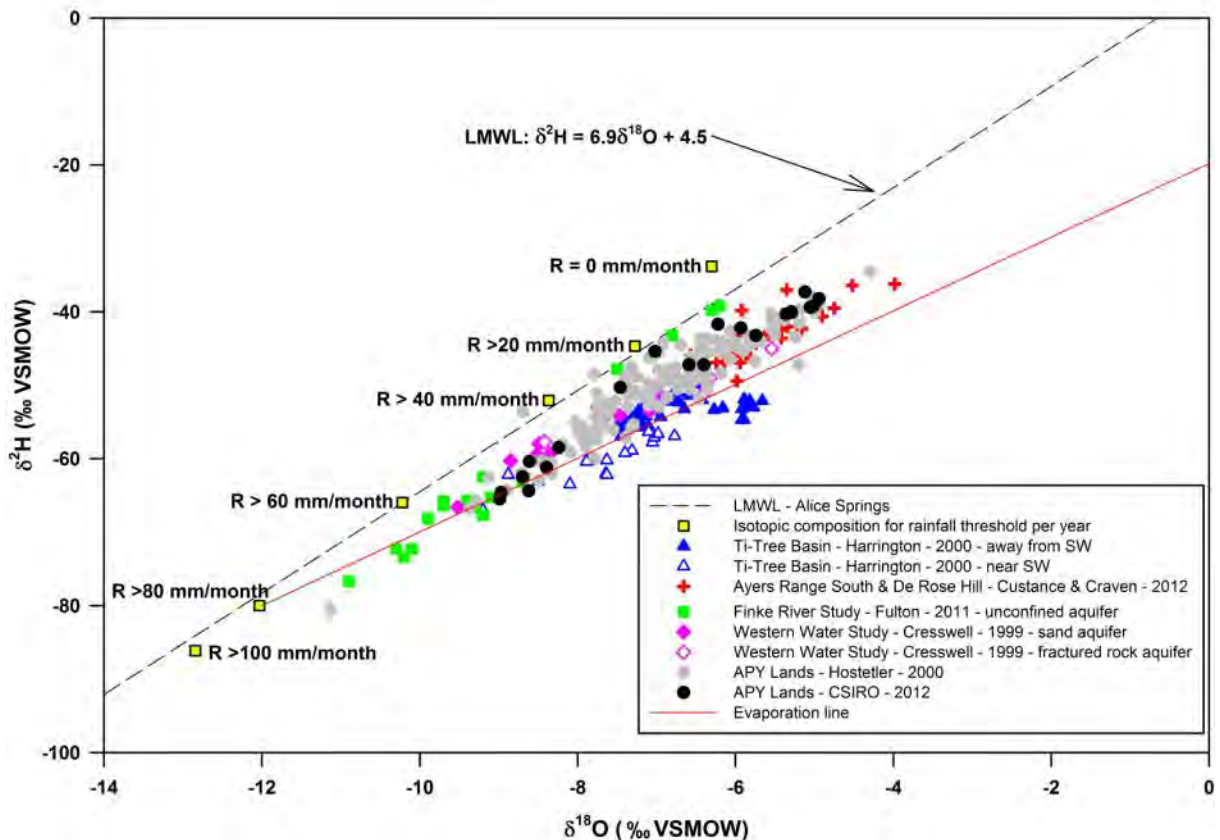


Figure 35. $\delta^2\text{H}$ and $\delta^{18}\text{O}$ results for current study compared to previous studies in surrounding areas. Note that the isotopic composition for monthly rainfall thresholds are shown on the LMWL.

Anthropogenic SF₆ and CFC analyses

CFC and SF₆ analysis of groundwater potentially provides a method for determining the mean residence time of groundwater that has recharged the aquifer since 1960. Use of the methods rely on the fact that concentrations of CFC and SF₆ have increased in the atmosphere since 1960 as their use in refrigeration (for CFC) and electrical insulation (for SF₆) also increased, and that their atmospheric concentrations from 1960 to present are well known. Atmospheric concentrations of CFCs reached their peak in the southern hemisphere 10-15 years ago and are now declining. This makes estimation of apparent groundwater ages over the past 20 or so years ambiguous. SF₆ on the other hand continues to rise exponentially and has supplanted CFCs as the age tracer of choice since the mid 1990s. For this reason, all samples were initially analysed for SF₆ concentration and most of the samples collected for CFC analysis were archived without analysis.

There is a very large range in the SF₆ concentrations in the groundwater (0.30 to 10.17 fmol L⁻¹;

Table 10). Concentrations below about 0.2 fmol L^{-1} are considered background for the SF_6 system and concentrations around $3\text{-}6 \text{ fmol L}^{-1}$ are considered modern (depending on a range of factors such as recharge temperature, recharge surface elevation and amounts of excess air entrained during recharge events). By using the ^{20}Ne and ^{40}Ar analyses, we are also able to estimate what is termed excess air in the groundwater samples. Excess air is the amount of "air" (usually ^{20}Ne) in the sample in excess of what is expected at the recharge temperature and tends to be greater when recharge takes place in large events rather than in events evenly distributed. Hence, episodic recharge tends to have high values for excess air.

What is clear from the SF_6 results is that there are groundwater samples in the area that are far in excess of maximum expected values for modern recharge and hence there must be another source of SF_6 leading to these high values. One possible source is upwelling of SF_6 from underlying rocks and or the mantle. If this is the case, one would expect to see similarly high values of other dissolved gases such as ^4He . This does appear to be the case for at least the well samples with the highest ^4He results (APY-14 and APY-15). These wells have ^4He concentrations in excess of $6 \times 10^{-8} \text{ ccSTP g}^{-1}$ (

Table 10) and SF6 concentrations of 10.17 and 6.86 fmol L⁻¹ respectively. However, there are other wells (e.g. APY-10 and APY-12) where this does not appear to be the case.

Table 10. Environmental tracer SF₆, CFC and noble gas analysis.

Unit Number	Location	Sample ID	SF ₆ fmol L ⁻¹	CFC-11 pg kg ⁻¹	CFC-12 pg kg ⁻¹	He-4 cc g ⁻¹ @ STP	Ne-20 cc g ⁻¹ @ STP	Ar-40 cc g ⁻¹ @ STP	Ae cc g ⁻¹ @ STP
534500079	Umawa	APY - 1	1.55	–	–	6.01E-08	2.23E-07	5.56E-04	5.33E-03
534500080	Umawa	APY - 2	1.01	–	–	7.28E-08	2.90E-07	4.18E-04	9.86E-03
524300010	Walalkara	APY - 3	0.65	–	–	3.49E-07	2.22E-07	5.19E-04	5.27E-03
534400031	Fregon	APY - 4	0.50	–	–	1.89E-07	2.17E-07	5.00E-04	4.97E-03
534400047	Fregon	APY - 5	0.41	–	–	1.30E-07	1.91E-07	3.17E-04	3.23E-03
534500033	Ernabella	APY - 6	2.40	–	–	8.53E-08	2.54E-07	8.41E-04	7.43E-03
534500084	Ernabella	APY - 7	2.22	–	–	8.05E-08	2.95E-07	5.35E-04	1.02E-02
534500068	Kenmore Park	APY - 8	3.51	258	154	5.37E-07	2.65E-07	3.95E-04	8.17E-03
534500120	Ernabella	APY - 9	0.97	–	–	2.53E-07	2.74E-07	7.60E-04	8.74E-03
534500024	Ernabella	APY - 10	8.54	221	164	8.93E-08	3.48E-07	8.25E-04	1.37E-02
514300006	Makari	APY - 11	3.97	35	21	2.06E-07	1.77E-07	3.04E-04	2.30E-03
484300012	Wataru	APY - 12	7.25	11	1	6.52E-07	2.00E-07	5.75E-04	3.80E-03
484400002	Wataru	APY - 13	1.61	–	–	5.79E-08	1.90E-07	6.20E-04	3.14E-03
494300007	Wataru/Iltur	APY - 14	10.17	47	29	6.86E-06	9.25E-07	1.23E-03	5.23E-02
484400003	Wataru/Kunytjanu	APY - 15	6.86	16	8	6.82E-06	2.15E-07	3.77E-04	4.81E-03
474400010	Kunytjanu	APY - 16	0.30	–	–	1.41E-07	1.86E-07	6.66E-04	2.86E-03
474500096	Pipalyatjara	APY - 17	0.63	–	–	1.38E-07	2.14E-07	3.85E-04	4.79E-03
514500084	Amata	APY - 18	0.47	–	–	6.15E-08	2.97E-07	7.31E-04	1.03E-02
514500109	Amata	APY - 19	0.89	–	–	8.53E-08	3.65E-07	8.14E-04	1.49E-02
524400021	Watinuma	APY - 20	1.79	–	–	1.22E-07	2.75E-07	8.12E-04	8.87E-03
554400101	Indulkana	APY - 21	0.32	–	–	4.46E-07	2.39E-07	4.62E-04	6.41E-03

* Excess air (Ae) was calculated using excess Ne-20 and assuming a recharge temperature of 20°C.

Given the potential problems in using some, if not all, SF₆ results, it was decided to analyse a 6 sample subset of the groundwater samples (2 modern groundwater samples with ¹⁴C >100 pMC and 4 older groundwater samples with ¹⁴C compositions between ~40 and 70 pMC) for CFC11 and CFC12. CFC results for modern groundwater samples (APY-8 and APY-11) range from 205 to 261 pg kg⁻¹ for CFC11 and from 145 to 180 pg kg⁻¹ for CFC12 (

Table 10). CFC results for the older groundwater samples ranged from below limit of detection levels (<25 pg kg⁻¹ for CFC11 and <20 pg kg⁻¹ for CFC12) for APY-12 and APY-15 to slightly above detection levels for APY-11 and APY-14. Detection level is considered to be <25 pg kg⁻¹ for CFC11 and <20 pg kg⁻¹ for CFC12.

Noble gas analyses

The noble gases are the elements ⁴He, ⁴⁰Ar, ²⁰Ne, krypton (Kr), xenon (Xe) and radon (²²²Rn). Because they form no compounds with other elements, their inert nature makes them excellent candidates as groundwater tracers. There are fundamentally two ways in which noble gases are used in groundwater studies. ⁴He is produced by decay of uranium and thorium in aquifer minerals and accumulates in groundwater over time. Its concentration in “old” groundwater is proportional to groundwater age. In certain circumstances, the release of ⁴He into much younger groundwater from minerals in recent geologic sediment may be used to estimate groundwater ages in the 100-10,000 year time scale. The atmospheric noble gases (²⁰Ne, ⁴⁰Ar, Kr, Xe) dissolve in water in the unsaturated zone and record the prevailing conditions just above the water table. They are most frequently used to estimate recharge temperatures that can be used to confirm the existence of fossil groundwater recharged under different climatic conditions of long ago. They can also be used to understand episodic recharge processes by way of estimating excess air in the groundwater. Excess air arises when there is a large amount of recharge over a short timeframe.

The noble gas analysis unit at CSIRO allows measurement for the lighter noble gases, ⁴He, ²⁰Ne and ⁴⁰Ar but not Kr nor Xe. Unfortunately, this prevents estimation of recharge temperature. However, the presence of high ⁴He in groundwater, compared to the equivalent concentration in modern recharge, can be used to indicate a component of old water in the groundwater or the presence of an external flux of ⁴He from underlying rocks or the mantle. Measured values of ²⁰Ne and /or ⁴⁰Ar also allows estimation of excess air, and this is a required input when calculating SF₆ groundwater “ages” from SF₆ analyses.

Results for ⁴He, ²⁰Ne and ⁴⁰Ar analyses on the APY Lands groundwater samples are given in Table 10. All of the groundwater samples except for the sample collected at APY-14 have Ne concentrations ranging from 1.77 to 3.65 x 10⁻⁷ ccSTP g⁻¹ and Ar concentrations ranging from ranging 3.17 to 8.25 x 10⁻⁴ ccSTP g⁻¹. The sample collected at APY-14 is significantly greater (²⁰Ne = 9.25 x 10⁻⁷ ccSTP g⁻¹ and ⁴⁰Ar = 1.2 x 10⁻³ ccSTP g⁻¹). The range in concentrations of ⁴He in groundwater is considerable, greater than two orders of magnitude (from 6.01 x 10⁻⁸ to 6.86 x 10⁻⁶ ccSTP g⁻¹) with the ⁴He concentrations at sites APY-14 and APY-15 significantly greater than those at the other sites.

When we consider excess air, excluding that at APY-14 excess air values in this study are in the range from about 0.003 -0.015 ccSTP g⁻¹ (about 30 to 150 % in excess of equilibration at 20 °C). At APY-14, the excess air was calculated at 52.3 ccSTP g⁻¹, a huge 500% in excess of equilibration. An immediate response to this would be to suggest a problem during sampling with air incorporated in the sample. However, with a similar anomalously high value measured for SF₆ on a sample collected separately in a different bottle, it is not obvious that sampling was a problem.

Spatial distribution in environmental tracer concentrations

Spatial distributions for the concentrations of the environmental tracers, ^{14}C , $\delta^2\text{H}$, Cl , ^4He , and SF_6 are shown against a background DEM map in, Figure 36, Figure 38, Figure 38, Figure 39 and Figure 40 respectively. Mountain Ranges are shown in white in the backing DEM. The spatial distribution for $\delta^{18}\text{O}$ is very similar to that for $\delta^2\text{H}$ and is not shown. Only 6 samples were analysed for CFC 11 and CFC12 and these are also not shown. ^{14}C , Cl and $\delta^2\text{H}$ concentrations correlate strongly with surface elevation with the higher elevations having a modern ^{14}C composition, a depleted $\delta^2\text{H}$ composition and low chloride concentrations (Figure 36,

Figure 37, and Figure 38).

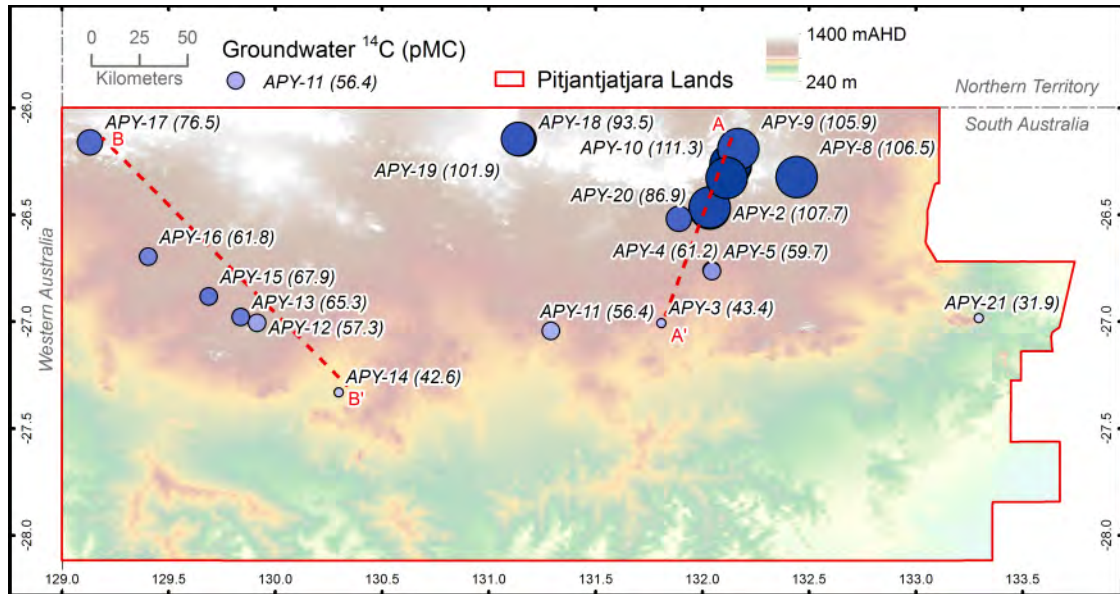


Figure 36. Spatial distribution of measured concentrations of ¹⁴C for groundwater wells sampled throughout the APY Lands, dashed red lines indicate hydrochemistry transects.

This is also indicated from the plots of ¹⁴C vs δ¹⁸O (Figure 34) and ground surface elevation vs ¹⁴C (Figure 46). Most of the modern groundwater samples in the valleys of the Musgrave and Mann Ranges (¹⁴C >100 pMC) also have a depleted δ¹⁸O signature (δ¹⁸O ≈ -8.4 to -9.0 ‰) compared to those in the southern/eastern most part of the study (¹⁴C ≈ 40 to 60 pMC; δ¹⁸O ≈ -4.9 to -6.0 ‰). There is a linear relationship between these possible end member compositions. Although not shown, a similar correlation exists for ¹⁴C vs δ²H. The only well that does not fit with this correlation, APY-21, is located close to the intersection of the Musgrave Province with the Great Artesian Basin and the Officer Basin.

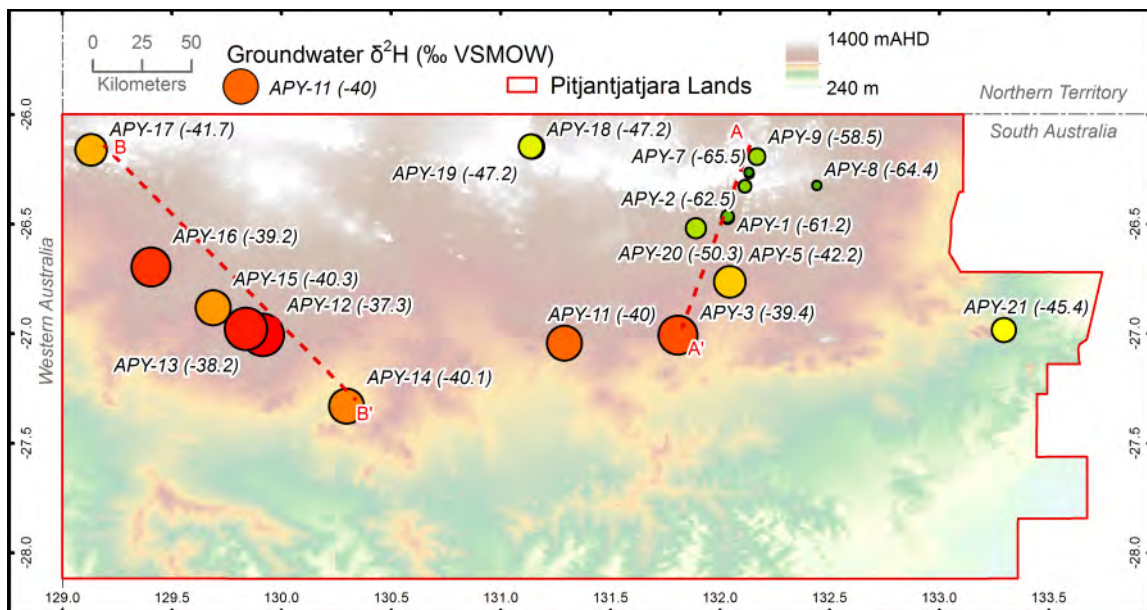


Figure 37. Spatial distribution of measured concentrations of δ²H for groundwater wells sampled throughout the APY Lands, dashed red lines indicate hydrochemistry transects.

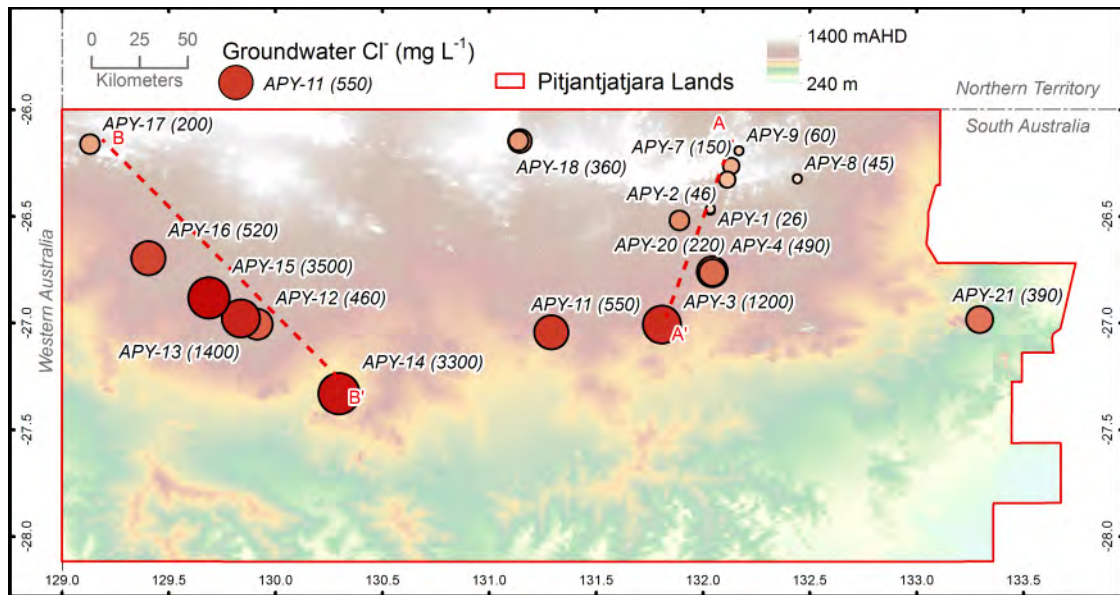


Figure 38. Spatial distribution of measured concentrations of Cl for groundwater wells sampled throughout the APY Lands, dashed red lines indicate hydrochemistry transects.

A similar spatial distribution is observed for ⁴He concentrations in the groundwater (Figure 39) although there are notable exceptions. Groundwater at the APY8 and APY9 sites have higher ⁴He concentrations than expected for modern groundwater while the ⁴He concentration at APY-13 is the second lowest measured in the study.

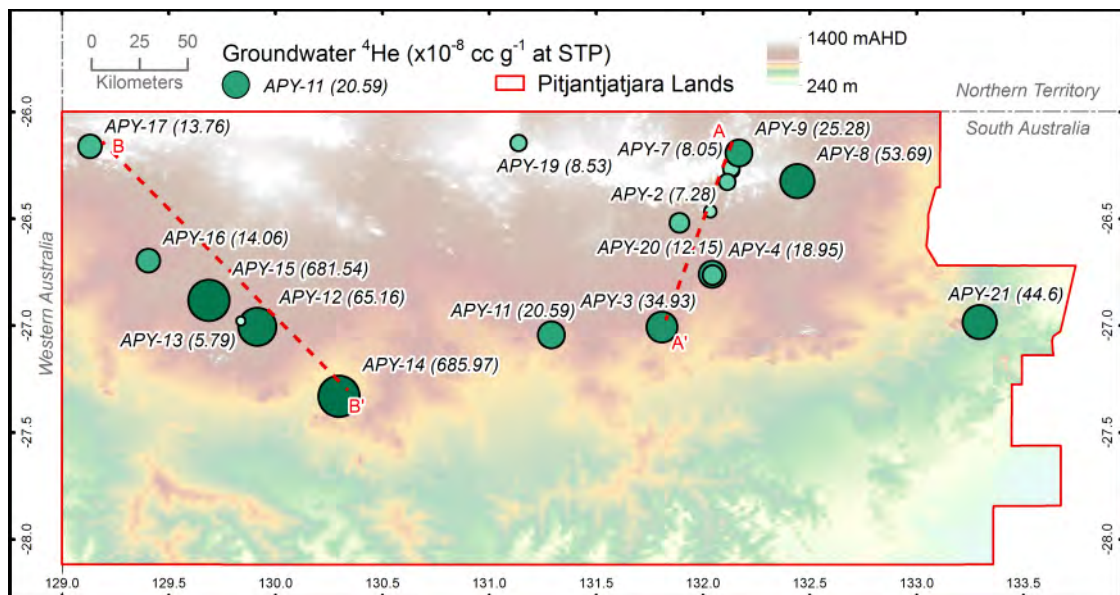


Figure 39. Spatial distribution of measured concentrations of ⁴He for groundwater wells sampled throughout the APY Lands, dashed red lines indicate hydrochemistry transects.

SF₆ a tracer for modern groundwater (Figure 40), should show higher concentrations in areas where ¹⁴C is modern (>100 pMC) and background or near background concentrations elsewhere. However, this is not the case with high concentrations to the south of the study area where ¹⁴C are significantly less than 100 pMC and where surface elevations are lower.

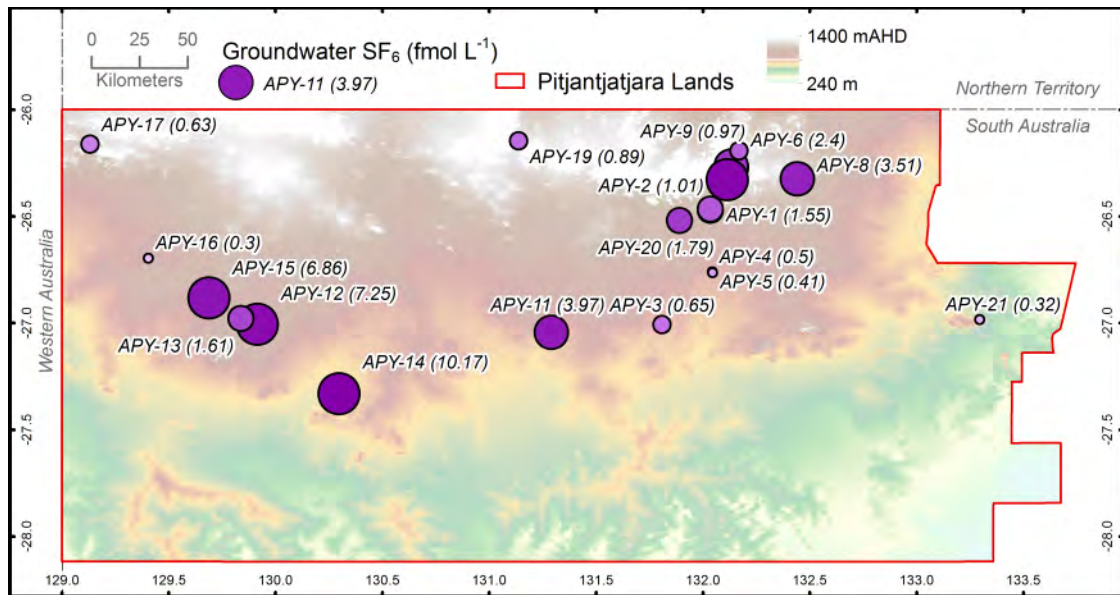


Figure 40. Spatial distribution of measured concentrations of SF₆ for groundwater wells sampled throughout the APY Lands.

Changes in hydrochemistry along inferred flow paths (transects).

Changes in [Cl], ¹⁴C, δ²H and ⁴He concentration are shown in groundwater hydrochemistry transects (red dashed lines) A to A' and B to B' (Figure 36,

Figure 37, Figure 38 and Figure 39). These transects were chosen based on the spatial distribution of wells sampled and the potential regional groundwater flow direction as indicated in Varma (2012). Each transect is in the vicinity of a number of sampled wells and in general trends north to south. Transect A commences near Ernabella at well APY-7 in the Musgrave Range (elevation ~700 m AHD) and continues approximately 100 km south along the 132 °E parallel longitude finishing at well APY-3 (elevation ~ 450 m AHD). This is approximately in the direction of flow which tends to follow topography (Varma, 2012). Transect B commences in the township of Pipalyatjara at well APY-17 (elevation ~650 m AHD) and continues southeast approximately 180 km passing through the homelands of Kuntjanu and Wataru finishing at APY-14 (elevation ~450 m AHD), ~13 km north-west of the Iltur homeland. There is currently insufficient groundwater level data to suggest whether or not this is along a flow line. However, the fact that a small hill, Mount Lindsay, is located about halfway along this transect would suggest that this transect does not follow a groundwater flow path.

For transect A (Figure 41) all of the measured tracers exhibit a consistent trend along the flow path consistent with modern recharge in the region of the Musgrave Ranges and progressive addition of diffuse recharge away from the Ranges. The majority of wells along this flow path are screened to the regolith (fractured granite) of the Precambrian basement rock.

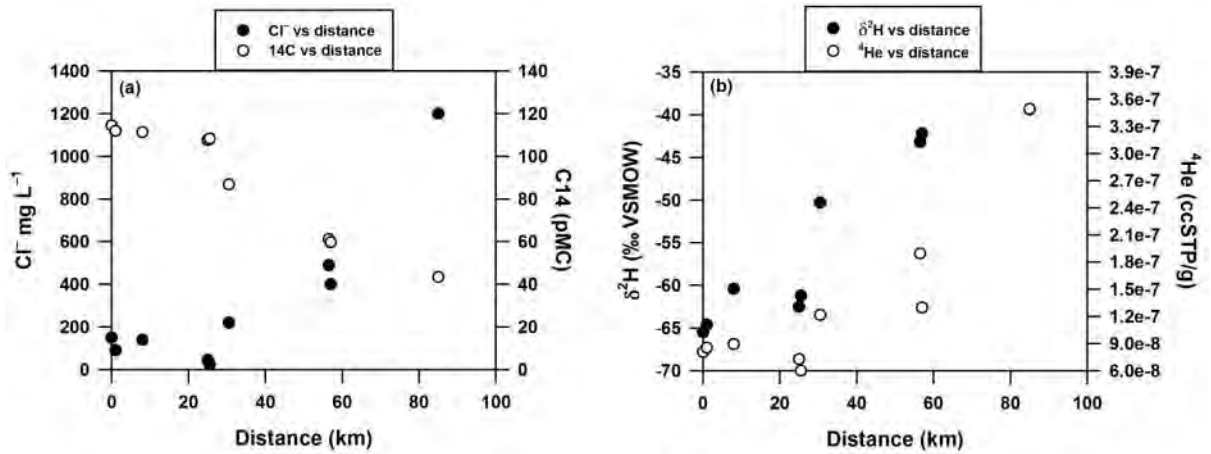


Figure 41. Transect A, concentration of environmental tracers, Cl⁻, ¹⁴C, δ²H and ⁴He versus distance along a potential groundwater flow path.

For transect B (Figure 42) [Cl] and ¹⁴C have a reasonably consistent trend along the inferred groundwater flow path, starting at values consistent with modern recharge. However the general trend in data for transect B relative to transect A exhibits some variability. Possible reasons for this include lower hydraulic conductivities associated with the calcrete and clay the majority of wells are screened too. Furthermore the inconsistent downward topographic gradient along this groundwater flow path due to the presence of Mount Lindsay has implications for the hydraulic gradient and a lower groundwater flow rate.

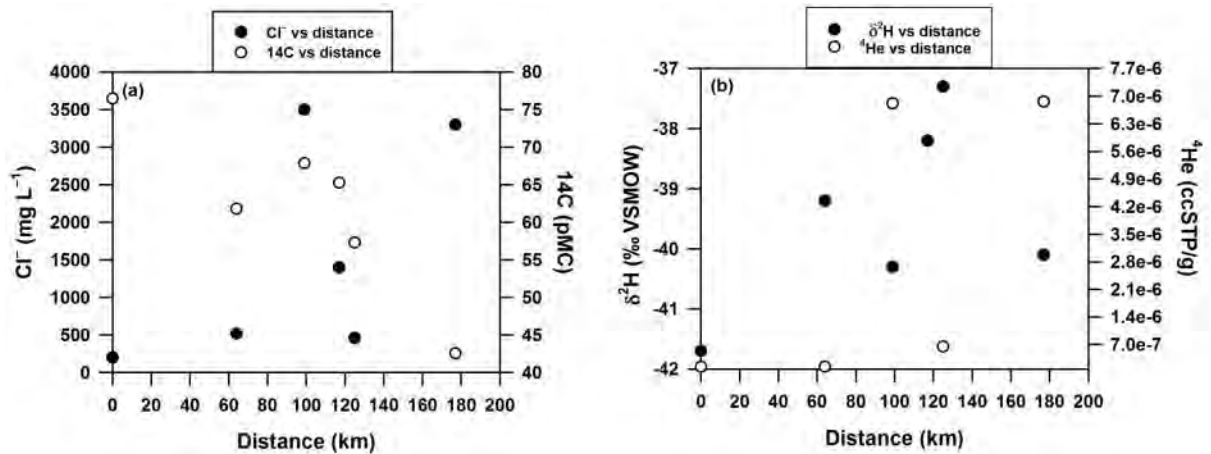


Figure 42. Transect B, concentration of environmental tracers, Cl⁻, ¹⁴C, δ²H and ⁴He versus distance along a potential groundwater flow path.

Discussion

Mean residence time of groundwater

In this study ^{14}C , ^4He , SF_6 , CFC11 and CFC12 have been measured on groundwater samples. When combined, these environmental tracers potentially provide dating for groundwater from modern up to 9200 years BP.

As discussed earlier in this report, correction of ^{14}C data for water-rock interaction using any of the hydrochemical and/or isotopic correction methods has not been attempted in this study. These types of corrections require detailed knowledge of aquifer properties and is something that requires further investigation in the APY lands. Hence, maximum or apparent ^{14}C ages have been determined for each site. The ages range from modern at eight sites to 9,200 years BP at the eastern most site, APY-21 (Table 11). Note however that such a simplistic approach assumes no groundwater mixing within the aquifer (piston flow scenario) as well as no water-rock interaction and such a scenario is highly unlikely.

Several of the sites have very high ^4He concentrations in the groundwater. No attempt has been made to estimate groundwater ages using the ^4He data. However, the ^4He concentrations are included in

Table 10 to compare trends with ages determined from the other tracers. At some of the sites with high ^4He concentrations, there are also inexplicably high SF_6 concentrations, suggesting either something in the groundwater affecting the SF_6 analysis or a source of SF_6 that is not anthropogenic. Hence, we have not used results from SF_6 analyses for estimation of groundwater age.

CFC analyses were undertaken at 6 sites (

Table 10). Assuming a recharge temperature of 20 °C (equal to the average of monthly maxima and minima temperatures at Ernabella) and again no groundwater mixing in the aquifer (piston flow scenario), this suggests CFC11 and CFC12 groundwater ages of 32 and 26 years respectively for groundwater at APY-8 and 34 and 25 years for groundwater at APY-10. If we assume that most recharge takes place during warmer months and use a slightly higher recharge temperature of 25°C, this suggests CFC11 and CFC12 groundwater ages of 27 and 22 years respectively for groundwater at APY-8 and 31 and 19 years for groundwater at APY-10. In most cases concentrations of CFC12 in groundwater are considered to be more reliable for determining apparent groundwater age than CFC11 because of the likelihood of CFC11 degradation in many groundwater systems. This being the case, the best estimate of mean residence time for groundwater at sites APY-8 and APY-10 is suggested to be about 20 years. The background, or near background levels at the sites APY-11, APY-12, APY-14 and APY-15 suggest much older groundwater ages, consistent with the results from ¹⁴C dating (Table 11).

Table 11. Apparent groundwater ages using CFC11, CFC12 and ¹⁴C.

Unit Number	Location	Sample ID	Apparent year of recharge			
			CFC11	CFC12	¹⁴ C	¹⁴ C error (± years)
534500079	Umawa	APY - 1	–	–	>MODERN	–
534500080	Umawa	APY - 2	–	–	>MODERN	–
524300010	Walalkara	APY - 3	–	–	6710	30
534400031	Fregon	APY - 4	–	–	3950	45
534400047	Fregon	APY - 5	–	–	4150	30
534500033	Ernabella	APY - 6	–	–	>MODERN	–
534500084	Ernabella	APY - 7	–	–	>MODERN	–
534500068	Kenmore Park	APY - 8	1985	1991	>MODERN	–
534500120	Ernabella	APY - 9	–	–	>MODERN	–
534500024	Ernabella	APY - 10	1982	1994	>MODERN	–
514300006	Makari	APY - 11	1966	1965	4610	30
484300012	Wataru	APY - 12	<1965	<1965	4480	25
484400002	Wataru	APY - 13	–	–	3430	25
494300007	Wataru/Iltur	APY - 14	1967	1968	6870	35
484400003	Wataru/Kunytjanu	APY - 15	<1965	<1965	3120	25
474400010	Kunytjanu	APY - 16	–	–	3870	25

474500096	Pipalyatjara	APY - 17	–	–	2160	30
514500084	Amata	APY - 18	–	–	540	25
514500109	Amata	APY - 19	–	–	>MODERN	–
524400021	Watinuma	APY - 20	–	–	1130	30
554400101	Indulkana	APY - 21	–	–	9190	30

New approach to interpreting stable isotope data in the arid regions of central Australia

Most of the previous studies in arid Central Australia with available $\delta^2\text{H}$ and $\delta^{18}\text{O}$ data have drawn a best fit line through the groundwater data and extrapolated it to an intersection point on the Alice Springs LMWL (IAEA/WMO (2006)). The intersection point was then compared to the mean isotopic composition for monthly rainfalls of 0-50 mm per month, 50-100 mm per month, 100-150 mm per month, etc. Using this approach, the authors then suggested that recharge in the Ti Tree Basin and the Finke River study area takes place when there is 150-200 mm per month rainfall, and recharge in the ARS and DRH takes place when there is 100-150 mm per month rainfall.

Our approach is slightly different and, we believe, more accurately fits with a conceptual model for intermittent recharge in arid zones. Instead of determining the stable isotope composition for different monthly rainfall amounts (0-50, 50-100, 100-150, 150-200, >200 mm per month), we determine the stable isotope composition for monthly rainfalls in excess of a monthly threshold (all rainfall, rainfall >20, >40, >60, >80, >100 mm per month). The reason for this change is that using a threshold rainfall assumes that recharge takes place for all events equal to or greater than the threshold value. Using a rainfall interval approach ignores recharge originating from larger events and this is conceptually incorrect.

The other change in our approach is to assume that rainfall is evaporated prior to recharge and that the enrichment in isotopic composition as rain (or ponded water) evaporates proceeds on a $\Delta\delta^2\text{H}/\delta^{18}\text{O}$ slope of 5. This is different from previous studies where evaporation is assumed to proceed on the $\delta^2\text{H}$ vs $\delta^{18}\text{O}$ line of best fit slope for the isotopic composition of the groundwater samples (usually less than 5). A $\delta^2\text{H}$ vs $\delta^{18}\text{O}$ evaporating line of slope 5 can be obtained theoretically assuming that evaporation takes place from a surface water body in an area with an average relative humidity of 50% and with the amount of recharge equal to the amount of evaporation. Varying the ratio of recharge to evaporation and/or the relative humidity may change the slope slightly but the value of 5 is consistent with what is normally assumed for an evaporating surface water body.

Extrapolating from the $\delta^2\text{H}$ and $\delta^{18}\text{O}$ composition of the groundwater at a $\Delta\delta^2\text{H}/\delta^{18}\text{O}$ slope of 5 to the LMWL allows calculation of the rainfall “threshold” at each well site (R_{th}). The term threshold is used loosely here. Some recharge can, and most likely will, occur when monthly rainfalls are less than the threshold value. However, most of the recharge, by volume, is related to the threshold value.

The distance from the LMWL $\delta^2\text{H}$ and $\delta^{18}\text{O}$ composition at R_{th} and the $\delta^2\text{H}$ and $\delta^{18}\text{O}$ composition (ΔEvap) of the groundwater at each well is indicative of the amount of evaporation occurring before

recharge takes place. Note that ΔEvap is linearly related to deuterium deficit, a term often referred to in isotope hydrological studies. We prefer to use ΔEvap because, in vector form, this value suggests the extent of evaporation taking place along the evaporating line. However, it should be noted that neither deuterium deficit nor ΔEvap are linearly related to evaporation.

$\delta^2\text{H}$ and $\delta^{18}\text{O}$ composition for sites in the APY land for this study and for the previous study are shown in relation to the results for previous studies in arid central Australia (Figure 35). The groupings become more obvious if the $\delta^2\text{H}$ vs $\delta^{18}\text{O}$ displacement (ΔEvap) is plotted against R_{th} (Figure 43). The summary of previous studies in the arid regions of Central Australia presented earlier in this report indicated that the freshest groundwater is found near the Ranges in the APY Lands and near river samples in the Finke River study area and the Ti-Tree Basin. These also tend to have a similar $\delta^2\text{H}$ and $\delta^{18}\text{O}$ signature with a relatively low value for ΔEvap (2 to 4 ‰) but a relatively high value for R_{th} (as shown in blue ellipse in Figure 43). This would be consistent with a recharge mechanism where not only does a large amount of rain fall in a short time but also that most of the rain presents as recharge (ie low ratio of evaporation to recharge). The concentrating of rain from run-off in the Ranges of the APY Lands and rivers in the Finke River study area and Ti-Tree Basin would provide such a recharge mechanism.

The most enriched $\delta^2\text{H}$ and $\delta^{18}\text{O}$ groundwater signatures are found in areas south of the Ranges in the APY Lands and east of the Ranges in the ARS/DRH study areas. At these sites, ΔEvap values are similar to those in the Ranges (2 to 4 ‰) but the value for R_{th} is less (shown in red ellipse in Figure 43). These areas have more saline groundwater and the topography precludes large amounts of run-off to concentrate in recharge areas and have a $\delta^2\text{H}$ and $\delta^{18}\text{O}$ signature more consistent with diffuse recharge. The ΔEvap vs R_{th} signature for the “away from river” groundwater in the Ti-Tree Basin and the groundwater in the Western water study area (shown in green ellipse) is between that for high recharge areas and diffuse recharge areas and suggests mixing of groundwater with different recharge mechanisms.

This approach has assumed that the changes in $\delta^2\text{H}$ and $\delta^{18}\text{O}$ composition of rainfall, and hence groundwater, is due to the “amount (intensity)” effect and has not considered what is known as the “altitude” effect (Mazor, 1991). The altitude effect would result in depleted signature for rain falling on the Ranges but would be impossible to quantify without many years of measuring the isotopic composition of rainfall at a range of Central Australia sites. Siegenthaler and Oeschger, 1980 suggested that the $\delta^{18}\text{O}$ composition of rainfall decreases by about 0.25 ‰ for every 100 m rise in elevation but this was for studies in the Swiss mountains. A similar effect in the Ranges in the APY Lands would change $\delta^{18}\text{O}$ and $\delta^2\text{H}$ by approximately 1.0 and 8 ‰ respectively for groundwater collected in the northern part of the study area.

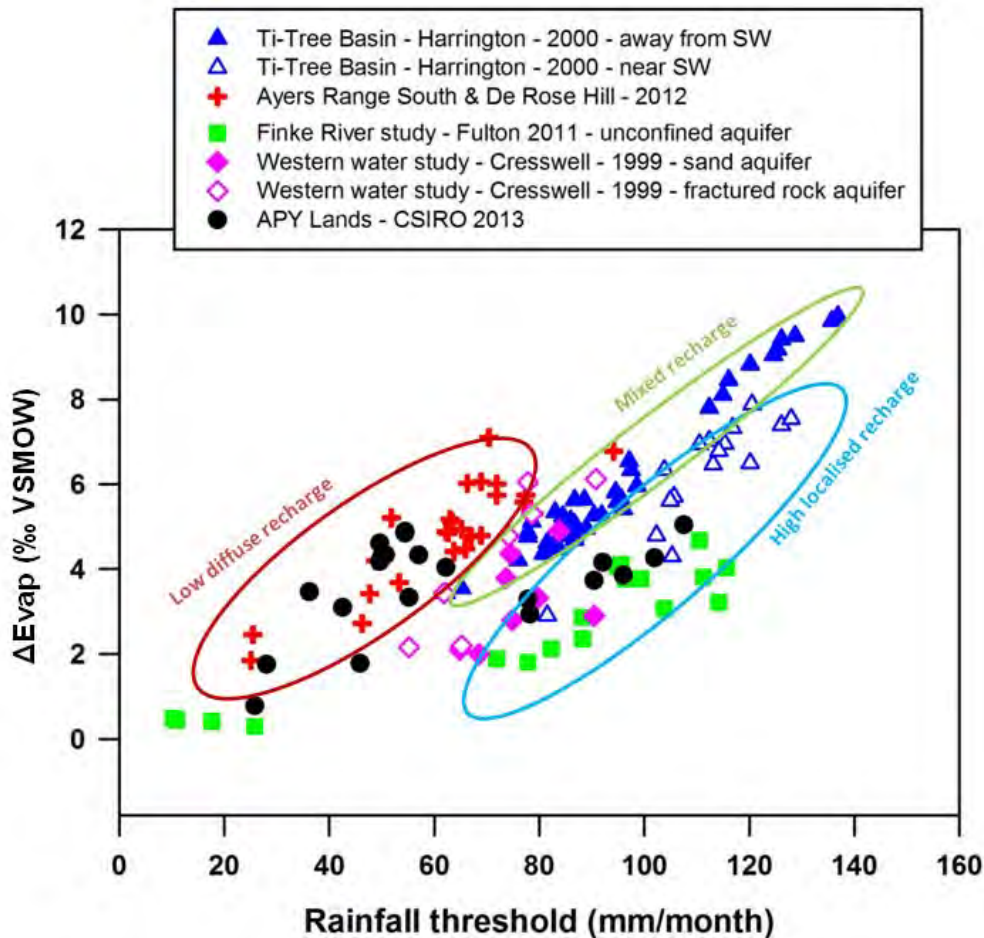


Figure 43. Plot of change in evaporative isotopic signature against rainfall threshold, the red ellipse represents low diffuse recharge, green represents mixed recharge mechanisms, and blue represents high localised recharge.

Temporal changes in groundwater level and $\delta^{18}\text{O}$, $\delta^2\text{H}$ and ^{14}C composition (1997-2012)

The 1997/1998 sampling trip was at the end of a decade of below average rainfall where the cumulative annual rainfall had decreased from slightly above the 120 year mean to a deviation of 350 mm below the mean (Figure 10). However, monthly rainfall amounts at Ernabella for the period from 1998-2012 are well above the average of 245 mm month⁻¹ including a few very wet months in 2011 (Figure 44, shown in blue). Also shown in Figure 44 are groundwater levels (shown in red) for wells located in the northern parts of the study area at (a) Pipalyatjara, (b) Amata, (c) Fregon, and (d) Ernabella respectively. While these plots no doubt reflect local changes in groundwater levels in the immediate areas what is unclear is the rate and frequency of groundwater pumping taking place at each location. Each community in the APY lands is supplied with groundwater from several wells in order to diversify supplies and provide redundancy in periods of dry weather and peak demand for water resources. AGT (2008) provides an in depth report on sustainability of water resources in the APY lands including data on water usage from individual production wells at 8 communities.

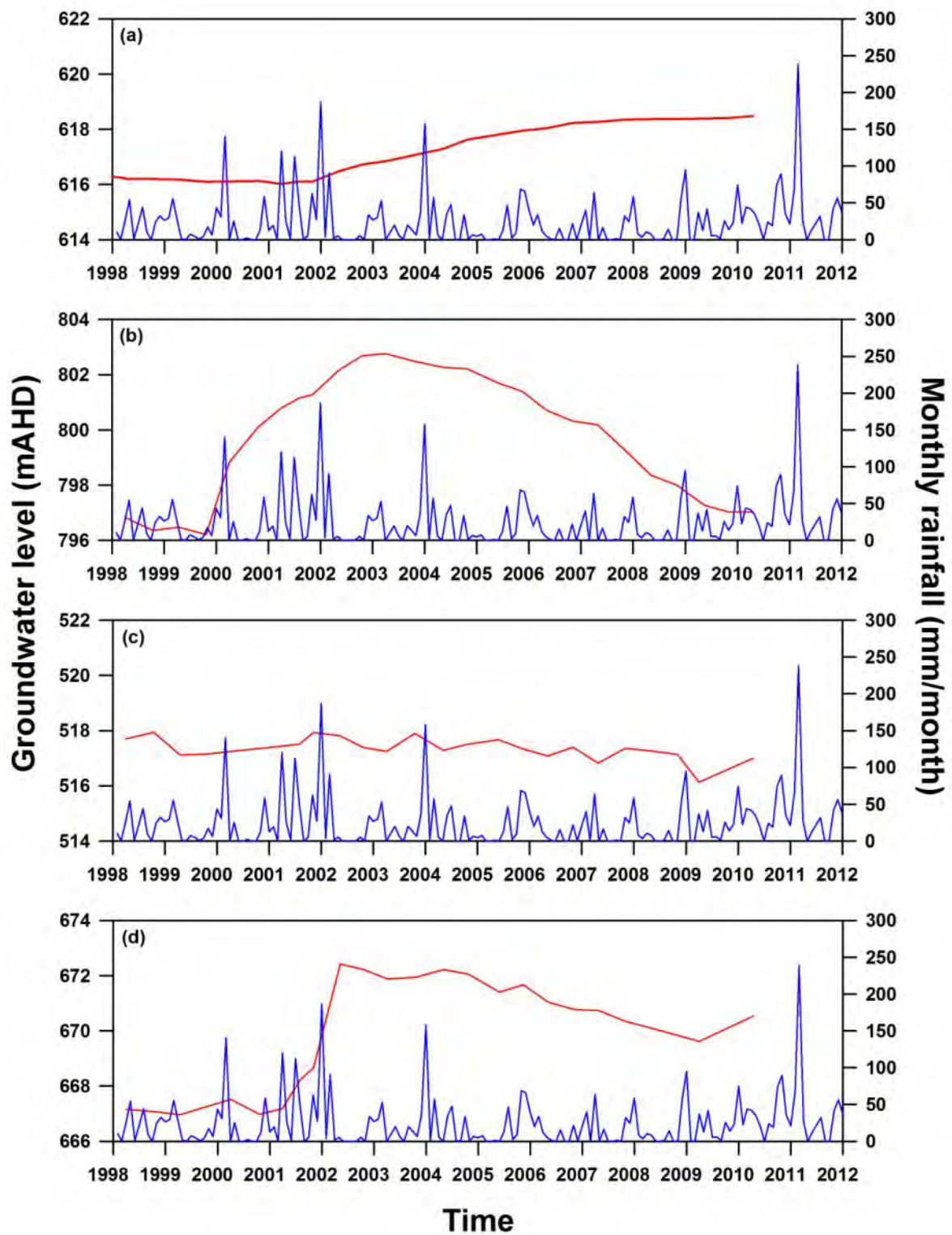


Figure 44. Plots of monthly rainfall at Ernabella versus mean monthly groundwater levels from selected groundwater production wells at (a) Pipalyatjara, (b) Amata, (c) Fregon and (d) Ernabella.

The first and only groundwater samples collected for environmental tracer analysis in the APY Lands prior to this study were collected in 1997/98 (Hostetler 2000; Dodds et al., 2001). Several of the wells were re-sampled in this project. This has allowed a comparison of $\delta^2\text{H}$ and $\delta^{18}\text{O}$ analyses for 11 of the same wells (Figure 45).

The 2012 samples are consistently depleted by up to 1.0 and 7 ‰ for $\delta^{18}\text{O}$ and $\delta^2\text{H}$ respectively relative to the 1997/98 samples in the northern part of the study area, while the isotopic composition for samples collected from wells in the southern section (Figure 28) show little consistent change. The samples for isotopic analysis in 1997/98 were collected at the end of a lengthy dry period when the cumulative deficit from mean rainfall at Ernabella was about 2000 mm. The samples collected in 2012 were collected after a reasonably wet period when the cumulative rainfall deficit at Ernabella had returned to near mean values. This also includes a very wet year (2011) when 700 mm of rainfall was recorded at Ernabella. The depleted signature of the samples collected in 2012 is consistent with recent recharge resulting from much higher intensity rainfall events, as discussed earlier. Little or no change in the $\delta^2\text{H}$ and $\delta^{18}\text{O}$ composition of the groundwater away from the Ranges is also consistent with a more sluggish system in this area with a much larger component of low rate diffuse recharge.

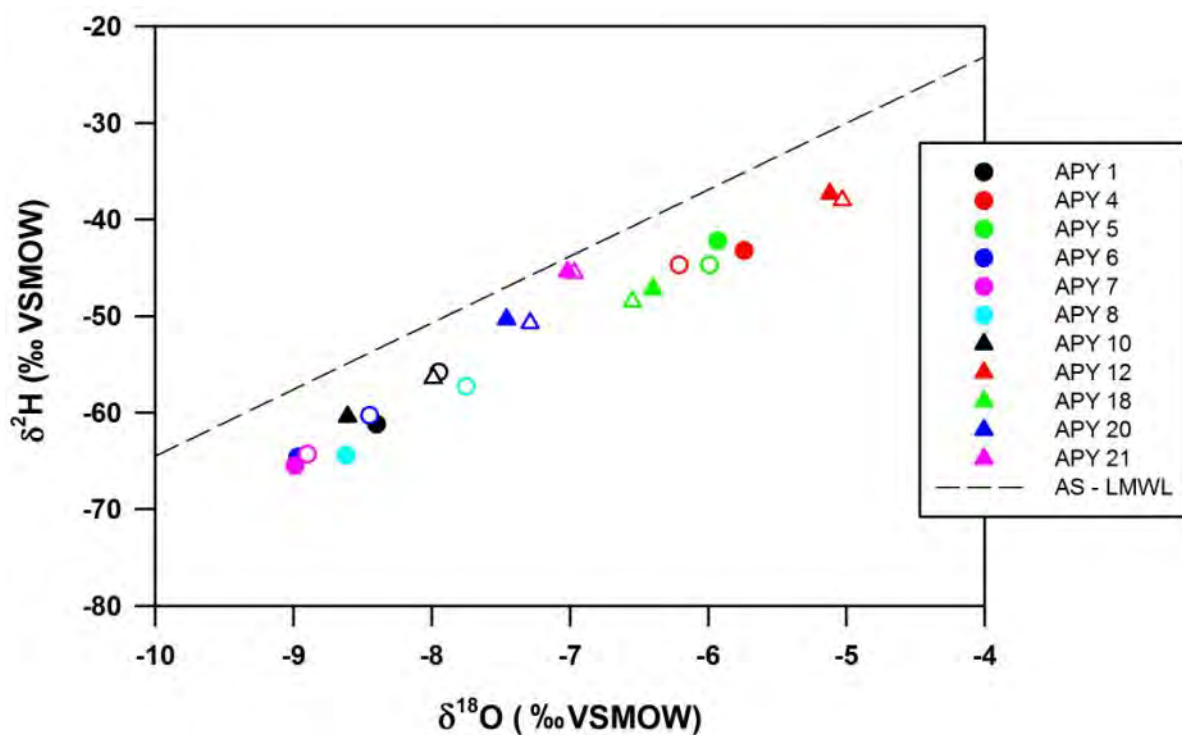


Figure 45. Temporal changes in $\delta^2\text{H}$ and $\delta^{18}\text{O}$ composition of groundwater (1997/98 samples shown with no fill, 2012 sampling shown as solid fill)

The comparison of ^{14}C for wells sampled in 1997/1998 and in 2012 (Figure 46a) shows that there has been a slight increase in the ^{14}C composition of the groundwater during that time. This most likely indicates a larger component of modern (post-bomb) recharge in the groundwater for the most recently collected samples. There is also a strong relationship between ^{14}C composition and ground surface elevation using all available ^{14}C data for the APY Lands (Figure 46b). This may be due to higher rainfall in the northern part of the APY lands relative to the central part and thus higher recharge rates. In addition to the potential differences in rainfall there are also differences in hydraulic conductivity associated with different geology. The majority of groundwater wells in the northern part of the APY lands are screened to the regolith (fractured granite) whereas those wells in the central parts of the APY lands are screened to calcrete and clay.

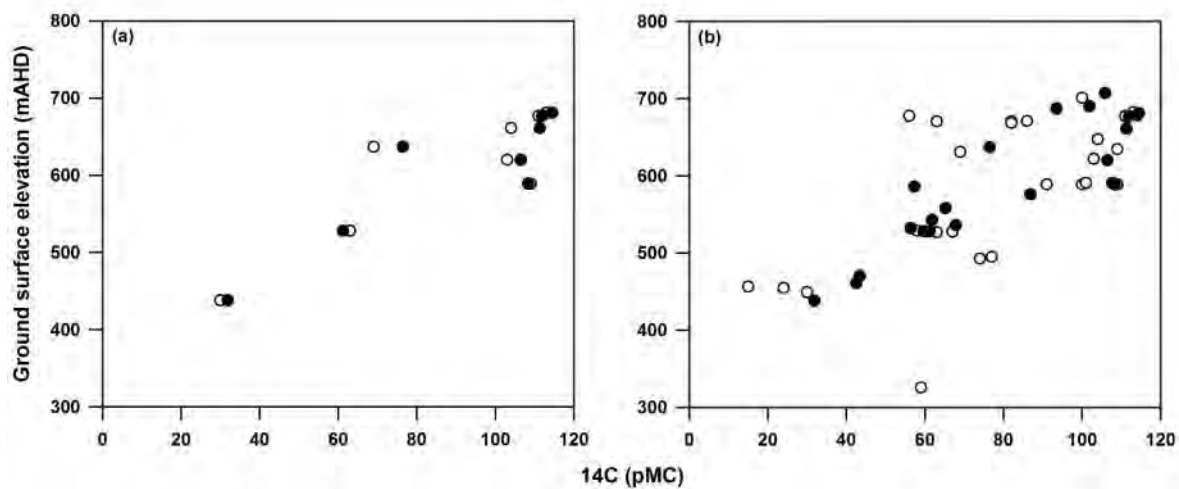


Figure 46. Comparison of ^{14}C on the same wells (a) for Dodds et al. (2001) study (open circles) and the present study by CSIRO (closed circles) as a function of ground surface elevation. All available ^{14}C data (b) as a function of ground surface elevation.

In summary, the temporal changes observed in $\delta^{18}\text{O}$ and $\delta^2\text{H}$ compositions of the groundwater in the northern area can be explained by rainfall changes taking place in the preceding years to decades while the lack of change observed in the southern areas are indicative of a much more sluggish system in that area. This observation is consistent with the ages of the groundwater suggested from ^{14}C and CFC dating. An interesting observation to add to this is that from 1889 to the early 1970s, rainfall was predominantly significantly less than the current mean (Figure 10). The decade from the early 1970s to early 1980s was the wettest on record with rainfall returning to average or near average since until the recent wet year in 2011.

Recharge rates, mechanisms and groundwater flow

The best estimates of groundwater “age” in the valleys of the Musgrave Range come from the CFC dating of groundwater (Table 11) at these sites, and to a lesser extent from the results of the ^{14}C analyses. Results of CFC-12 analyses in these valleys suggest the groundwater to be about 20 years old but only two samples were analysed. Results from ^{14}C analyses for the Musgrave Ranges are consistently close to or greater than 100 pMC suggesting groundwater younger than 50 years. The temporal changes in the $\delta^{18}\text{O}$ and $\delta^2\text{H}$ compositions of the groundwater in the recharge valleys suggest responses to recent recharge within a similar timeframe. The well sampled at Pipalyatjara, near the Tomkinson Range has a ^{14}C concentration of 76.5 pMC, slightly less than that measured in valleys in the Musgrave Ranges but greater than that for wells to the south. It is believed that this result may be a combination of the well being screened in the calcrete and not in the fractured rock as well as slightly less rainfall as a result of smaller ranges.

In order to convert this “groundwater age” to a recharge estimate would require an estimate of the porosity of the aquifer matrix at each of the wells and a knowledge of screen depths and also the amount of water being pumped from the wells. These are beyond the scope of this study. It was not possible to use the results of SF_6 analyses on groundwater in this study because inexplicably high values were measured. It is not clear why this was the case but, for most of the wells, the high SF_6 results were found for wells also with high ^4He concentrations.

An analysis of the $\delta^{18}\text{O}$ and $\delta^2\text{H}$ compositions of wells in the APY Lands has shown that recharge in the valleys takes place when rainfall exceeds 80-100 mm per month. There is evidence of some evaporation taking place prior to recharge, consistent with a run-on scenario in the streams in the Ranges. This recharge mechanism and $\delta^{18}\text{O}$ and $\delta^2\text{H}$ signature is similar to that in the Finke River study area, where large amounts of fresh groundwater can be observed. The high values for excess air are consistent with the main mechanism for recharge to the groundwater being from river recharge in the valleys and alluvium after large episodic rainfall events.

Groundwater in the southern parts of the APY Lands have background or near background CFC11 and CFC12 concentrations, lesser ^{14}C concentrations (~32 to 68 pMC), higher salinities, an enriched $\delta^{18}\text{O}$ and $\delta^2\text{H}$ signature and in general higher ^4He concentrations than groundwater in the fractured rock and alluvial plains areas to the north. The gradual changes observed in ^{14}C concentrations, [Cl], $\delta^{18}\text{O}$ and $\delta^2\text{H}$ composition from the high recharge areas in the north to the diffuse recharge areas in the south suggests that progressing south there is an increasing component of saline diffuse recharge and decreasing component of recharge from the Ranges.

Conclusions

The desktop study involved detailed analyses of the available historical rainfall and potential evaporation data at 8 stations (Barton, Coober Pedy, Cook, Ernabella, Maralinga, Marla, Nullarbor and Tarcoola) in the Alinytjara-Wilurara/western South Australian Arid lands Natural Resources Management regions, and the production of maps of recharge across the whole of the far north using the Method of Last Resort (MOLR) and Chloride Mass Balance (CMB) methods. These analyses have shown that:

- The study area is extremely arid with a seasonal pattern in rainfall that varies from winter dominant in the south (i.e. Nullarbor) to summer dominant in the north (i.e. Ernabella) and in most of the rest there is no clear seasonal trend. This behaviour in rainfall seasonality reflects the fact that most of the far north is influenced by both the winter rainfall patterns of the Southern Ocean and the summer monsoonal patterns from the north.
- There is some evidence of consistent patterns in the long-term mean annual rainfalls. There is a general trend of decreasing rainfalls (with some wetter periods) until around the 1970's, and then increasing rainfalls after that with variable behaviours during the last decade. This general trend is stronger at some sites (i.e. Barton) than others (i.e. Tarcoola).
- Recharge rates determined using the MOLR are in general very low ($<1 \text{ mm yr}^{-1}$) across all of the far north and are indicative of the diffuse recharge regimes.
- Recharge rates determined using the CMB are often greater than those determined using the MOLR because the CMB method is more likely to identify areas where surface run-on leads to localised recharge whereas the MOLR does not.

The field study, involving the use of environmental tracers to estimate recharge rates and determine recharge processes in Central Australia, was carried out in the APY Lands of the Musgrave Province. The study used a comprehensive range of chemical and isotopic analyses on 21 groundwater samples collected in late 2012. Results from this study have shown that:

- There are high rates of recharge that occur within the fractured and weathered regolith of the Precambrian basement rocks in the areas of the Musgrave and potentially in the Mann and Tomkinson Ranges. This results in fresh groundwater reserves in these areas.
- Groundwater pumped from the wells in the Musgrave Ranges is modern with a mean residence time of less than 50 (and probably less than 30) years old.
- The fresh groundwater reserves result from recharge during large episodic rainfall events where the monthly rainfall exceeds 80 mm month^{-1} . The rainfall needs to be sufficient to cause overland flow to the rivers and valleys in these areas for significant recharge to occur.
- A revised evaluation using the $\delta^2\text{H}$ vs $\delta^{18}\text{O}$ signature of groundwater from this and previous studies in central arid Australia may be used to suggest different recharge mechanisms for different areas.
- Away from the Ranges in the shallow poorly consolidated Tertiary and Quaternary sediments, saline diffuse recharge dominates with recharge rates significantly less than 1 mm yr^{-1} .

- Progressing south of the Ranges, groundwater has an increasing component of saline diffuse recharge and decreasing component of recharge from the Ranges.
- There is a large range in the ^4He concentration in groundwater in the area. In general, higher He concentrations are found in the Tertiary and Quaternary sediments to the south of the study area and, as such, are consistent with older groundwater.
- SF_6 analyses have not proved useful to estimate the age of groundwater in this study. It is believed that this may be related to the high concentrations of ^4He in groundwater at some well sites but further study is required to confirm this.

Further work

When undertaking a groundwater study utilising environmental tracers, there is quite a spectrum of potential tracers available but there are usually also time and funding constraints on what is achievable. In using a multi-tracer approach, we hope that the tracers tell a consistent story. If not, we have the advantage to use those that are consistent and disregard those that aren't.

Understanding why we disregard some results sometimes also adds to the overall understanding of the hydrology of the system. In this study, we collected samples for both SF_6 and CFC analysis amongst other analyses but, because CFC and SF_6 are both considered "tracers of modern recharge" and SF_6 has advantages over CFCs for dating post year 2000 water, we chose initially to analyse only SF_6 . This proved to be a mistake for the reasons discussed in this report. A subset of the CFC samples were analysed and they appear to be giving results consistent with the other tracers. Time and funding constraints prevented undertaking the remaining analyses. However, the CFC samples have been stored should funding be available in the future.

One of the main aims of this study was to estimate recharge rates in the study area, particularly near the major towns. Whilst groundwater ages have been determined using ^{14}C and CFC techniques, recharge rates were not estimated. Estimation of recharge rates using ^{14}C and CFC techniques require detailed knowledge of aquifer properties and this is an area where further work is required. However recharge rates have been determined using the MOLR and GCMB methods. In order to convert the recharge age to a recharge rate, more information is required on the geology of the water bearing aquifers, particularly in the Ranges valleys where most of the APY settlements are located. This, along with information on groundwater use and more refined ages from the CFC dating would allow a much better estimate of recharge and hence better management of the groundwater resource. When doing so, however, it is important to correlate the recharge rates thus determined with rainfall during that period because, as seen from the rainfall records at Ernabella, there are considerable short and long-term variations observed.

This study has indicated that high ^4He concentrations in groundwater may correlate with high SF_6 concentrations, thus preventing SF_6 to be used to estimate groundwater age. The reasons why this is so are not completely understood although both may be the result of a component of deep groundwater in the sample. It would be useful to see whether there is any correlation between high ^4He and high SF_6 and faulting in the area along with correlation with uranium bearing rocks in the aquifer matrix.

References

- AGT (2008). Sustainability of Water Resources in the Anangu Pitjantjatjara Yankunytjatjara Lands, Maralinga Tjarutja Lands and Aboriginal Lands Trust Lands, South Australia. AGT Report No. 2008/31 prepared for Department of Water, Land and Biodiversity Conservation and South Australian Water Corporation by Australian Groundwater Technologies, Adelaide.
- AGT (2010). Review of the Basic Capacity of the Groundwater Resources in the Far North, Australian Groundwater Technologies, Mile End.
- Appelo, CAJ & Postma, D 1993, *Geochemistry, Groundwater and Pollution*, Balkema, Rotterdam.
- AWNRMB (2011). Natural Resources Management Plan for the Alinytjara Wilurara Natural Resources Management Region. Alinytjara Wilurara Natural Resources Management Board, Adelaide.
- Coram JE, Dyson PR, Houlder PA and Evans WR. (2000) Australian groundwater flow systems contributing to dryland salinity. Bureau of Rural Sciences: Canberra.
- Craven, C.B. (2012). Sustainability of regolith hosted aquifers in the Musgrave Province: Northern South Australia. Honours Thesis. Flinders University.
- Cook, PG & Bohlke, JK 2000, 'Determining timescales for groundwater flow and solute transport, in environmental tracers', in: Cook, P & Herczeg, AL (eds), *Subsurface Hydrology*, Kluwer Academic Publishers, Massachusetts, USA, pp. 1–30.
- Cresswell, R., Wischusen, J., Jacobson, G. and Fifield, K. (1999) Assessment of recharge to groundwater systems in the arid southwestern part of Northern Territory, Australia, using chlorine-36. *Hydrogeology Journal*, 7: 393-404.
- Cresswell, R.G., Hostetler, S., Jacobson, G. and Fifield, L.K. (2002) Rapid, episodic recharge in the arid north of South Australia. Proceedings of International Association of Hydrogeologists Groundwater Conference "Balancing the Groundwater Budget", May 14-17 2002, Darwin.
- Crosbie, R.S., Jolly, I.D., Leaney, F.W., Petheram, C. and Wohling, D. (2010a). Review of Australian groundwater recharge studies, CSIRO Water for a Healthy Country National Research Flagship Report, Canberra.
- Crosbie, R.S., Jolly, I.D., Leaney, F.W. and Petheram, C. (2010b). Can the dataset of field based recharge estimates in Australia be used to predict recharge in data-poor areas? *Hydrology and Earth System Sciences*, 14: 2023-2038.
- Crosbie, R.S., Pollock, D.W., Mpelasoka, F.S., Barron, O.V., Charles, S.P. and Donn, M.J., 2012. Changes in Köppen-Geiger climate types under a future climate for Australia: hydrological implications. *Hydrol. Earth Syst. Sci.*, 16(9): 3341-3349.
- Custance, H.E. (2012). Hydrochemistry of shallow regolith hosted aquifers in the eastern Musgrave Province of South Australia. Honours Thesis. Flinders University.
- Dodds, A.R. (1996). Report on a Groundwater Search Program over Various Pitjantjatjara Homelands in the Musgrave Ranges Area, South Australia. Department of Mines and Energy, South Australia, Report Book 96/37, Adelaide.

- Dodds, S. and Sampson, L. (2000). The Sustainability of Water Resources in the Anangu Pitjantjatjara Lands, South Australia. Department for Water Resources, PIRSA RB 2000/00027, Adelaide.
- Dodds, A.R., Hostetler, S. and Jacobson, G. (2001). Community Water Supplies in the Anangu Pitjantjatjara Lands, South Australia: Sustainability of Groundwater Resources. Bureau of Rural Sciences, Canberra.
- Fitzgerald, J., Cunliffe, D., Dodds, S., Hostetler, S., Rainow, S. and Jacobson, G. (2000). Groundwater Quality and Environmental Health Implications, Anangu Pitjantjatjara Lands, South Australia. Bureau of Rural Sciences, Canberra.
- Gallant, J.C. and Dowling, T.I. (2003). A multiresolution index of valley bottom flatness for mapping depositional areas. *Water Resources Research*, 39(12): 1347, doi:10.1029/2002WR001426.
- GHD (2009). Report for Future Management of Water Resources: Consolidated Report for Stages, 3, 4 and 5. Unpublished draft report (August 2009) prepared for the Alinytjara Wilurara Natural Resources Management Board by GHD, Adelaide.
- Harrington, G.A., Herczeg, A.L. and Cook, P.G. (1999). Groundwater Sustainability and water Quality in the Ti-Tree Basin, Central Australia. CSIRO Land and Water Technical Report 53/99, Adelaide.
- Harrington, G.A., Cook, P.G. and Herczeg, A.L. (2002). Spatial and temporal variability of ground water recharge in central Australia: a tracer approach. *Ground Water*, 40(5): 518-528.
- Harrington, G., and Herczeg, A. (2003). The importance of silicate weathering of a sedimentary aquifer in arid Central Australia indicated by very high $^{87}\text{Sr}/^{86}\text{Sr}$ ratios. *Chemical Geology*, 199: 281-292
- Hou, B., Frakes, L.A., Alley, N.F. and Clarke, J.D.A. (2003). Characteristics and evolution of the Tertiary Palaeovalleys in the North-west Gawler Craton, South Australia, *Australian Journal of Earth Sciences*, 50: 215-230.
- IAEA/WMO (2006). Global Network of Isotopes in Precipitation. The GNIP Database. Accessible at: <http://www.iaea.org/water>
- Jeffrey, S.J., Carter, J.O., Moodie, K.B. and Beswick, A.R. (2001). Using spatial interpolation to construct a comprehensive archive of Australian climate data. *Environmental Modelling & Software*, 16(4): 309-330.
- Jolly, I., Gow, L., Davies, P., O'Grady, A., Leaney, F., Crosbie, R., Wilford, J. and Kilgour, P. (2011). Recharge and Discharge Estimation in Data Poor Areas: User Guide for the Recharge and Discharge Estimation Spreadsheets and MapConnect. CSIRO Water for a Healthy Country National Research Flagship Report, Canberra.
- Köppen, W., 1936. Das geographische System der Klimate. In: W. Köppen and G. Geiger (Editors), *Handbuch der Klimatologie*. Borntraeger, pp. 1-44.
- Leaney, F., Crosbie, R., O'Grady, A., Jolly, I., Gow, L., Davies, P., Wilford, J. and Kilgour, P. (2011). Recharge and Discharge Estimation in Data Poor Areas: Scientific Reference Guide. CSIRO Water for a Healthy Country National Research Flagship Report, Canberra.

- Lewis, S.J., English, P.M., Wischusen, J.D.H., Woodgate, M.F., Gow, L.J., Hanna, A.L. and Kilgour, P.L. (2010). The Palaeovalley Groundwater Project: Operational Update on Demonstration Study Sites July 2009 to April 2010. Milestone 5 Report by Geoscience Australia for the National Water Commission, April 2010, 302p.
- Love et al. (eds) 2013, *Allocating Water and Maintaining Springs in the Great Artesian Basin, Volume II: Groundwater Recharge, Hydrodynamics and Hydrochemistry of the Western Great Artesian Basin*, National Water Commission, Canberra.
- Magee, J.W., 2009. Palaeovalley Groundwater Resources in Arid and Semi-Arid Australia – A Literature Review. *Geoscience Australia Record* 2009/03. 224 pp.
- Major, RB & Connor, CHH 1993, 'Musgrave Province', in Drexel, JF & Preiss, WV (eds), *The Geology of South Australia, Vol. 1, The Precambrian*, Bulletin 54, Geological Survey, Adelaide, pp.156-167.
- Mazor, E. 1991, *Applied chemical and isotopic groundwater hydrology*. Open University Press Buckingham, United Kingdom MK181XW
- SAALNRMB (2010). *Regional Natural Resources Management Plan for the SA Arid Lands Natural Resources Management Region - Volume 1 Ten-year Strategic plan*. South Australian Arid Lands Natural Resource Management Board, Port Augusta.
- Siegenthaler, U. and Oeschger, H. (1980) Correlation of O-18 in precipitation with temperature and altitude. *Nature* 285, 314-317.
- Tewkesbury, P. and Dodds, A.R. (1997). *An Appraisal of the Water Resources of the Musgrave Province, South Australia*. Department of Mines and Energy Resources, South Australia Report Book No. 97/22, Adelaide.
- Varma, S., 2012, *Hydrogeological review of the Musgrave Province, South Australia*, Goyder Institute for Water Research Technical Report Series No. 12/8.
- Venables, M.N., Smith, D.H. and the R Development Core Team (2011). *An Introduction to R. Notes on R: A programming Environment for Data Analysis and Graphics Version 2.14.1 (2011-12-22)*. (<http://cran.r-project.org/doc/manuals/R-intro.pdf>)
- Vogel, JC 1967, *Investigation of groundwater flow with radiocarbon: Isotopes in Hydrology*, International Atomic Energy Agency, Vienna, pp 355–369.
- Watt, E. and Berens, V. (2011). *Non-Prescribed Groundwater Resources Assessment – Alinytjara Wilurara Natural Resources Management Region. Phase 1 – Literature and Data Review*. DFW Technical Report 2011/18, Government of South Australia, through Department for Water, Adelaide.
- Weiss, RF (1968) Piggyback sampler for dissolved gas studies on sealed water samples. *Deep Sea Research and Oceanographic Abstracts* 15, 695-699.

Zambrano-Bigiarini, M. (2011). Package 'hydroTSM': Time series management, analysis and interpolation for hydrological modelling.

(<http://cran.csiro.au/web/packages/hydroTSM/hydroTSM.pdf>)

Appendix A – Further analysis of historical rainfall and evaporation

Barton

Time series of daily, monthly and annual rainfall, with one and three year moving averages are shown in Figure 47. A boxplot of the monthly rainfall is shown in Figure 48. A plot of the cumulative annual deviation from the mean annual rainfall is shown in Figure 49. A summary of the daily, monthly and annual rainfall statistics is given in Table 12.

Barton is located in the south-central part of the study area in a BWh climate zone. It has mean daily, monthly and annual rainfalls of 0.6, 16.9 and 202.6 mm respectively. The highly variable rainfall regime is illustrated by the high standard deviations of the daily, month and annual rainfalls. The variability is most extreme in the daily rainfall, followed by the monthly rainfall and then the annual rainfall, as illustrated by the coefficients of variation of each. There boxplot suggests that there is a slight winter dominance of the rainfall. The cumulative deviation from the mean plot shows that the mean annual rainfalls generally declined until the mid 1970's, then increased until the mid 1980's, and have been declining since then.

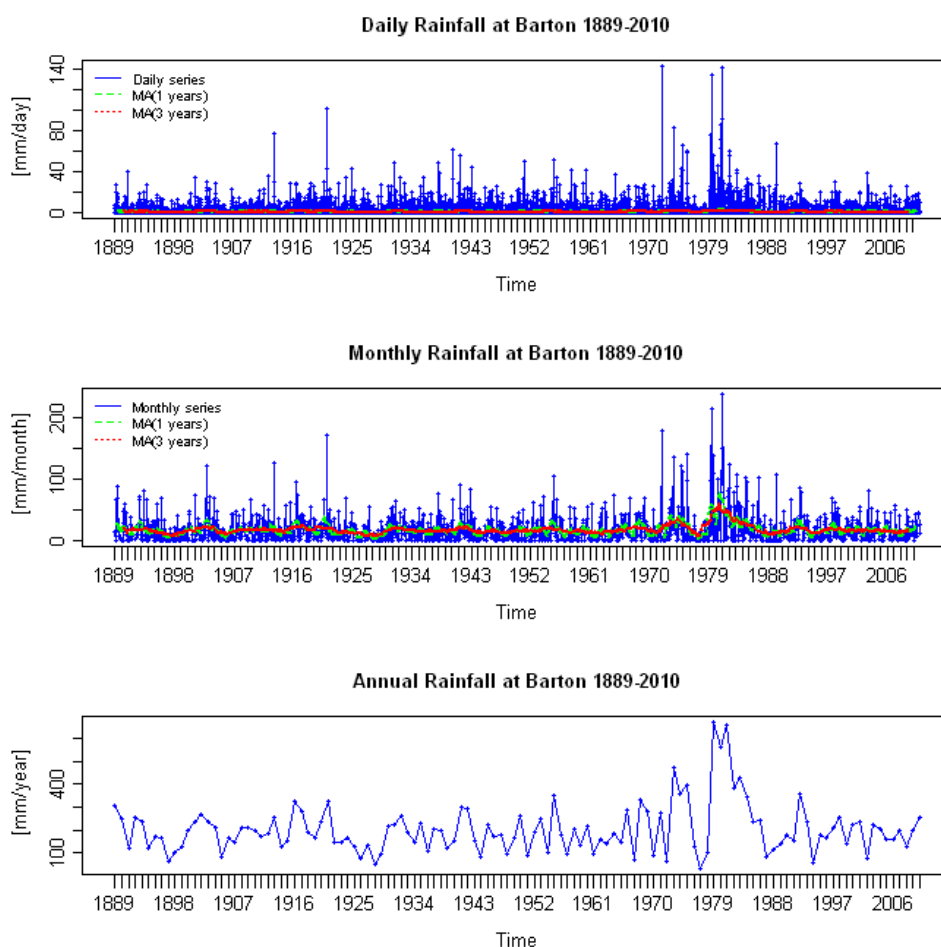


Figure 47. Time series of daily, monthly and annual rainfall at Barton. One year and three year moving averages are shown in green and red respectively.

Monthly Rainfall at Barton 1889-2010

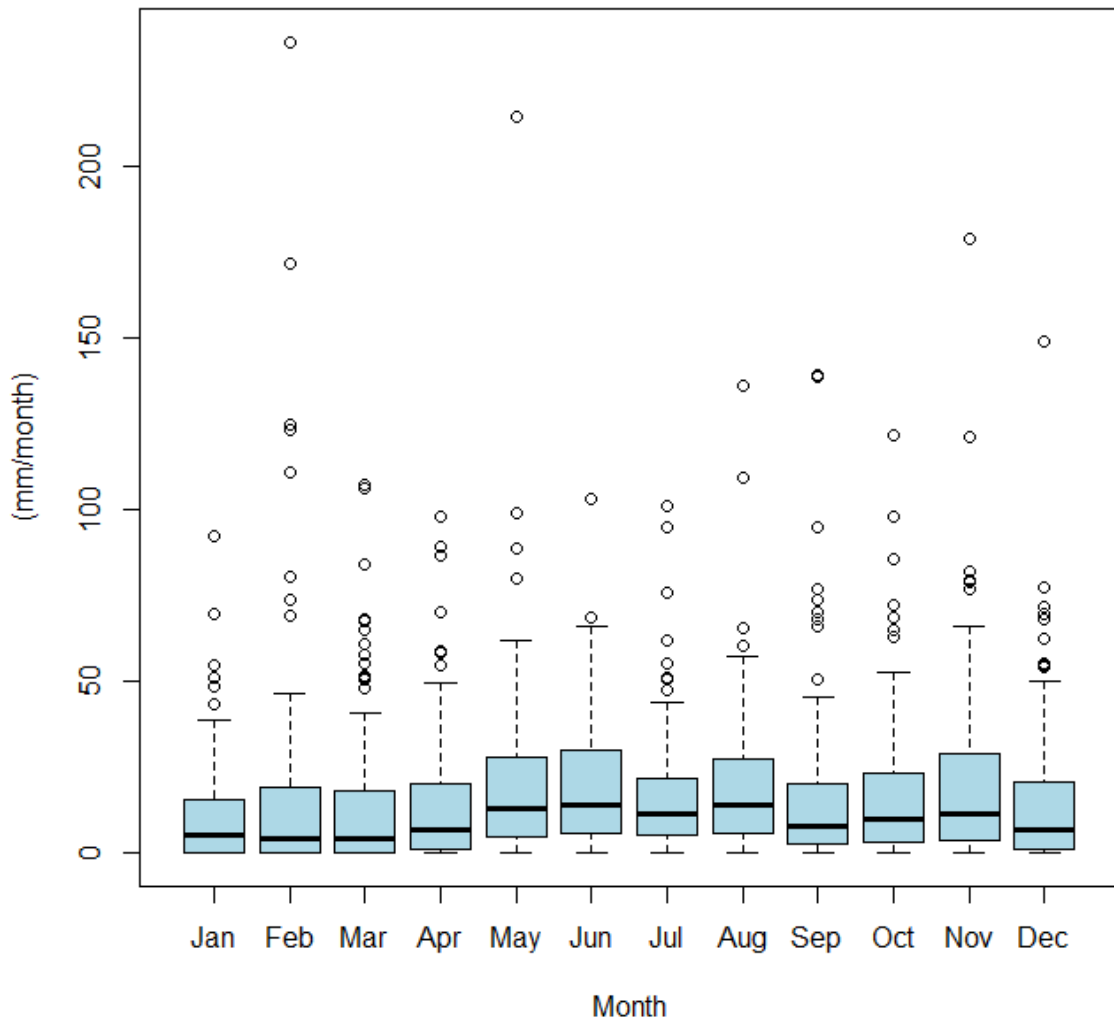


Figure 48. Boxplot of the monthly rainfall at Barton. The bottom and top of each box are the first and third quartiles, the band inside each box is the second quartile (the median), the ends of each of the whiskers are 1.5 times the interquartile range of the lower and upper quartiles, and the circles are outliers.

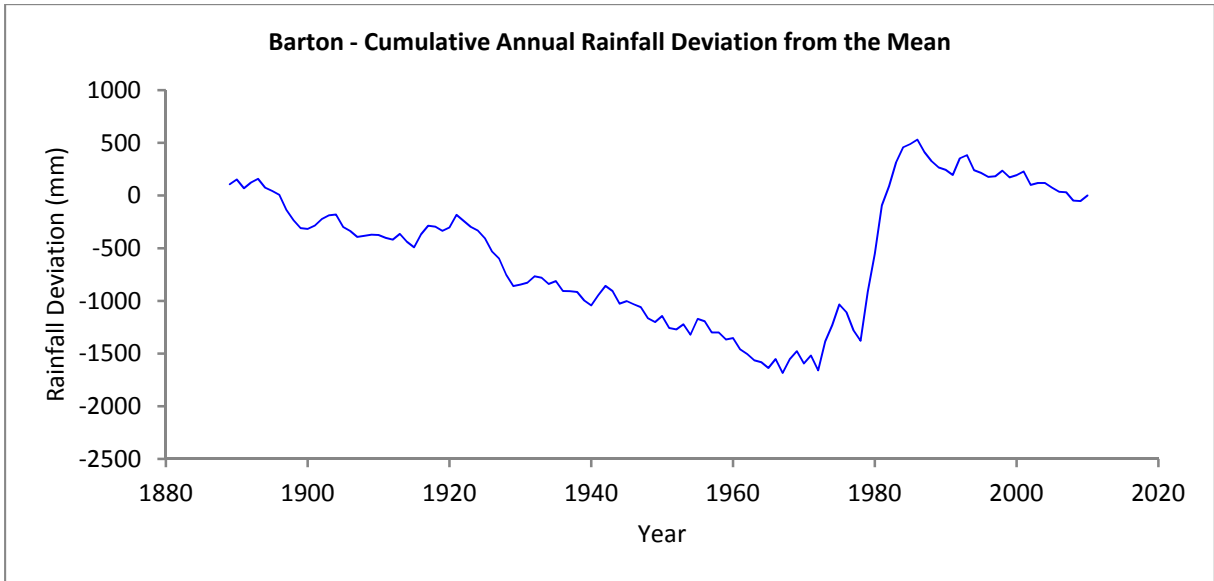


Figure 49. Plot of the cumulative annual deviation from the mean annual rainfall at Barton.

Table 12. Summary of the daily, monthly and annual rainfall statistics at Barton.

Statistic	Daily	Monthly	Annual
Minimum (mm)	0.0	0.0	31.8
First quartile (mm)	0.0	2.1	135.6
Median (mm)	0.0	9.1	185.2
Mean (mm)	0.6	16.9	202.6
Third quartile (mm)	0.0	22.8	243.3
Maximum (mm)	142.2	236.0	669.7
Interquartile range (mm)	0.0	20.7	107.8
Standard deviation (mm)	3.0	22.9	108.6
Coefficient of variation	5.3	1.4	0.5
Number of points	14975	492	41

Time series of daily, monthly and annual pan evaporation, with one and three year moving averages are shown in Figure 50. A boxplot of the monthly pan evaporation is shown in Figure 51. A summary of the daily, monthly and annual pan evaporation statistics is given in Table 13.

The pan evaporation at Barton is very high, with the mean daily, monthly and annual values of 7.1, 216.5 and 2598.0 mm respectively far exceeding those of the rainfall. The monthly boxplot shows that there is a strong seasonal pattern with lowest values in winter and highest values in summer. Whilst the pan evaporation is highly variable, the coefficients of variation are all much lower than those for rainfall.

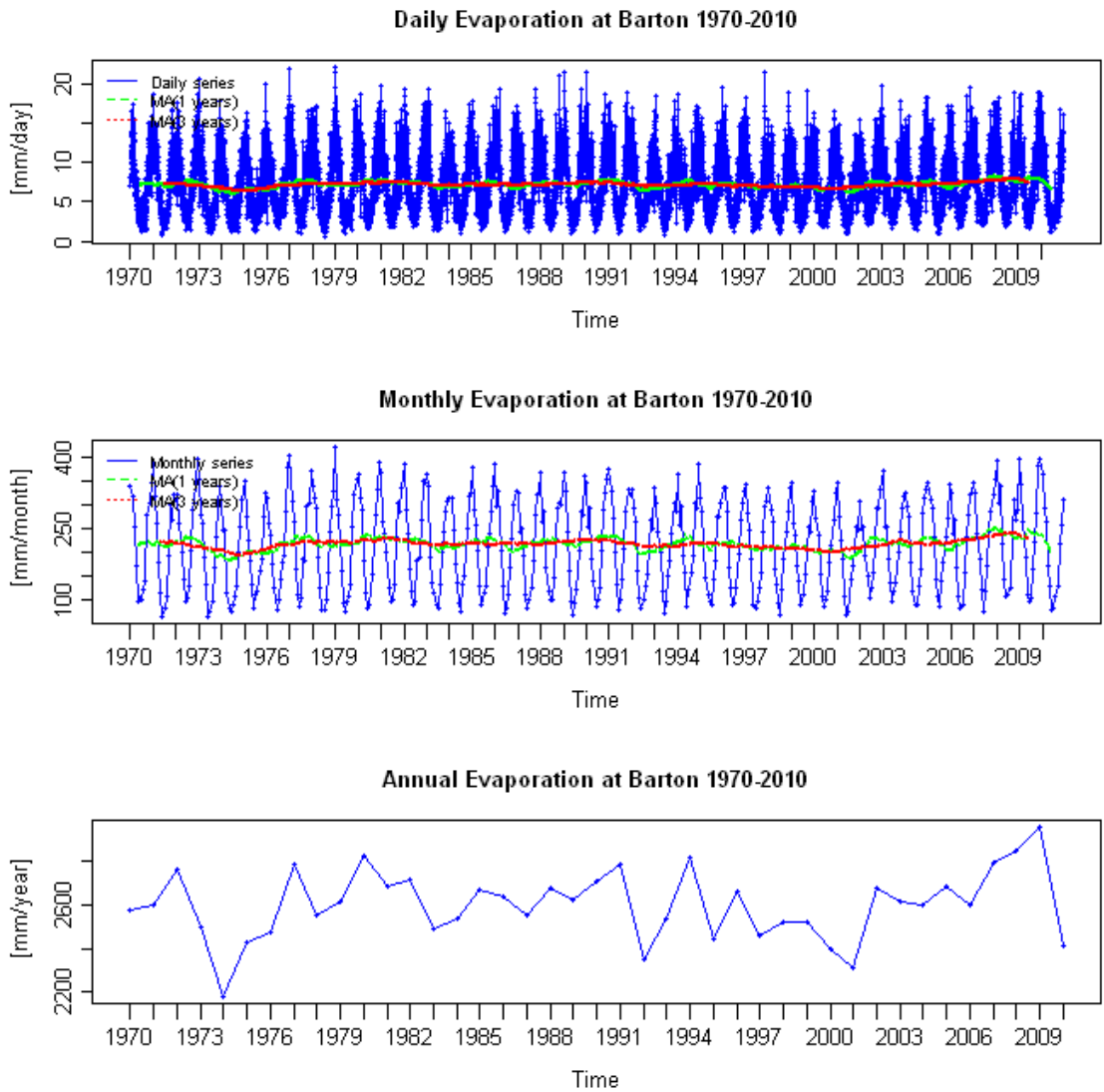


Figure 50. Time series of daily, monthly and annual pan evaporation at Barton. One year and three year moving averages are shown in green and red respectively.

Monthly Evaporation at Barton 1970-2010

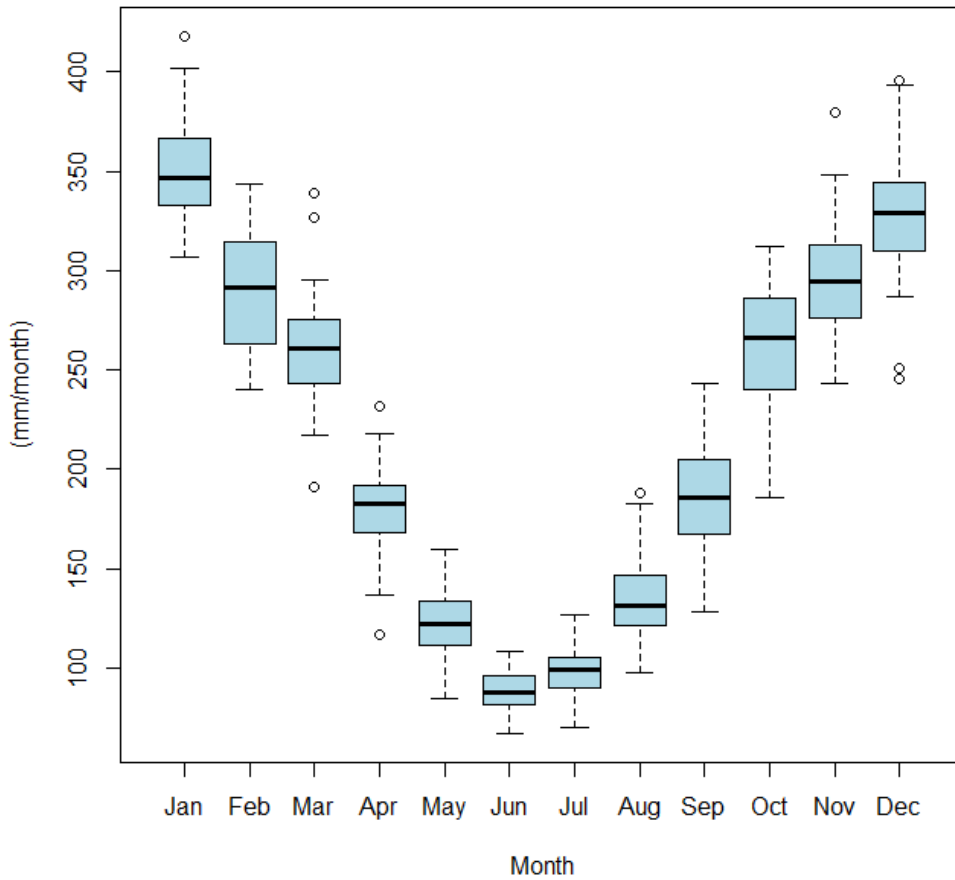


Figure 51. Boxplot of the monthly pan evaporation at Barton. The bottom and top of each box are the first and third quartiles, the band inside each box is the second quartile (the median), the ends of each of the whiskers are 1.5 times the interquartile range of the lower and upper quartiles, and the circles are outliers.

Table 13. Summary of the daily, monthly and annual pan evaporation statistics at Barton.

Statistic	Daily	Monthly	Annual
Minimum (mm)	0.6	66.8	2181.0
First quartile (mm)	4.0	127.8	2495.0
Median (mm)	6.8	218.9	2601.0
Mean (mm)	7.1	216.5	2598.0
Third quartile (mm)	9.8	295.0	2686.0
Maximum (mm)	22.0	418.2	2951.0
Interquartile range (mm)	5.8	167.3	191.0
Standard deviation (mm)	3.6	92.4	158.2
Coefficient of variation	0.5	0.4	0.1
Number of points	14975	492	41

Coober Pedy

Time series of daily, monthly and annual rainfall, with one and three year moving averages are shown in Figure 52. A boxplot of the monthly rainfall is shown in Figure 53. A plot of the cumulative annual deviation from the mean annual rainfall is shown in Figure 54. A summary of the daily, monthly and annual rainfall statistics is given in Table 14.

Coober Pedy is located in the central-west part of the study area in a BWh climate zone. It has mean daily, monthly and annual rainfalls of 0.4, 12.5 and 150.0 mm respectively. The highly variable rainfall regime is illustrated by the high standard deviations of the daily, month and annual rainfalls. The variability is most extreme in the daily rainfall, followed by the monthly rainfall and then the annual rainfall, as illustrated by the coefficients of variation of each. The boxplot suggests that there is a no clear seasonal behaviour of the rainfall. The cumulative deviation from the mean plot shows that the mean annual rainfalls generally declined until the mid 1970's, then increased until around 2000, and have been declining slowly since then.

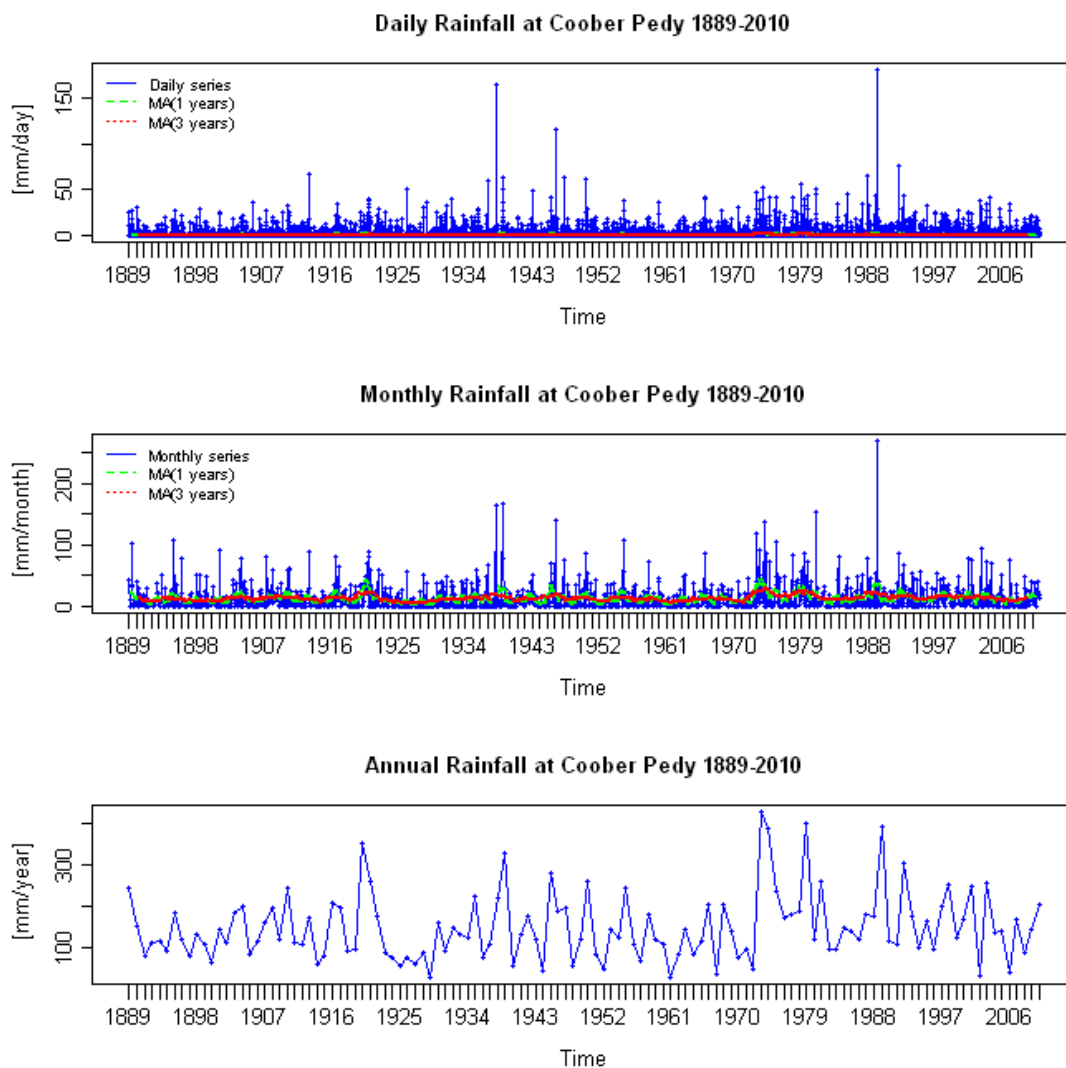


Figure 52. Time series of daily, monthly and annual rainfall at Coober Pedy. One year and three year moving averages are shown in green and red respectively.

Monthly Rainfall at Cobber Pedy 1889-2010

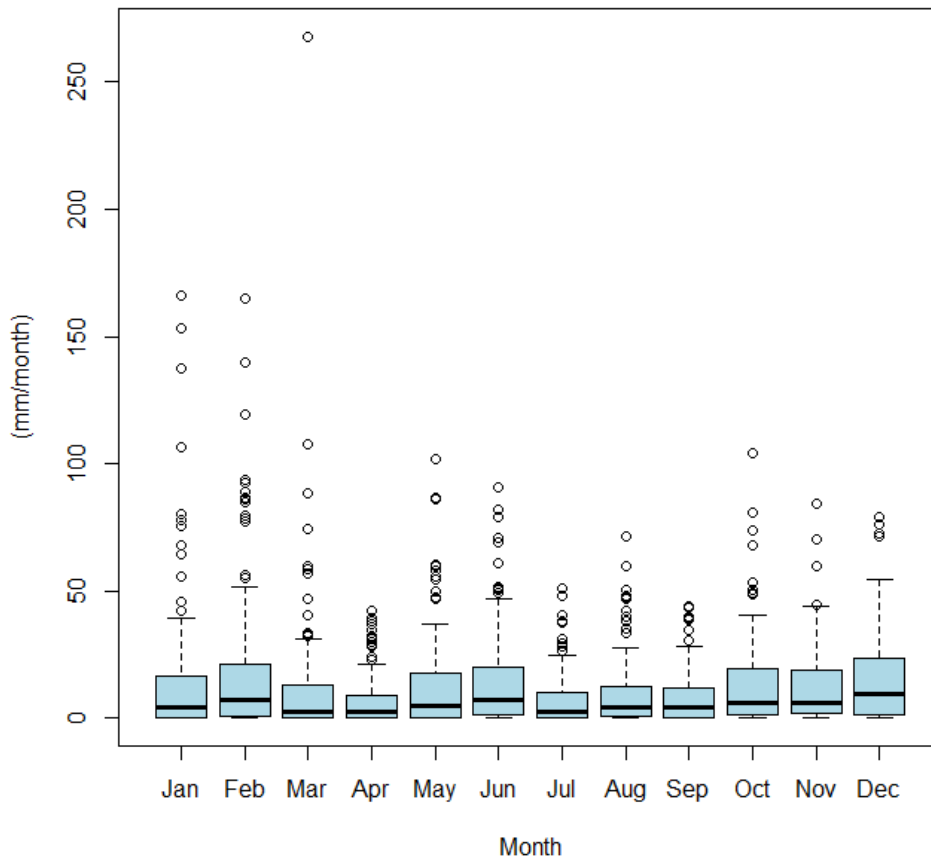


Figure 53. Boxplot of the monthly rainfall at Coober Pedy. The bottom and top of each box are the first and third quartiles, the band inside each box is the second quartile (the median), the ends of each of the whiskers are 1.5 times the interquartile range of the lower and upper quartiles, and the circles are outliers.

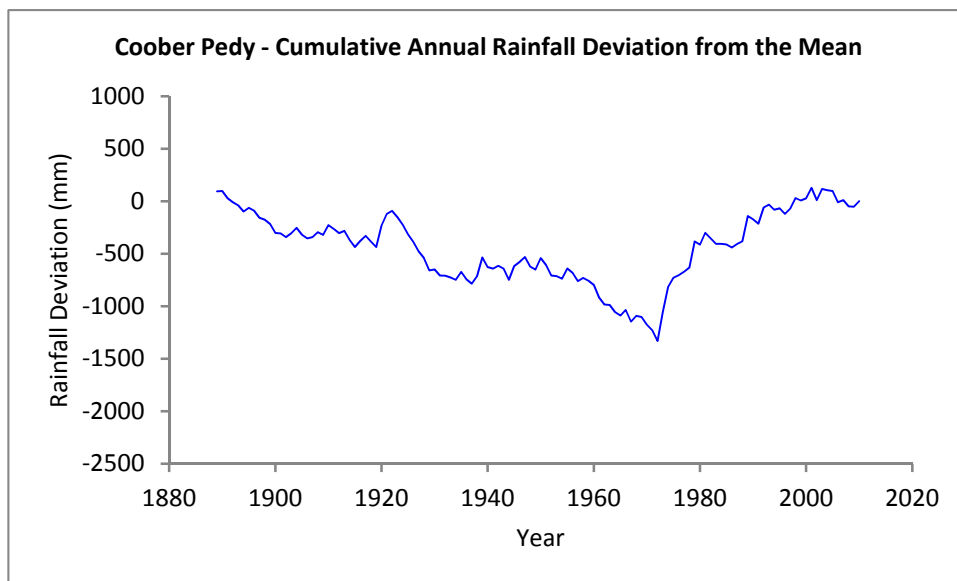


Figure 54. Plot of the cumulative annual deviation from the mean annual rainfall at Coober Pedy.

Table 14. Summary of the daily, monthly and annual rainfall statistics at Coober Pedy.

Statistic	Daily	Monthly	Annual
Minimum (mm)	0.0	0.0	29.9
First quartile (mm)	0.0	0.5	93.3
Median (mm)	0.0	4.8	129.9
Mean (mm)	0.4	12.5	150.0
Third quartile (mm)	0.0	16.0	187.8
Maximum (mm)	180.0	268.0	427.2
Interquartile range (mm)	0.0	15.5	94.6
Standard deviation (mm)	2.7	20.4	80.8
Coefficient of variation	6.6	1.6	0.5
Number of points	44599	1464	122

Time series of daily, monthly and annual pan evaporation, with one and three year moving averages are shown in Figure 55. A boxplot of the monthly pan evaporation is shown in Figure 56. A summary of the daily, monthly and annual pan evaporation statistics is given in Table 15.

The pan evaporation at Coober Pedy is extremely high, with the mean daily, monthly and annual values of 8.1, 247.1 and 2965.0 mm respectively far exceeding those of the rainfall. The monthly boxplot shows that there is a strong seasonal pattern with lowest values in winter and highest values in summer. Whilst the pan evaporation is highly variable, the coefficients of variation are all much lower than those for rainfall.

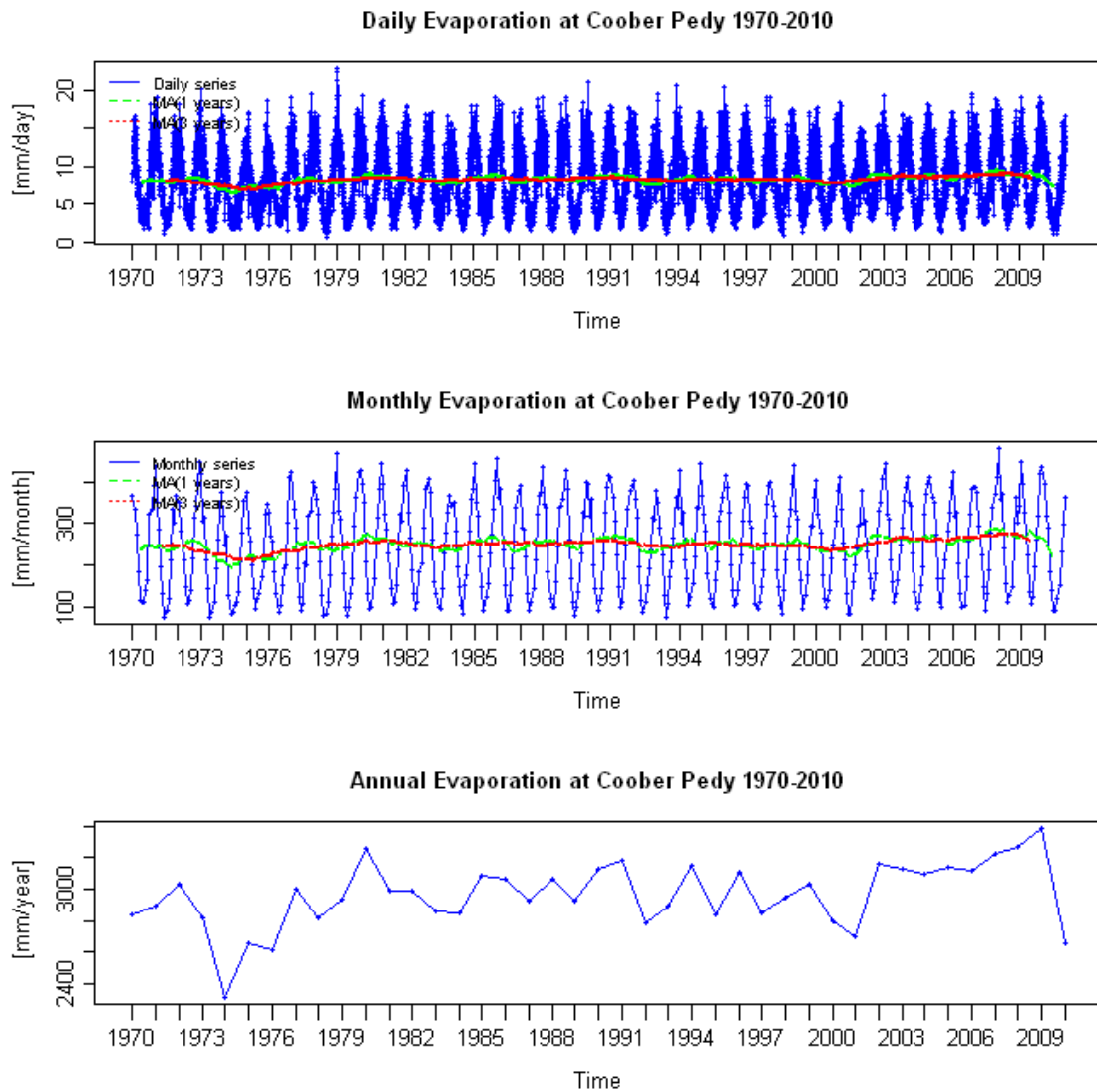


Figure 55. Time series of daily, monthly and annual pan evaporation at Coober Pedy. One year and three year moving averages are shown in green and red respectively.

Monthly Evaporation at Coober Pedy 1970-2010

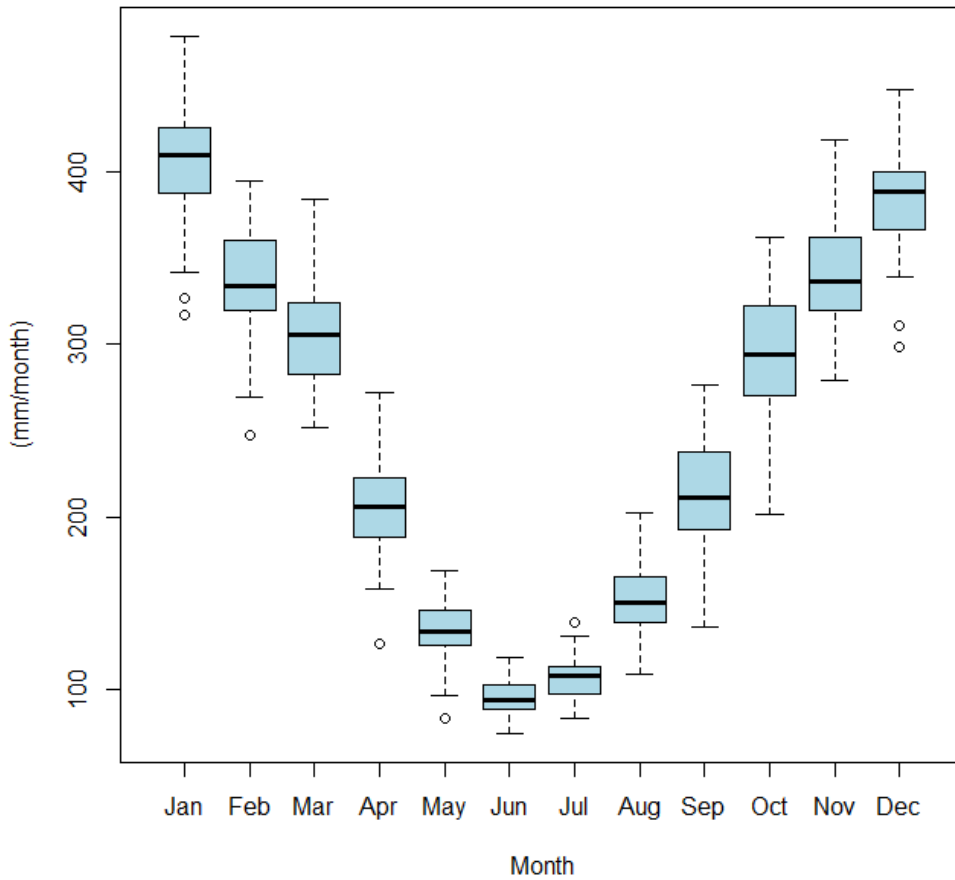


Figure 56. Boxplot of the monthly pan evaporation at Coober Pedy. The bottom and top of each box are the first and third quartiles, the band inside each box is the second quartile (the median), the ends of each of the whiskers are 1.5 times the interquartile range of the lower and upper quartiles, and the circles are outliers.

Table 15. Summary of the daily, monthly and annual pan evaporation statistics at Coober Pedy.

Statistic	Daily	Monthly	Annual
Minimum (mm)	0.6	74.4	2316.0
First quartile (mm)	4.4	142.1	2838.0
Median (mm)	7.8	249.0	2995.0
Mean (mm)	8.1	247.1	2965.0
Third quartile (mm)	11.4	339.2	3121.0
Maximum (mm)	22.8	478.4	3383.0
Interquartile range (mm)	7.0	197.1	283.0
Standard deviation (mm)	4.1	109.4	207.1
Coefficient of variation	0.5	0.4	0.1
Number of points	14975	492	41

Cook

Time series of daily, monthly and annual rainfall, with one and three year moving averages are shown in Figure 57. A boxplot of the monthly rainfall is shown in Figure 58. A plot of the cumulative annual deviation from the mean annual rainfall is shown in Figure 59. A summary of the daily, monthly and annual rainfall statistics is given in Table 16.

Cook is located in the south-western part of the study area in a BWh climate zone. It has mean daily, monthly and annual rainfalls of 0.5, 14.9 and 178.7 mm respectively. The highly variable rainfall regime is illustrated by the high standard deviations of the daily, month and annual rainfalls. The variability is most extreme in the daily rainfall, followed by the monthly rainfall and then the annual rainfall, as illustrated by the coefficients of variation of each. The boxplot suggests that there is a no clear seasonal behaviour of the rainfall. The cumulative deviation from the mean plot shows that the mean annual rainfalls generally declined until the late 1960's and have been increasing since then.

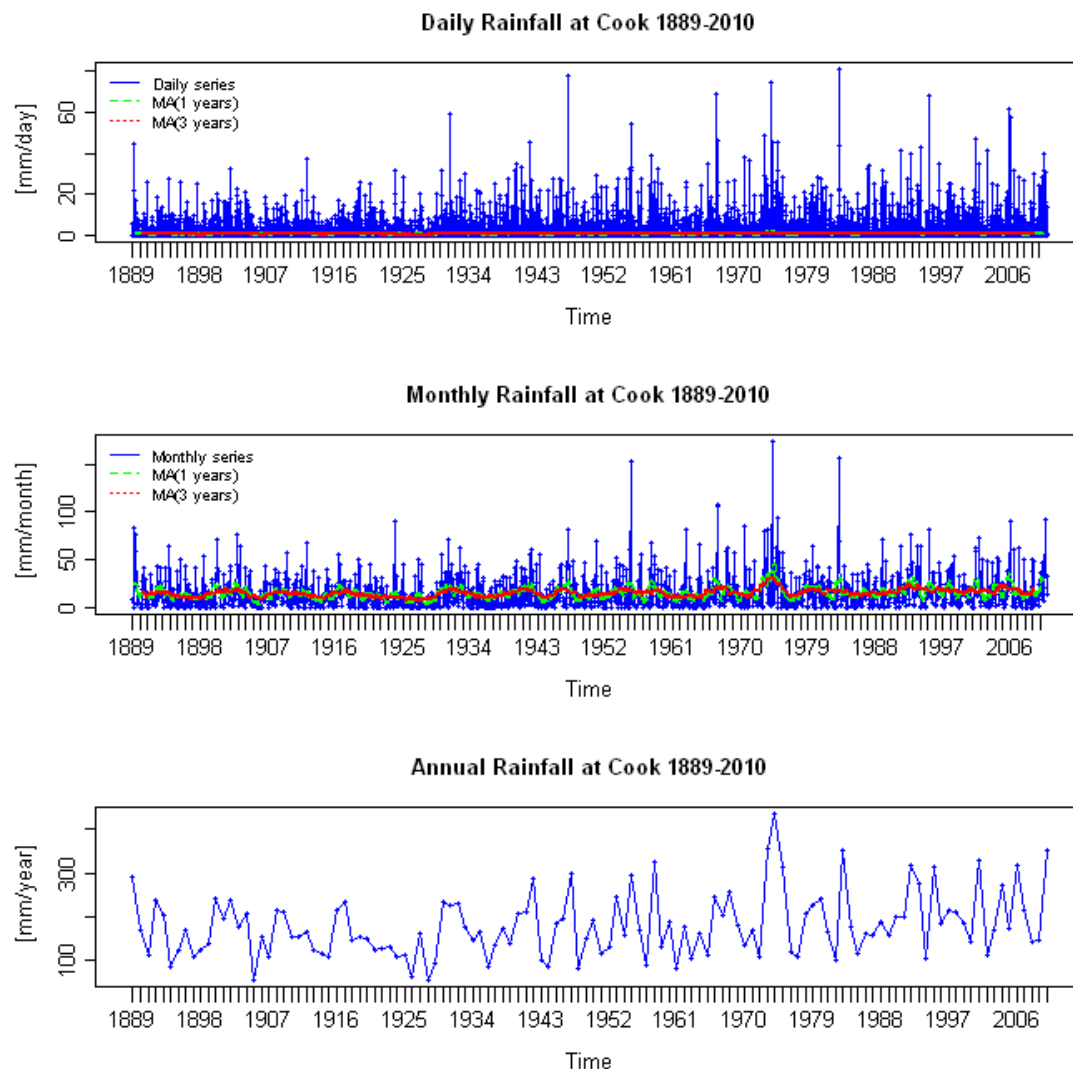


Figure 57. Time series of daily, monthly and annual rainfall at Cook. One year and three year moving averages are shown in green and red respectively.

Monthly Rainfall at Cook 1889-2010

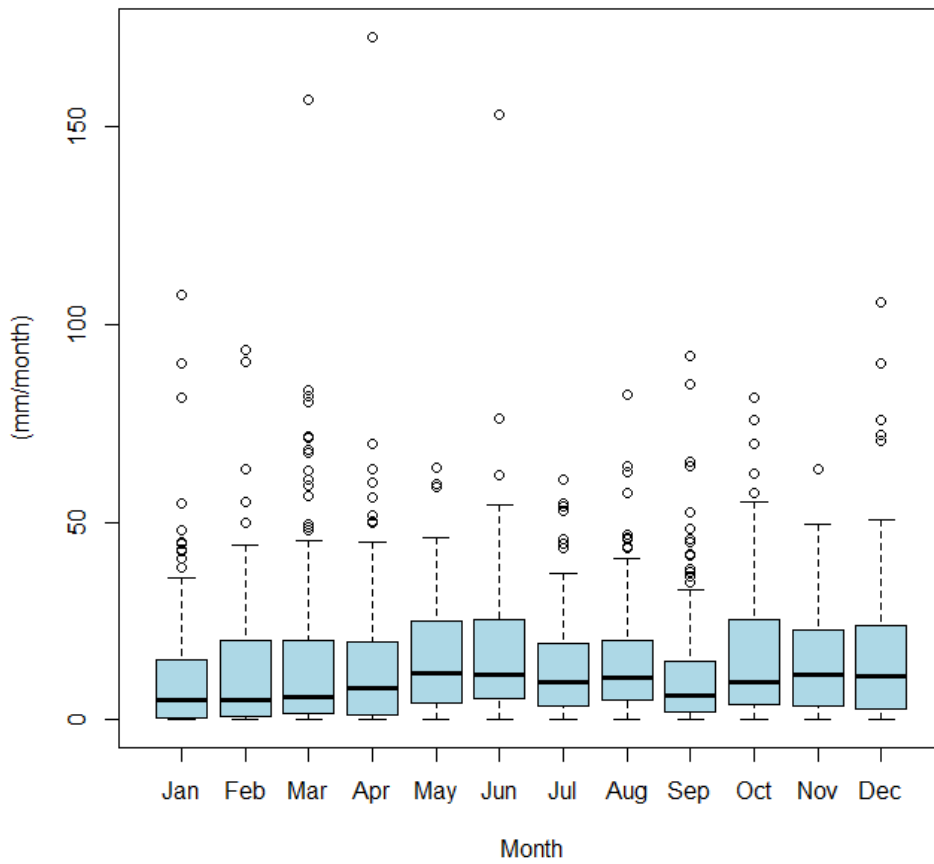


Figure 58. Boxplot of the monthly rainfall at Cook. The bottom and top of each box are the first and third quartiles, the band inside each box is the second quartile (the median), the ends of each of the whiskers are 1.5 times the interquartile range of the lower and upper quartiles, and the circles are outliers.

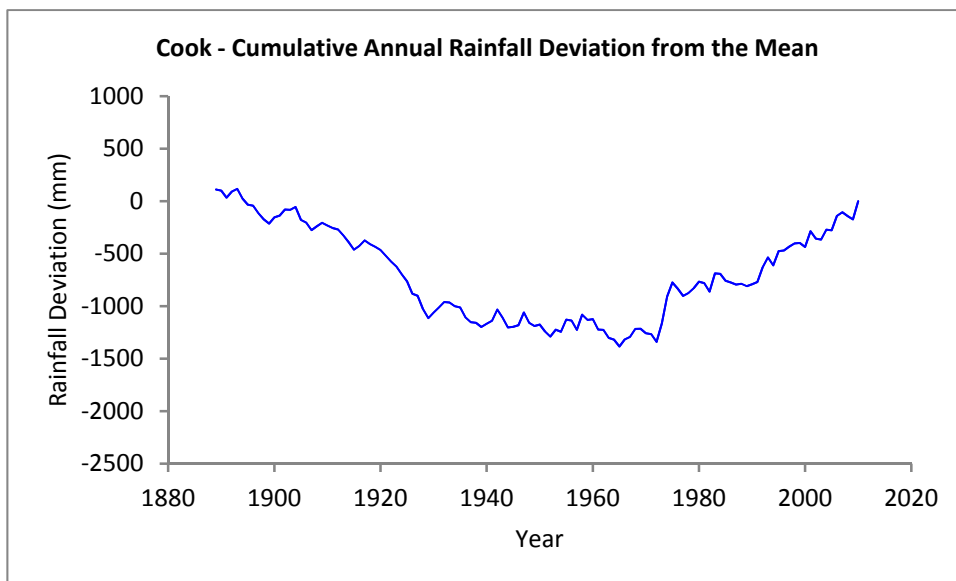


Figure 59. Plot of the cumulative annual deviation from the mean annual rainfall at Cook.

Table 16. Summary of the daily, monthly and annual rainfall statistics at Cook.

Statistic	Daily	Monthly	Annual
Minimum (mm)	0.0	0.0	53.8
First quartile (mm)	0.0	2.8	123.2
Median (mm)	0.0	8.7	168.4
Mean (mm)	0.5	14.9	178.7
Third quartile (mm)	0.0	21.3	213.9
Maximum (mm)	80.8	172.8	434.6
Interquartile range (mm)	0.0	18.6	90.8
Standard deviation (mm)	2.4	17.8	72.8
Coefficient of variation	5.0	1.2	0.4
Number of points	44599	1464	122

Time series of daily, monthly and annual pan evaporation, with one and three year moving averages are shown in Figure 60. A boxplot of the monthly pan evaporation is shown in Figure 61. A summary of the daily, monthly and annual pan evaporation statistics is given in Table 17.

The pan evaporation at Cook is very high, with the mean daily, monthly and annual values of 7.0, 214.0 and 2567.0 mm respectively far exceeding those of the rainfall. The monthly boxplot shows that there is a strong seasonal pattern with lowest values in winter and highest values in summer. Whilst the pan evaporation is highly variable, the coefficients of variation are all much lower than those for rainfall.

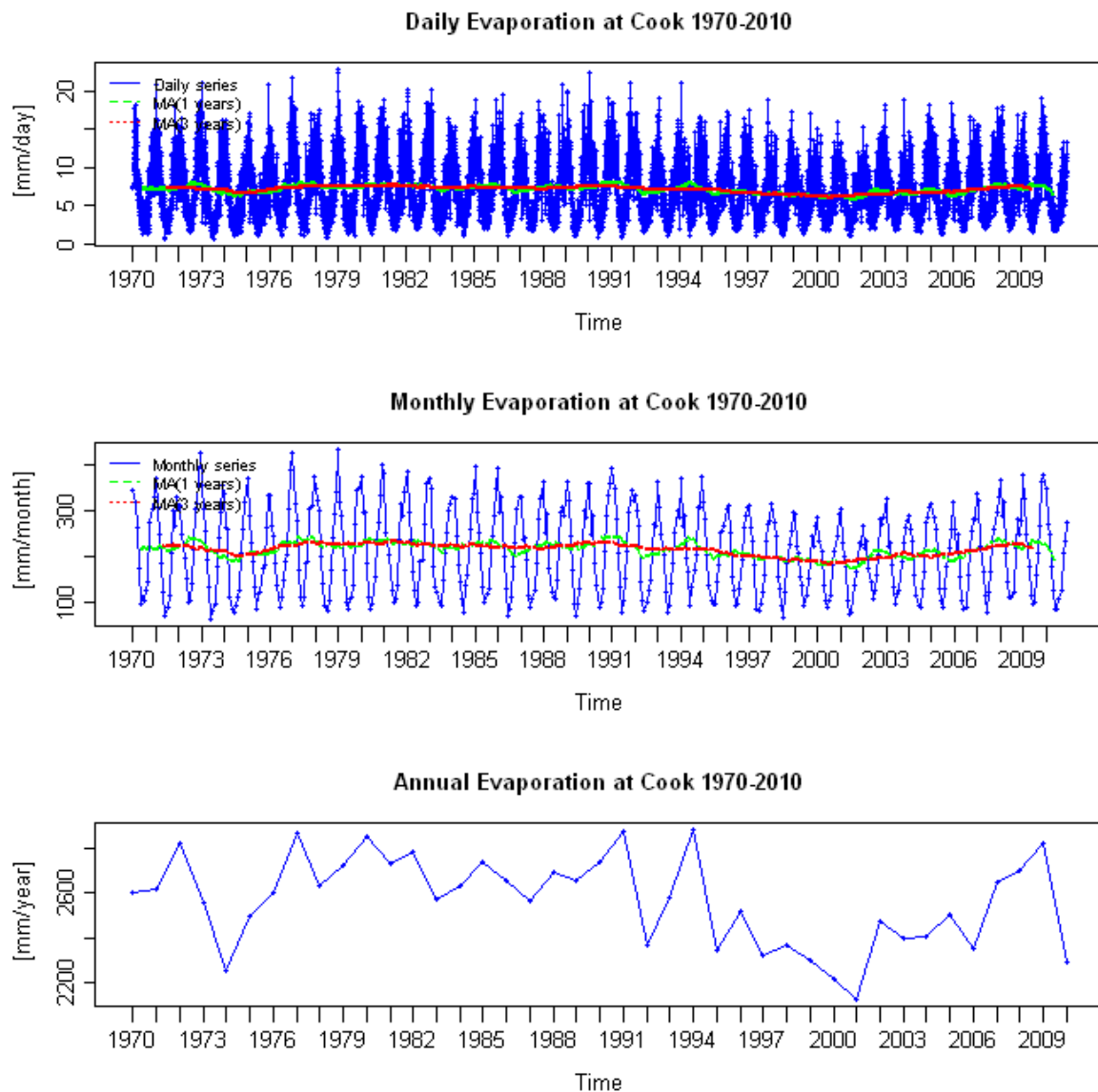


Figure 60. Time series of daily, monthly and annual pan evaporation at Cook. One year and three year moving averages are shown in green and red respectively.

Monthly Evaporation at Cook 1970-2010

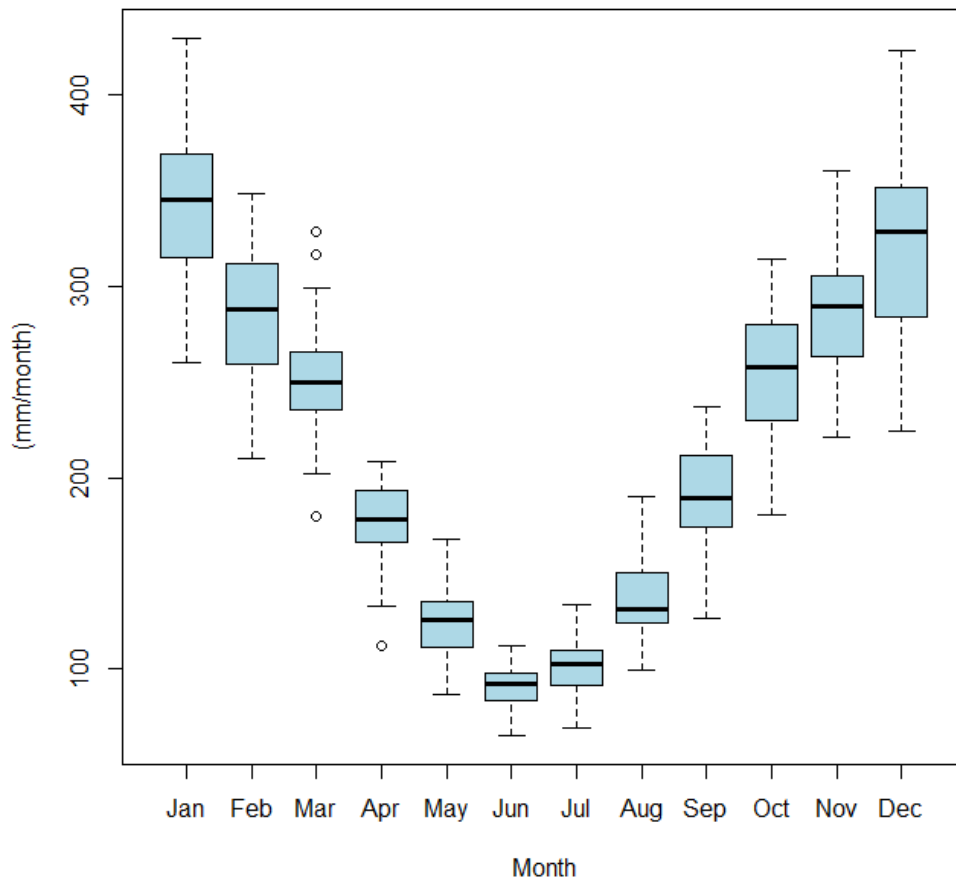


Figure 61. Boxplot of the monthly pan evaporation at Cook. The bottom and top of each box are the first and third quartiles, the band inside each box is the second quartile (the median), the ends of each of the whiskers are 1.5 times the interquartile range of the lower and upper quartiles, and the circles are outliers.

Table 17. Summary of the daily, monthly and annual pan evaporation statistics at Cook.

Statistic	Daily	Monthly	Annual
Minimum (mm)	0.6	65.0	2127.0
First quartile (mm)	4.0	128.0	2401.0
Median (mm)	6.6	211.2	2599.0
Mean (mm)	7.0	214.0	2567.0
Third quartile (mm)	9.6	288.4	2720.0
Maximum (mm)	22.8	430.2	2878.0
Interquartile range (mm)	5.6	160.5	319.2
Standard deviation (mm)	3.6	89.7	199.0
Coefficient of variation	0.5	0.4	0.1
Number of points	14975	492	41

Maralinga

Time series of daily, monthly and annual rainfall, with one and three year moving averages are shown in Figure 62. A boxplot of the monthly rainfall is shown in Figure 63. A plot of the cumulative annual deviation from the mean annual rainfall is shown in Figure 64. A summary of the daily, monthly and annual rainfall statistics is given in Table 18.

Maralinga is located in the south-central part of the study area in a BWh climate zone. It has mean daily, monthly and annual rainfalls of 0.5, 16.6 and 198.7 mm respectively. The highly variable rainfall regime is illustrated by the high standard deviations of the daily, month and annual rainfalls. The variability is most extreme in the daily rainfall, followed by the monthly rainfall and then the annual rainfall, as illustrated by the coefficients of variation of each. The boxplot suggests that there is a no clear seasonal behaviour of the rainfall. The cumulative deviation from the mean plot shows that the mean annual rainfalls generally declined until the mide 1960's and have been increasing since then.

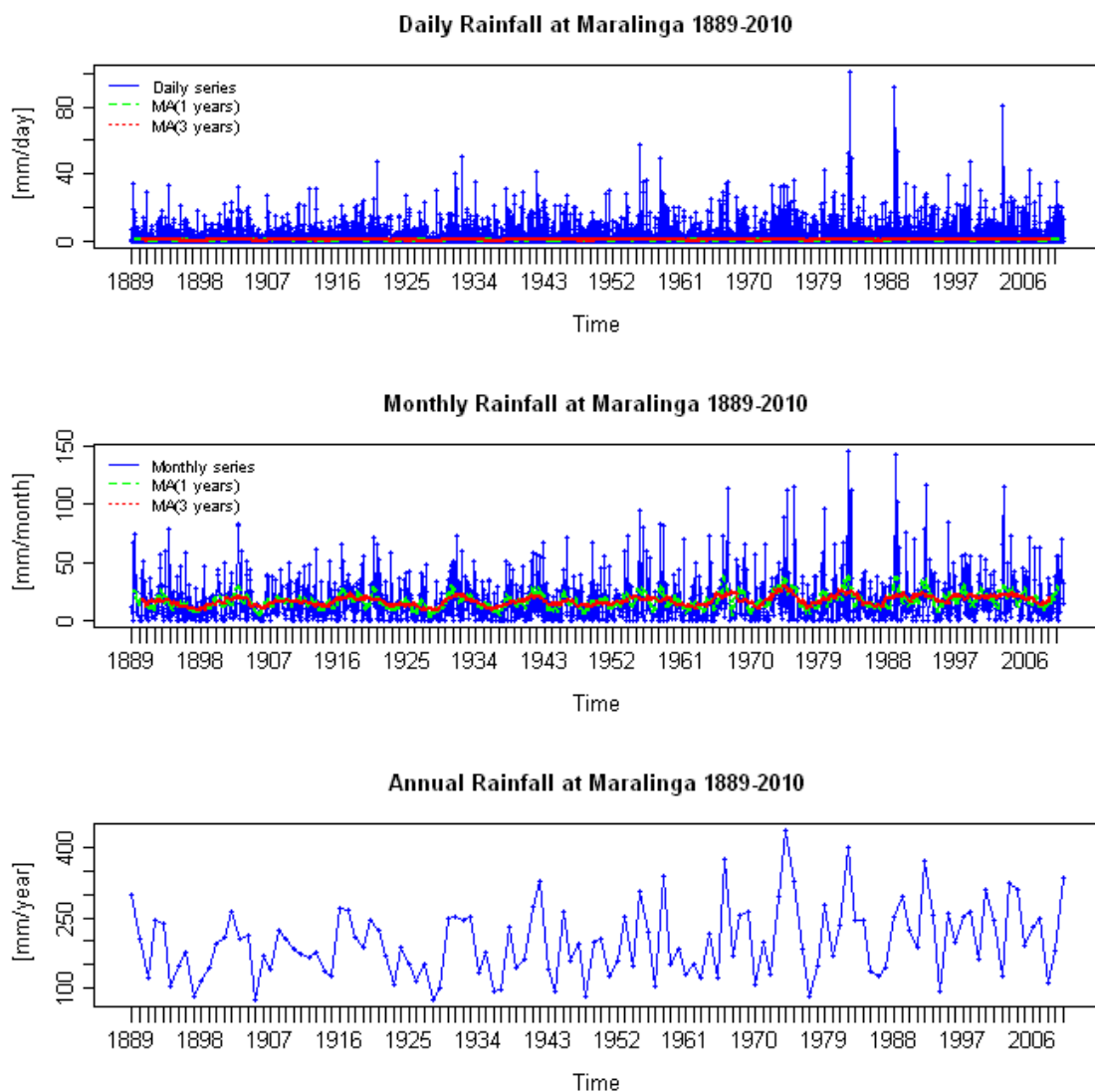


Figure 62. Time series of daily, monthly and annual rainfall at Maralinga. One year and three year moving averages are shown in green and red respectively.

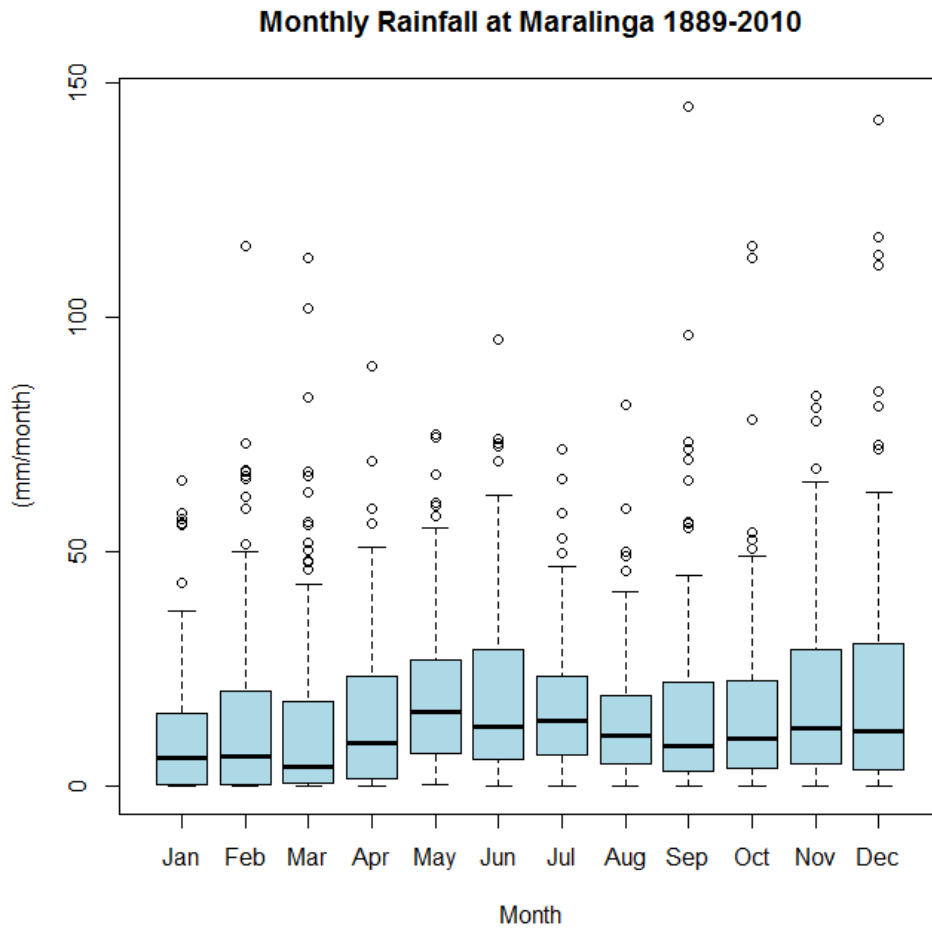


Figure 63. Boxplot of the monthly rainfall at Maralinga. The bottom and top of each box are the first and third quartiles, the band inside each box is the second quartile (the median), the ends of each of the whiskers are 1.5 times the interquartile range of the lower and upper quartiles, and the circles are outliers.

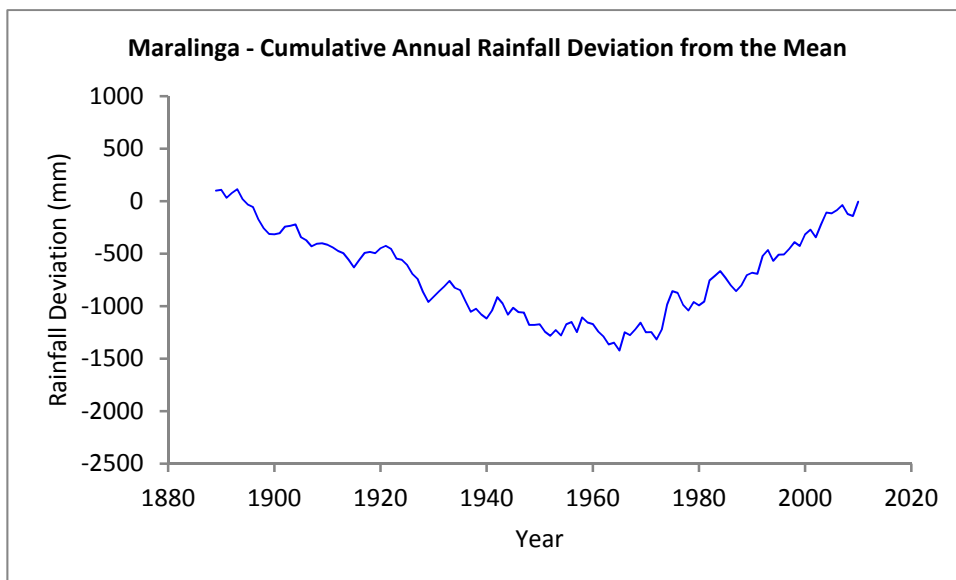


Figure 64. Plot of the cumulative annual deviation from the mean annual rainfall at Maralinga.

Table 18. Summary of the daily, monthly and annual rainfall statistics at Maralinga.

Statistic	Daily	Monthly	Annual
Minimum (mm)	0.0	0.0	75.8
First quartile (mm)	0.0	3.3	141.2
Median (mm)	0.0	10.3	189.6
Mean (mm)	0.5	16.6	198.7
Third quartile (mm)	0.0	23.3	249.8
Maximum (mm)	100.4	145.0	434.0
Interquartile range (mm)	0.0	20.0	108.5
Standard deviation (mm)	2.5	18.8	75.1
Coefficient of variation	4.5	1.1	0.4
Number of points	44599	1464	122

Time series of daily, monthly and annual pan evaporation, with one and three year moving averages are shown in Figure 65. A boxplot of the monthly pan evaporation is shown in Figure 66. A summary of the daily, monthly and annual pan evaporation statistics is given in Table 19.

The pan evaporation at Maralinga is very high, with the mean daily, monthly and annual values of 7.1, 217.5 and 2611.0 mm respectively far exceeding those of the rainfall. The monthly boxplot shows that there is a strong seasonal pattern with lowest values in winter and highest values in summer. Whilst the pan evaporation is highly variable, the coefficients of variation are all much lower than those for rainfall.

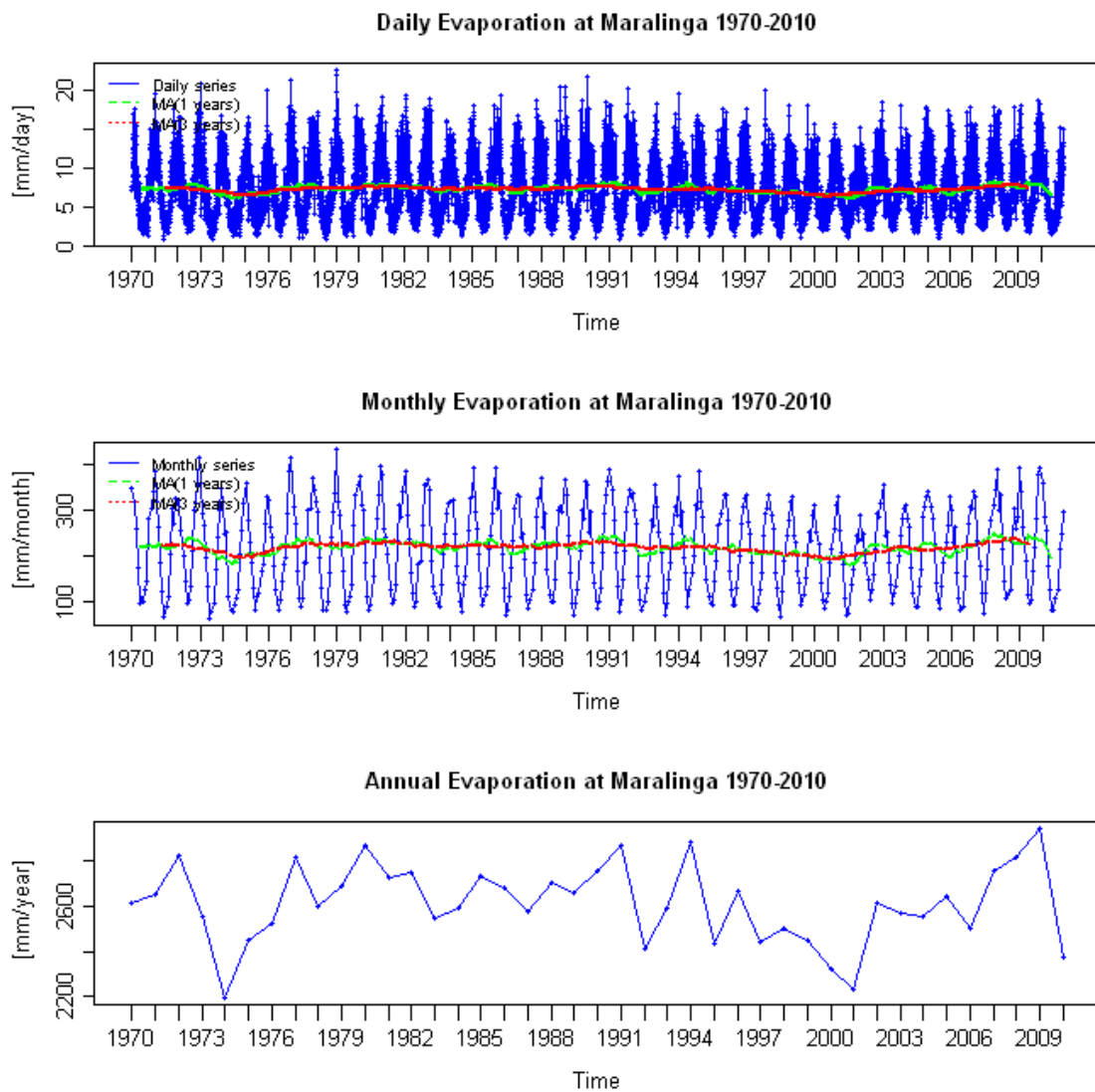


Figure 65. Time series of daily, monthly and annual pan evaporation at Maralinga. One year and three year moving averages are shown in green and red respectively.

Monthly Evaporation at Maralinga 1970-2010

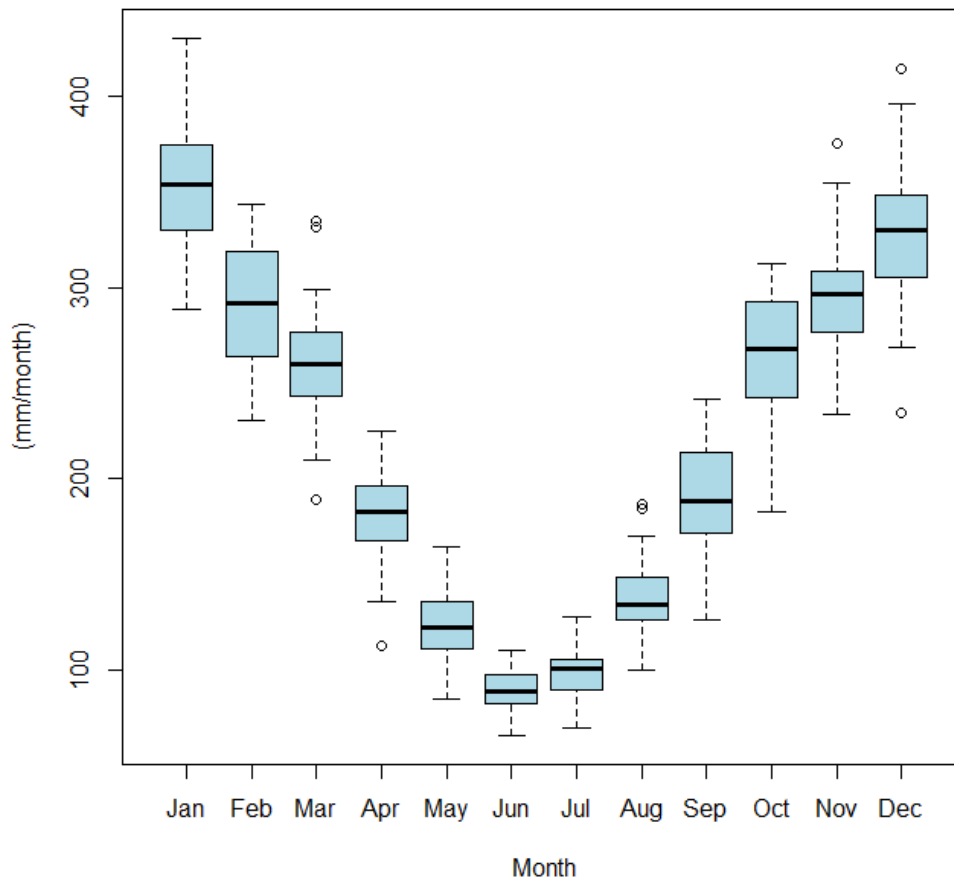


Figure 66. Boxplot of the monthly pan evaporation at Maralinga. The bottom and top of each box are the first and third quartiles, the band inside each box is the second quartile (the median), the ends of each of the whiskers are 1.5 times the interquartile range of the lower and upper quartiles, and the circles are outliers.

Table 19. Summary of the daily, monthly and annual pan evaporation statistics at Maralinga.

Statistic	Daily	Monthly	Annual
Minimum (mm)	0.8	65.2	2196.0
First quartile (mm)	4.0	128.5	2504.0
Median (mm)	6.8	216.3	2612.0
Mean (mm)	7.1	217.5	2611.0
Third quartile (mm)	9.8	298.1	2729.0
Maximum (mm)	22.6	431.0	2938.0
Interquartile range (mm)	5.8	169.6	224.8
Standard deviation (mm)	3.6	92.6	173.6
Coefficient of variation	0.5	0.4	0.1
Number of points	14975	492	41

Marla

Time series of daily, monthly and annual rainfall, with one and three year moving averages are shown in Figure 67. A boxplot of the monthly rainfall is shown in Figure 68. A plot of the cumulative annual deviation from the mean annual rainfall is shown in Figure 69. A summary of the daily, monthly and annual rainfall statistics is given in Table 20.

Marla is located in the north-east part of the study area in a BWh climate zone. It has mean daily, monthly and annual rainfalls of 0.5, 14.3 and 171.7 mm respectively. The highly variable rainfall regime is illustrated by the high standard deviations of the daily, month and annual rainfalls. The variability is most extreme in the daily rainfall, followed by the monthly rainfall and then the annual rainfall, as illustrated by the coefficients of variation of each. The boxplot suggests that there is a slight summer dominance in the rainfall (although June rainfall is similar to the summer months). The cumulative deviation from the mean plot shows that the mean annual rainfalls generally declined until the early 1970's (with some wetter years in the early 1920's and the late 1940's and early 1950's), and have been increasing since then.

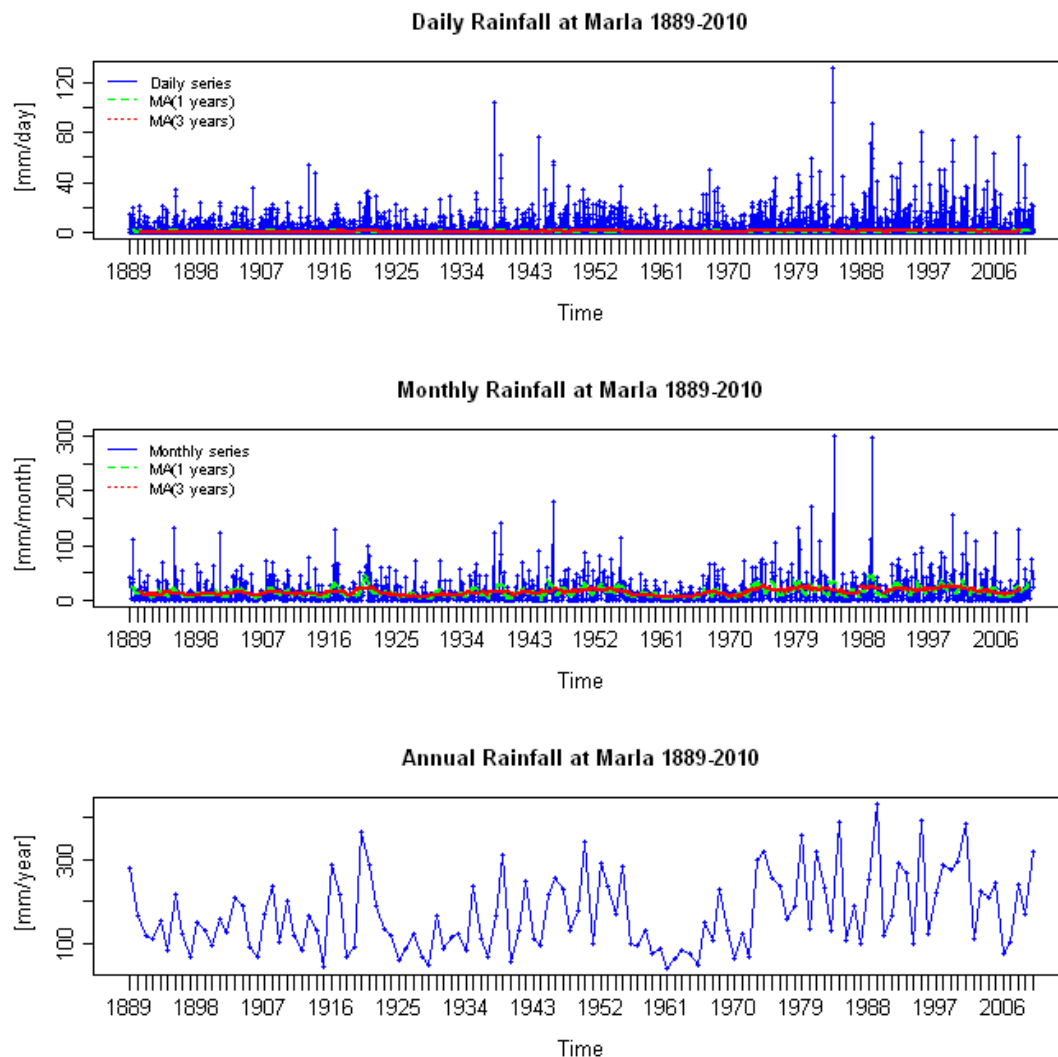


Figure 67. Time series of daily, monthly and annual rainfall at Marla. One year and three year moving averages are shown in green and red respectively.

Monthly Rainfall at Marla 1889-2010

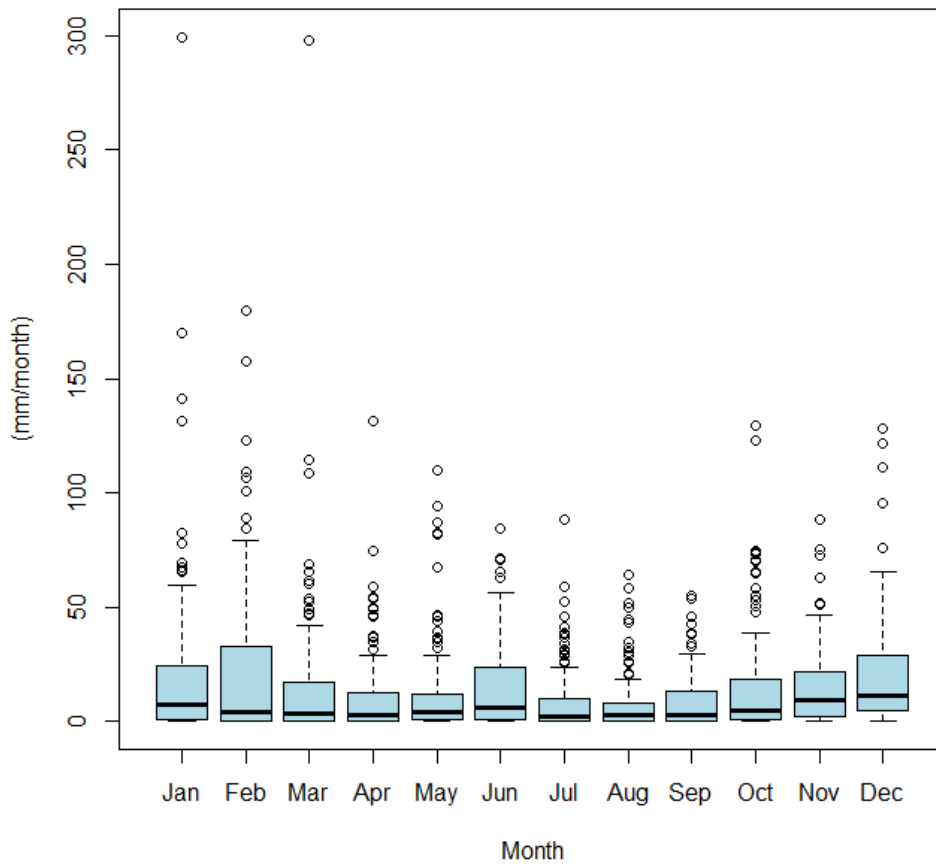


Figure 68. Boxplot of the monthly rainfall at Marla. The bottom and top of each box are the first and third quartiles, the band inside each box is the second quartile (the median), the ends of each of the whiskers are 1.5 times the interquartile range of the lower and upper quartiles, and the circles are outliers.

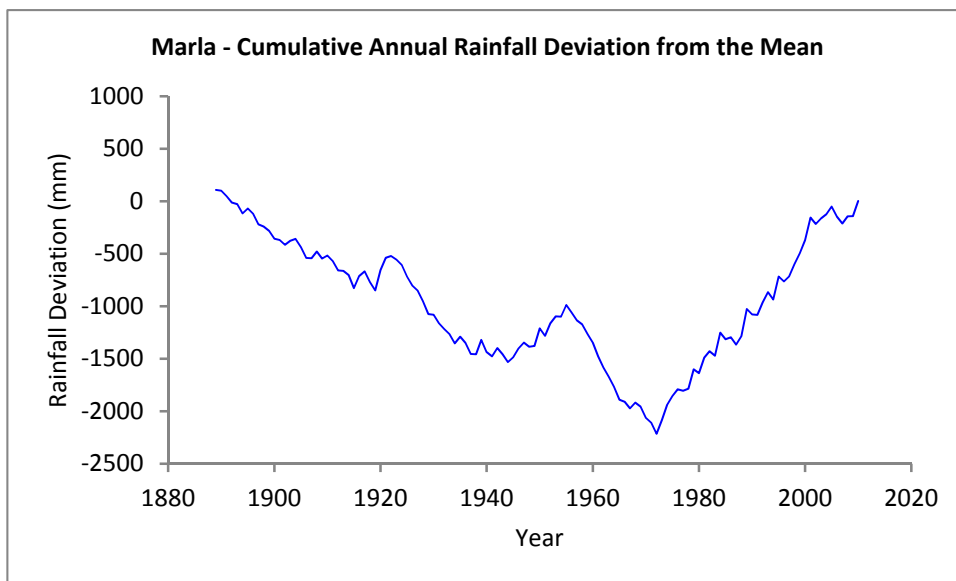


Figure 69. Plot of the cumulative annual deviation from the mean annual rainfall at Marla.

Table 20. Summary of the daily, monthly and annual rainfall statistics at Marla.

Statistic	Daily	Monthly	Annual
Minimum (mm)	0.0	0.0	42.0
First quartile (mm)	0.0	0.5	100.5
Median (mm)	0.0	4.8	144.0
Mean (mm)	0.5	14.3	171.7
Third quartile (mm)	0.0	18.4	235.6
Maximum (mm)	131.4	299.5	430.3
Interquartile range (mm)	0.0	17.9	135.2
Standard deviation (mm)	2.8	24.3	90.7
Coefficient of variation	5.9	1.7	0.5
Number of points	44599	1464	122

Time series of daily, monthly and annual pan evaporation, with one and three year moving averages are shown in Figure 70. A boxplot of the monthly pan evaporation is shown in Figure 71. A summary of the daily, monthly and annual pan evaporation statistics is given in Table 21.

The pan evaporation at Marla is extremely high, with the mean daily, monthly and annual values of 8.3, 252.5 and 3030.0 mm respectively far exceeding those of the rainfall. The monthly boxplot shows that there is a strong seasonal pattern with lowest values in winter and highest values in summer. Whilst the pan evaporation is highly variable, the coefficients of variation are all much lower than those for rainfall.

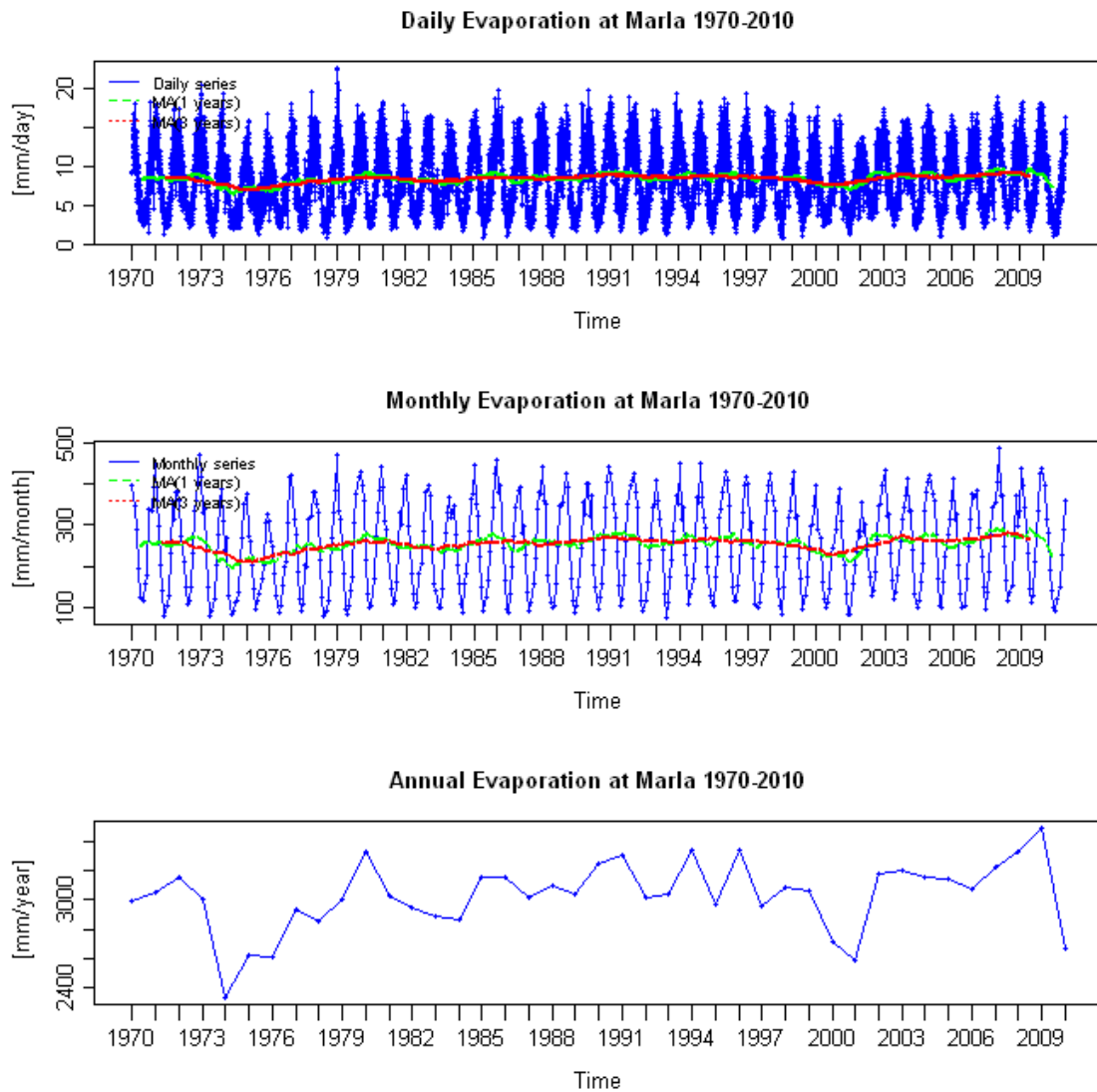


Figure 70. Time series of daily, monthly and annual pan evaporation at Marla. One year and three year moving averages are shown in green and red respectively.

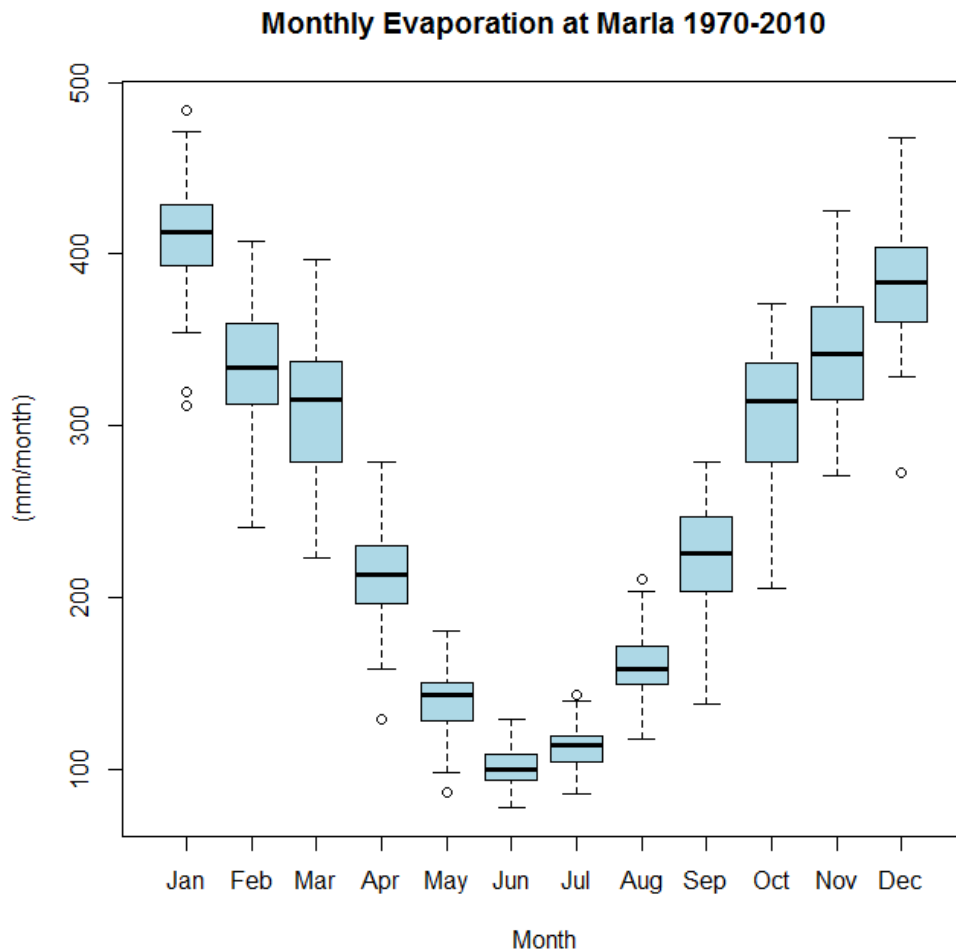


Figure 71. Boxplot of the monthly pan evaporation at Marla. The bottom and top of each box are the first and third quartiles, the band inside each box is the second quartile (the median), the ends of each of the whiskers are 1.5 times the interquartile range of the lower and upper quartiles, and the circles are outliers.

Table 21. Summary of the daily, monthly and annual pan evaporation statistics at Marla.

Statistic	Daily	Monthly	Annual
Minimum (mm)	0.8	77.2	2337.0
First quartile (mm)	4.6	149.4	2942.0
Median (mm)	8.0	250.5	3042.0
Mean (mm)	8.3	252.5	3030.0
Third quartile (mm)	11.6	347.8	3157.0
Maximum (mm)	22.6	484.0	3485.0
Interquartile range (mm)	7.0	198.5	215.0
Standard deviation (mm)	4.0	108.5	236.2
Coefficient of variation	0.5	0.4	0.1
Number of points	14975	492	41

Nullarbor

Time series of daily, monthly and annual rainfall, with one and three year moving averages are shown in Figure 72. A boxplot of the monthly rainfall is shown in Figure 73. A plot of the cumulative annual deviation from the mean annual rainfall is shown in Figure 74. A summary of the daily, monthly and annual rainfall statistics is given in Table 22.

Nullarbor is located in the north-east part of the study area and is the only site in a BSk climate zone. It has mean daily, monthly and annual rainfalls of 0.7, 20.3 and 243.6 mm respectively. The highly variable rainfall regime is illustrated by the high standard deviations of the daily, month and annual rainfalls. The variability is most extreme in the daily rainfall, followed by the monthly rainfall and then the annual rainfall, as illustrated by the coefficients of variation of each. The boxplot suggests that there is a clear winter dominance in the rainfall. The cumulative deviation from the mean plot shows that the mean annual rainfalls generally declined until the early 1970's and have been increasing since then.

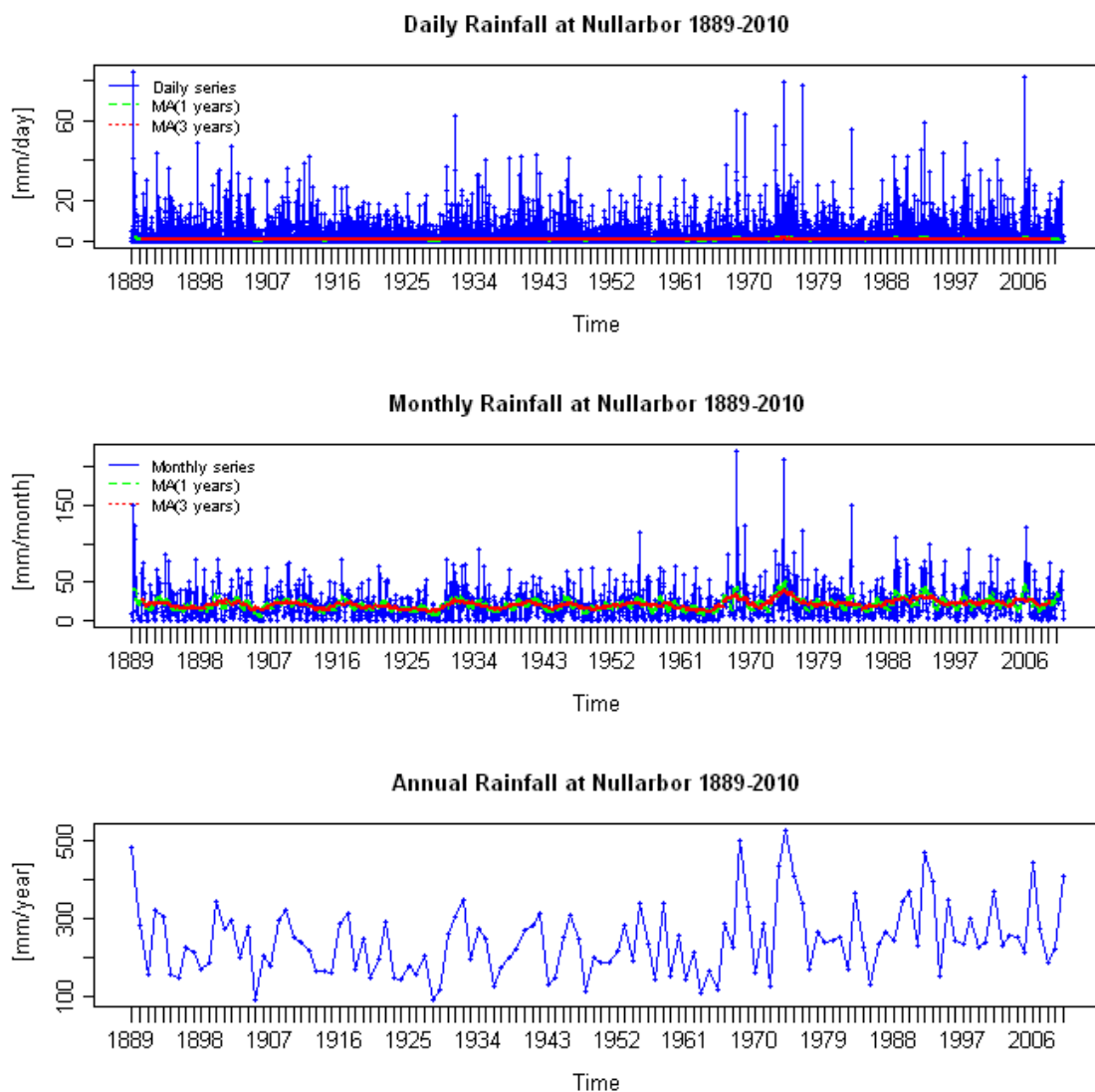


Figure 72. Time series of daily, monthly and annual rainfall at Nullarbor. One year and three year moving averages are shown in green and red respectively.

Monthly Rainfall at Nullarbor 1889-2010

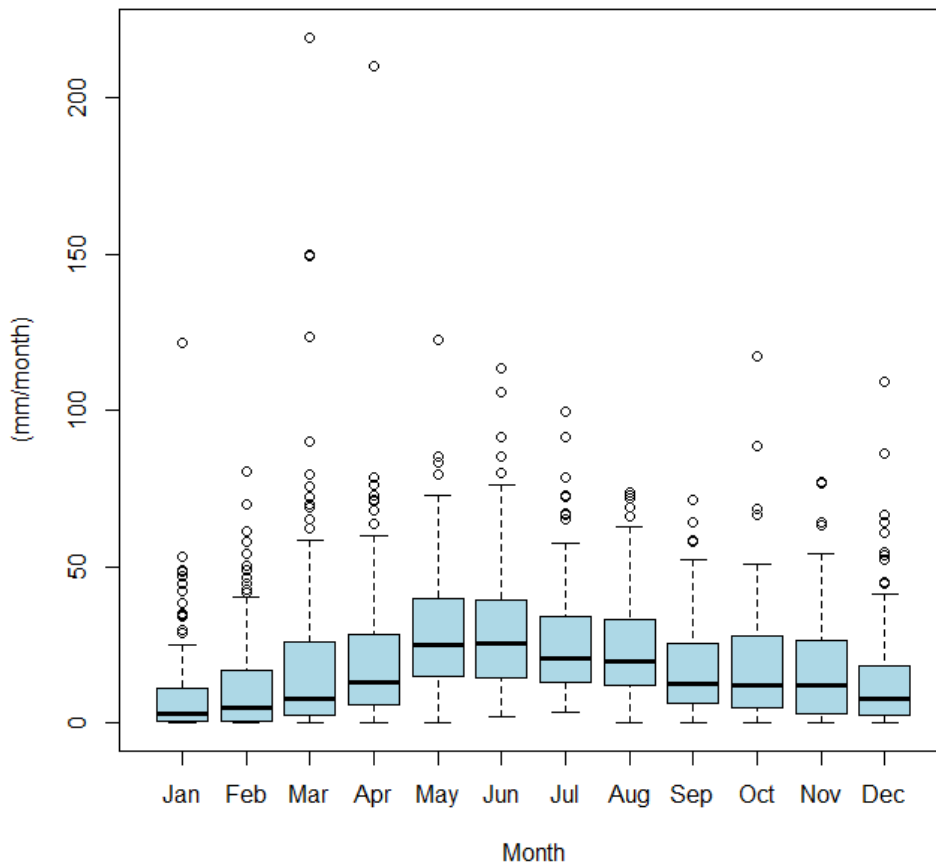


Figure 73. Boxplot of the monthly rainfall at Nullarbor. The bottom and top of each box are the first and third quartiles, the band inside each box is the second quartile (the median), the ends of each of the whiskers are 1.5 times the interquartile range of the lower and upper quartiles, and the circles are outliers.

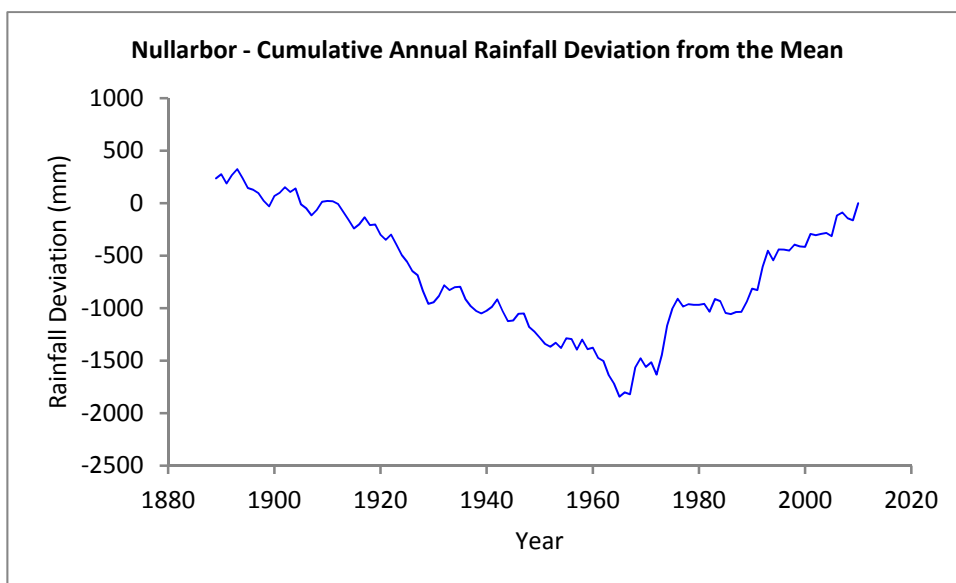


Figure 74. Plot of the cumulative annual deviation from the mean annual rainfall at Nullarbor.

Table 22. Summary of the daily, monthly and annual rainfall statistics at Nullarbor.

Statistic	Daily	Monthly	Annual
Minimum (mm)	0.0	0.0	92.4
First quartile (mm)	0.0	5.0	172.5
Median (mm)	0.0	14.0	234.8
Mean (mm)	0.7	20.3	243.6
Third quartile (mm)	0.1	28.4	291.2
Maximum (mm)	83.8	219.5	522.0
Interquartile range (mm)	0.1	23.4	118.7
Standard deviation (mm)	2.7	21.4	88.7
Coefficient of variation	4.1	1.1	0.4
Number of points	44599	1464	122

Time series of daily, monthly and annual pan evaporation, with one and three year moving averages are shown in Figure 75. A boxplot of the monthly pan evaporation is shown in Figure 76. A summary of the daily, monthly and annual pan evaporation statistics is given in Table 23.

The pan evaporation at Nullarbor is high, with the mean daily, monthly and annual values of 6.6, 201.4 and 2417.0 mm respectively far exceeding those of the rainfall. The monthly boxplot shows that there is a strong seasonal pattern with lowest values in winter and highest values in summer. Whilst the pan evaporation is highly variable, the coefficients of variation are all much lower than those for rainfall.

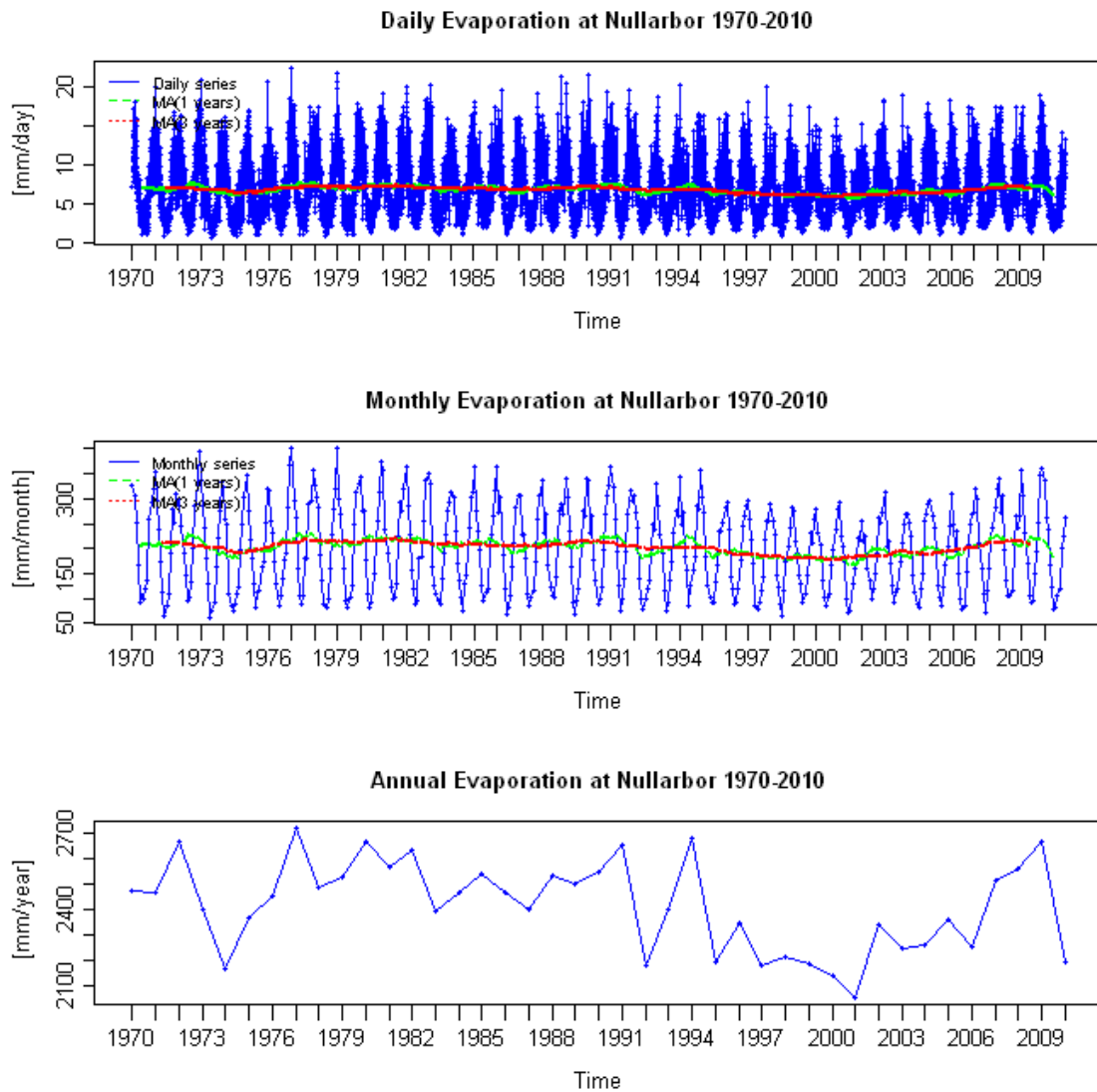


Figure 75. Time series of daily, monthly and annual pan evaporation at Nullarbor. One year and three year moving averages are shown in green and red respectively.

Monthly Evaporation at Nullarbor 1970-2010

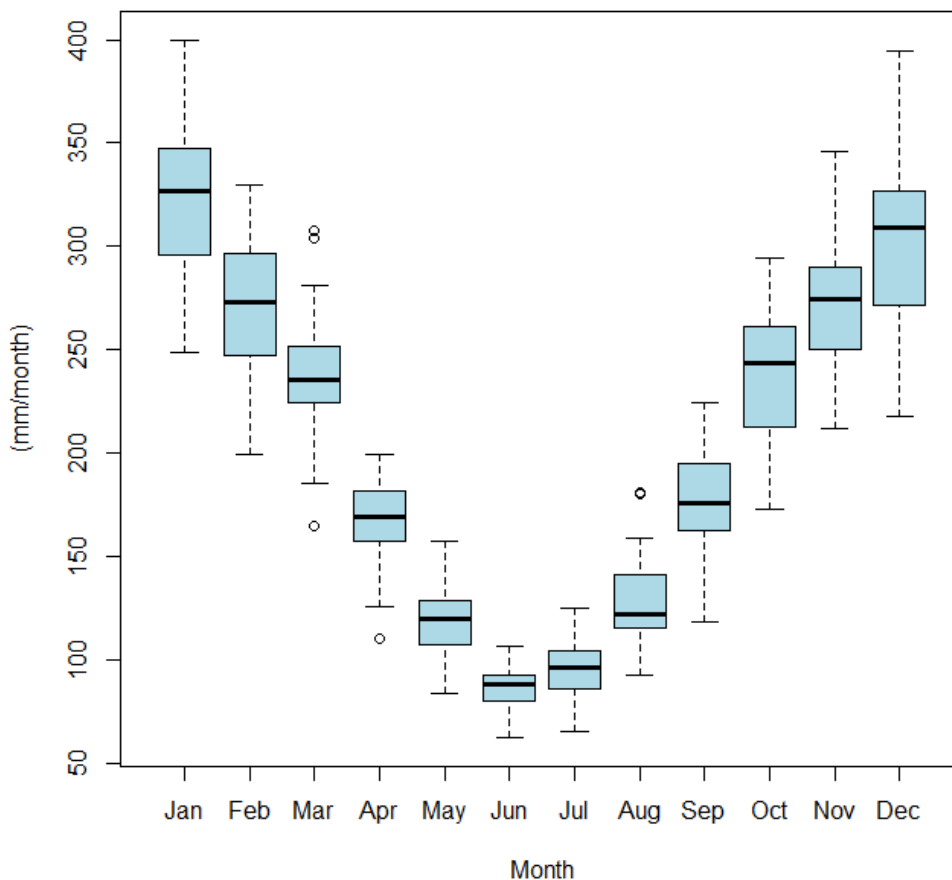


Figure 76. Boxplot of the monthly pan evaporation at Nullarbor. The bottom and top of each box are the first and third quartiles, the band inside each box is the second quartile (the median), the ends of each of the whiskers are 1.5 times the interquartile range of the lower and upper quartiles, and the circles are outliers.

Table 23. Summary of the daily, monthly and annual pan evaporation statistics at Nullarbor.

Statistic	Daily	Monthly	Annual
Minimum (mm)	0.6	62.0	2054.0
First quartile (mm)	3.6	120.8	2253.0
Median (mm)	6.2	199.1	2452.0
Mean (mm)	6.6	201.4	2417.0
Third quartile (mm)	9.0	272.0	2542.0
Maximum (mm)	22.2	400.0	2720.0
Interquartile range (mm)	5.4	151.3	289.0
Standard deviation (mm)	3.4	84.4	177.6
Coefficient of variation	0.5	0.4	0.1
Number of points	14975	492	41

Tarcoola

Time series of daily, monthly and annual rainfall, with one and three year moving averages are shown in Figure 77. A boxplot of the monthly rainfall is shown in Figure 78. A plot of the cumulative annual deviation from the mean annual rainfall is shown in Figure 79. A summary of the daily, monthly and annual rainfall statistics is given in Table 24.

Tarcoola is located in the south-eastern part of the study area in a BWh climate zone. It has mean daily, monthly and annual rainfalls of 0.5, 14.3 and 172.0 mm respectively. The highly variable rainfall regime is illustrated by the high standard deviations of the daily, month and annual rainfalls. The variability is most extreme in the daily rainfall, followed by the monthly rainfall and then the annual rainfall, as illustrated by the coefficients of variation of each. The boxplot suggests that there is a no clear seasonal behaviour of the rainfall. The cumulative deviation from the mean plot shows that the mean annual rainfalls have had no clear long-term trends.

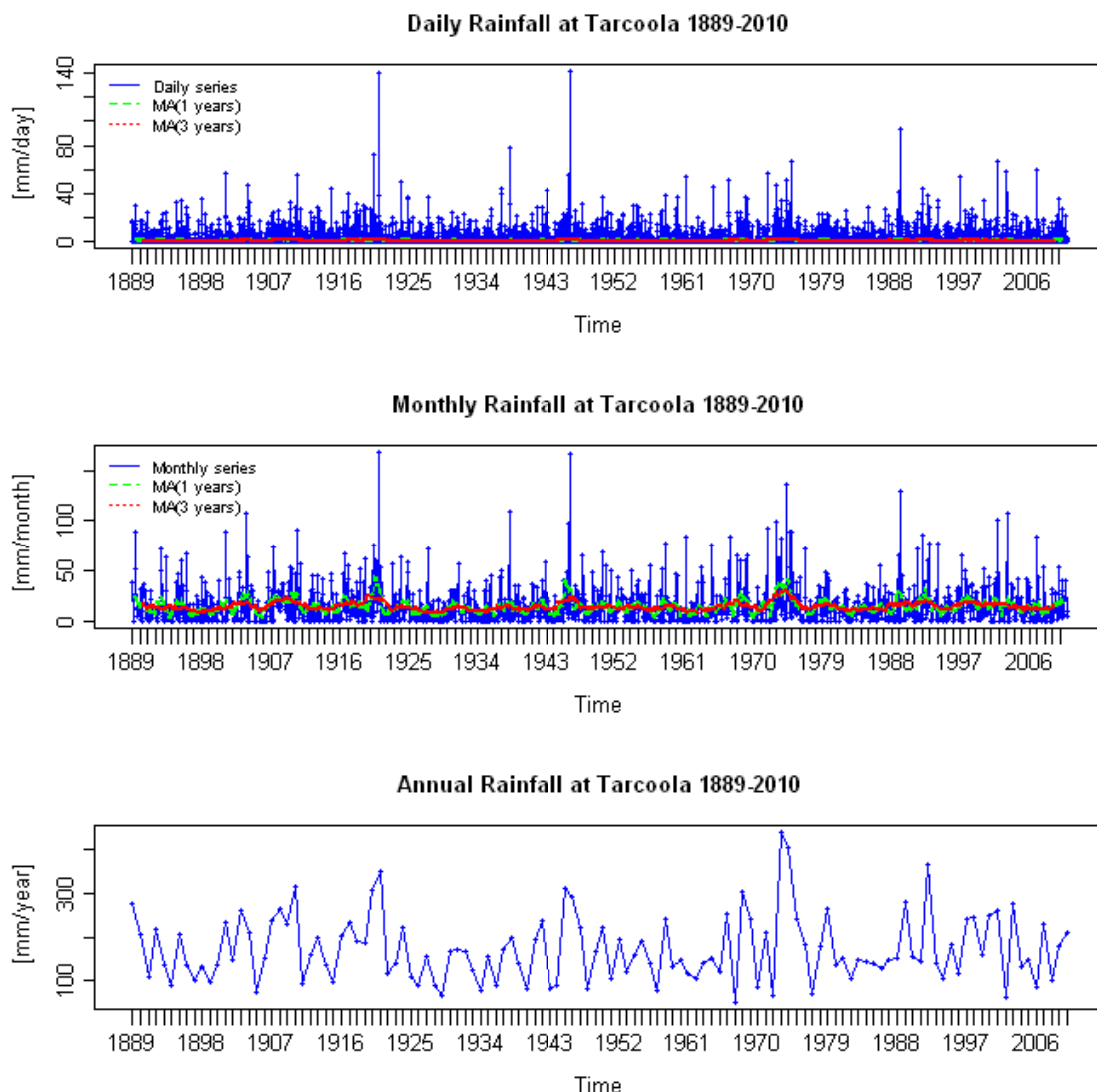


Figure 77. Time series of daily, monthly and annual rainfall at Tarcoola. One year and three year moving averages are shown in green and red respectively.

Monthly Rainfall at Tarcoola 1889-2010

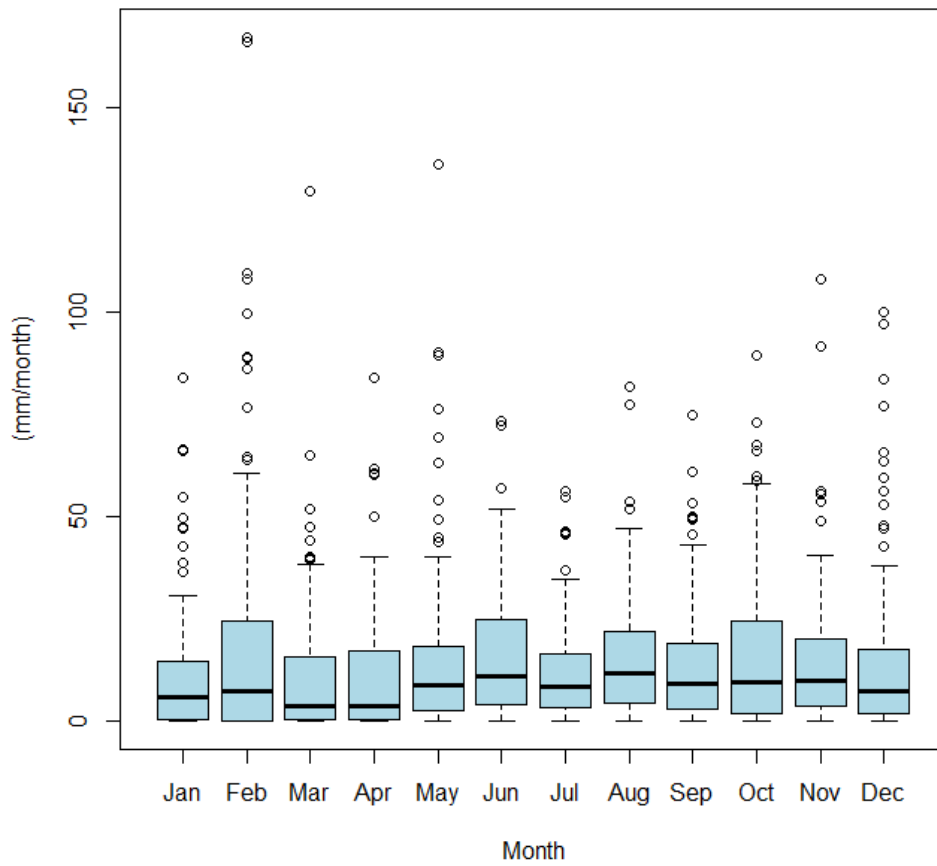


Figure 78. Boxplot of the monthly rainfall at Tarcoola. The bottom and top of each box are the first and third quartiles, the band inside each box is the second quartile (the median), the ends of each of the whiskers are 1.5 times the interquartile range of the lower and upper quartiles, and the circles are outliers.

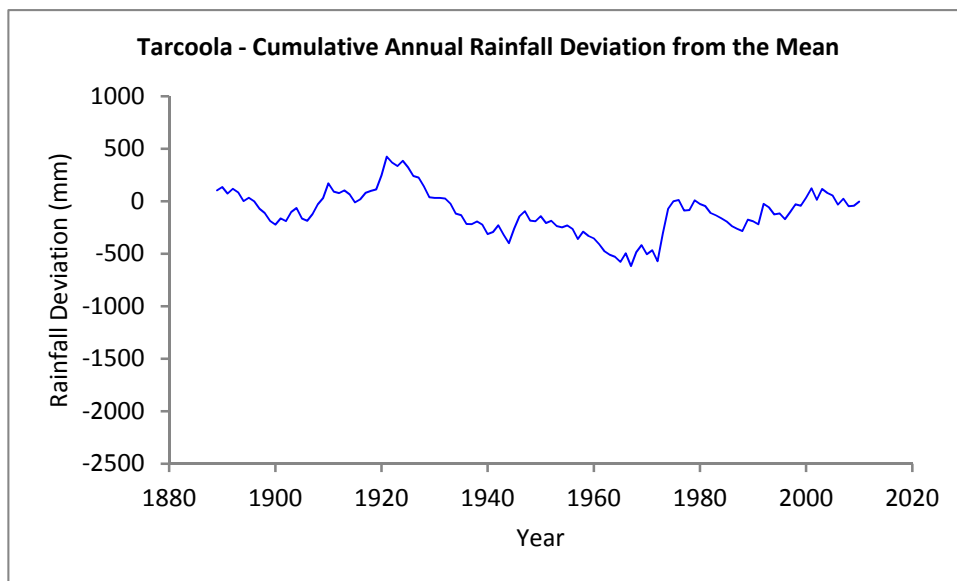


Figure 79. Plot of the cumulative annual deviation from the mean annual rainfall at Tarcoola.

Table 24. Summary of the daily, monthly and annual rainfall statistics at Tarcoola.

Statistic	Daily	Monthly	Annual
Minimum (mm)	0.0	0.0	50.8
First quartile (mm)	0.0	1.8	117.2
Median (mm)	0.0	8.4	154.2
Mean (mm)	0.5	14.3	172.0
Third quartile (mm)	0.0	19.3	221.0
Maximum (mm)	141.2	167.4	437.9
Interquartile range (mm)	0.0	17.5	103.7
Standard deviation (mm)	2.7	18.5	75.4
Coefficient of variation	5.7	1.3	0.4
Number of points	44599	1464	122

Time series of daily, monthly and annual pan evaporation, with one and three year moving averages are shown in Figure 80. A boxplot of the monthly pan evaporation is shown in Figure 81. A summary of the daily, monthly and annual pan evaporation statistics is given in Table 25.

The pan evaporation at Tarcoola is very high, with the mean daily, monthly and annual values of 7.4, 226.3 and 2715.0 mm respectively far exceeding those of the rainfall. The monthly boxplot shows that there is a strong seasonal pattern with lowest values in winter and highest values in summer. Whilst the pan evaporation is highly variable, the coefficients of variation are all much lower than those for rainfall.

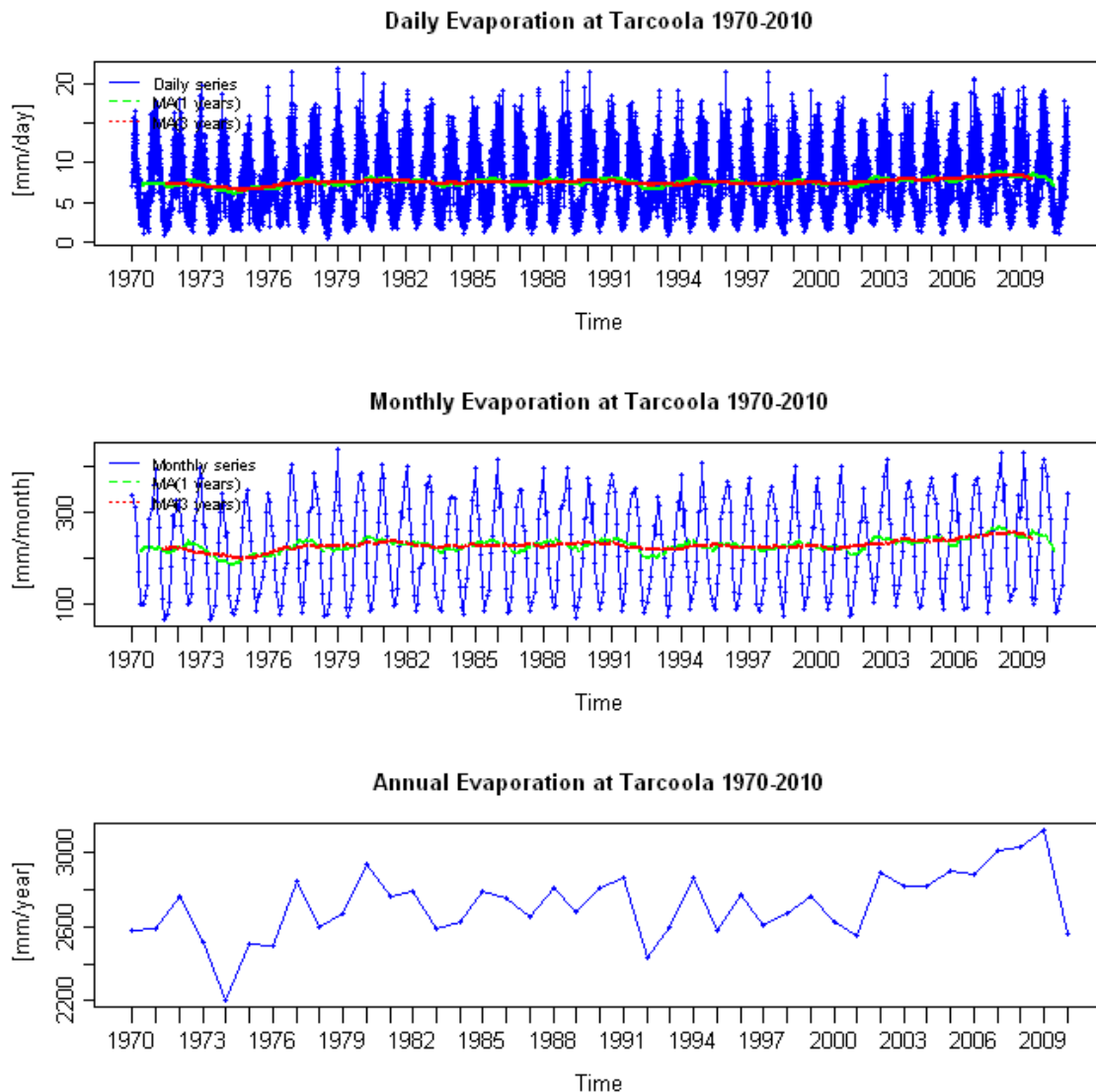


Figure 80. Time series of daily, monthly and annual pan evaporation at Tarcoola. One year and three year moving averages are shown in green and red respectively.

Monthly Evaporation at Tarcoola 1970-2010

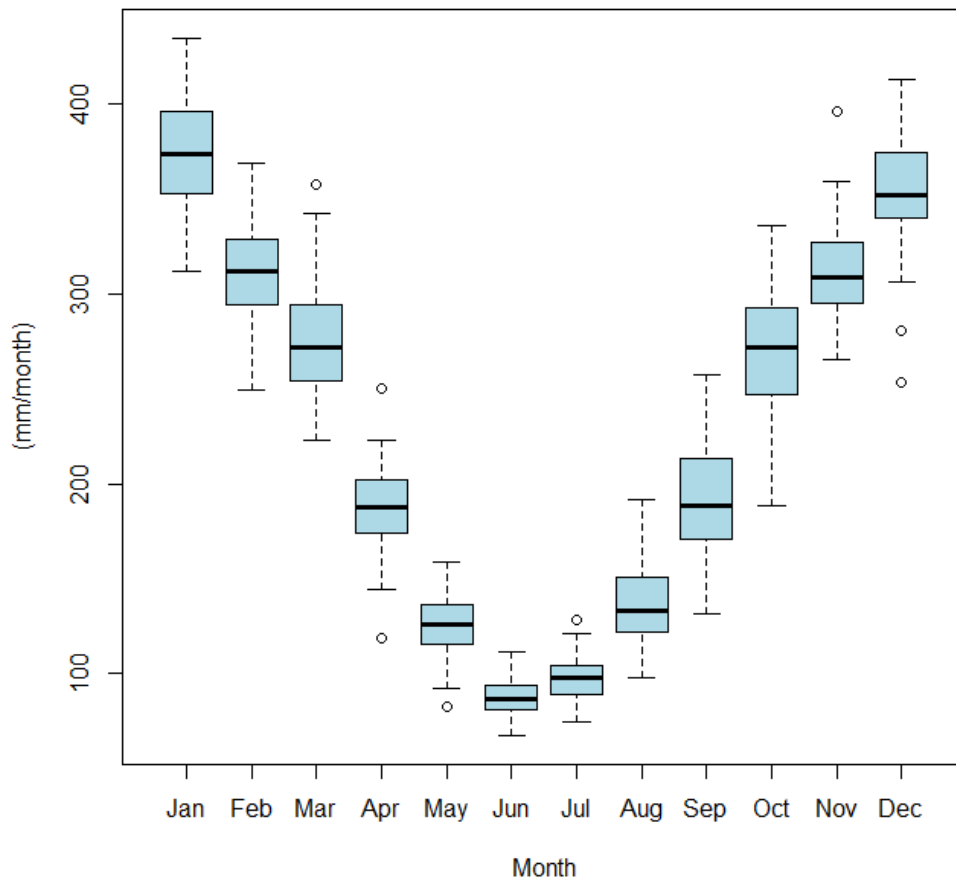


Figure 81. Boxplot of the monthly pan evaporation at Tarcoola. The bottom and top of each box are the first and third quartiles, the band inside each box is the second quartile (the median), the ends of each of the whiskers are 1.5 times the interquartile range of the lower and upper quartiles, and the circles are outliers.

Table 25. Summary of the daily, monthly and annual pan evaporation statistics at Tarcoola.

Statistic	Daily	Monthly	Annual
Minimum (mm)	0.4	67.2	2205.0
First quartile (mm)	4.0	129.6	2591.0
Median (mm)	7.0	230.4	2754.0
Mean (mm)	7.4	226.3	2715.0
Third quartile (mm)	10.4	311.7	2821.0
Maximum (mm)	21.8	435.2	3117.0
Interquartile range (mm)	6.4	182.1	229.8
Standard deviation (mm)	3.9	100.5	177.9
Coefficient of variation	0.5	0.4	0.1
Number of points	14975	492	41

Appendix B - Estimation of recharge using the Method of Last Resort

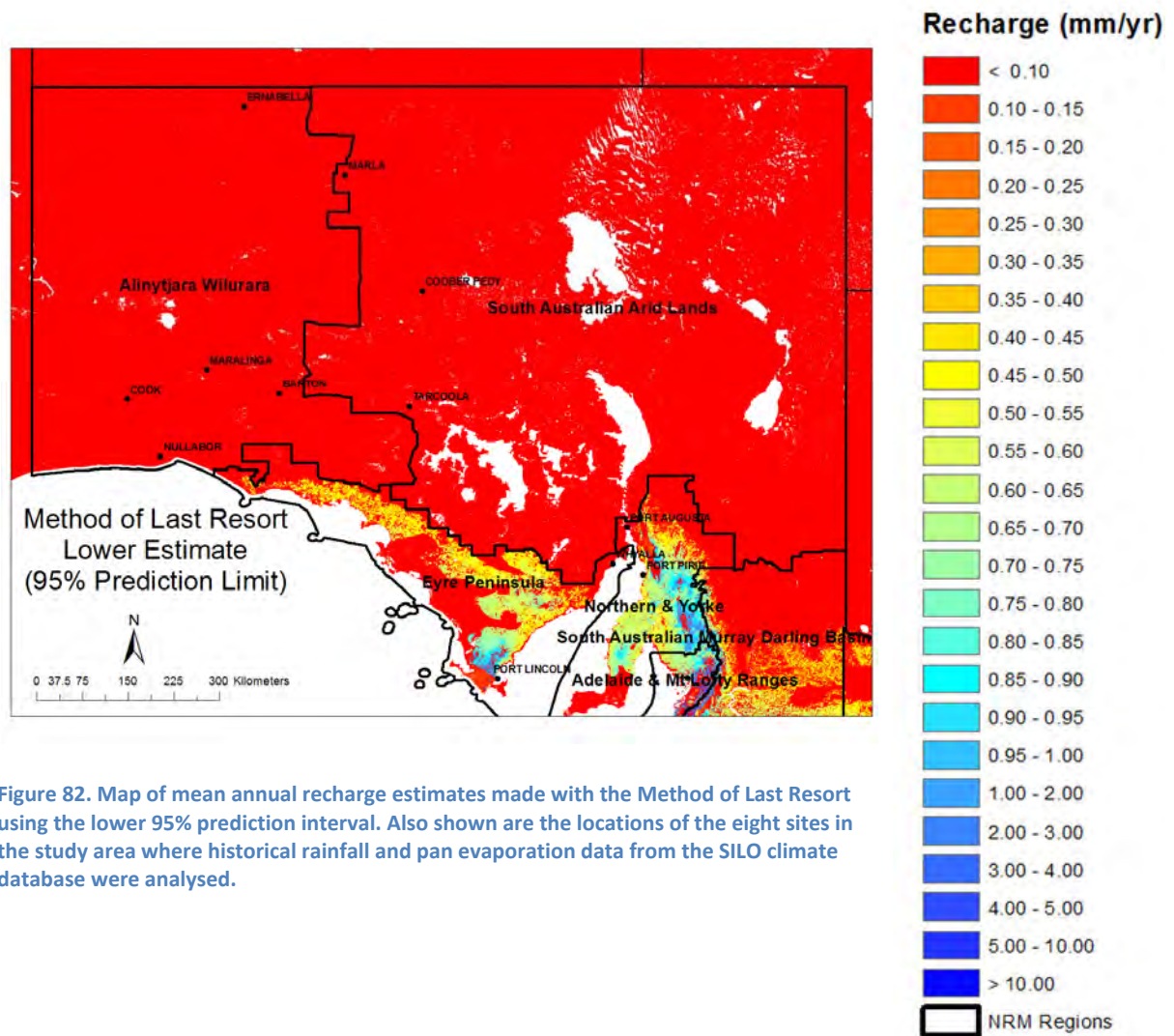


Figure 82. Map of mean annual recharge estimates made with the Method of Last Resort using the lower 95% prediction interval. Also shown are the locations of the eight sites in the study area where historical rainfall and pan evaporation data from the SILO climate database were analysed.

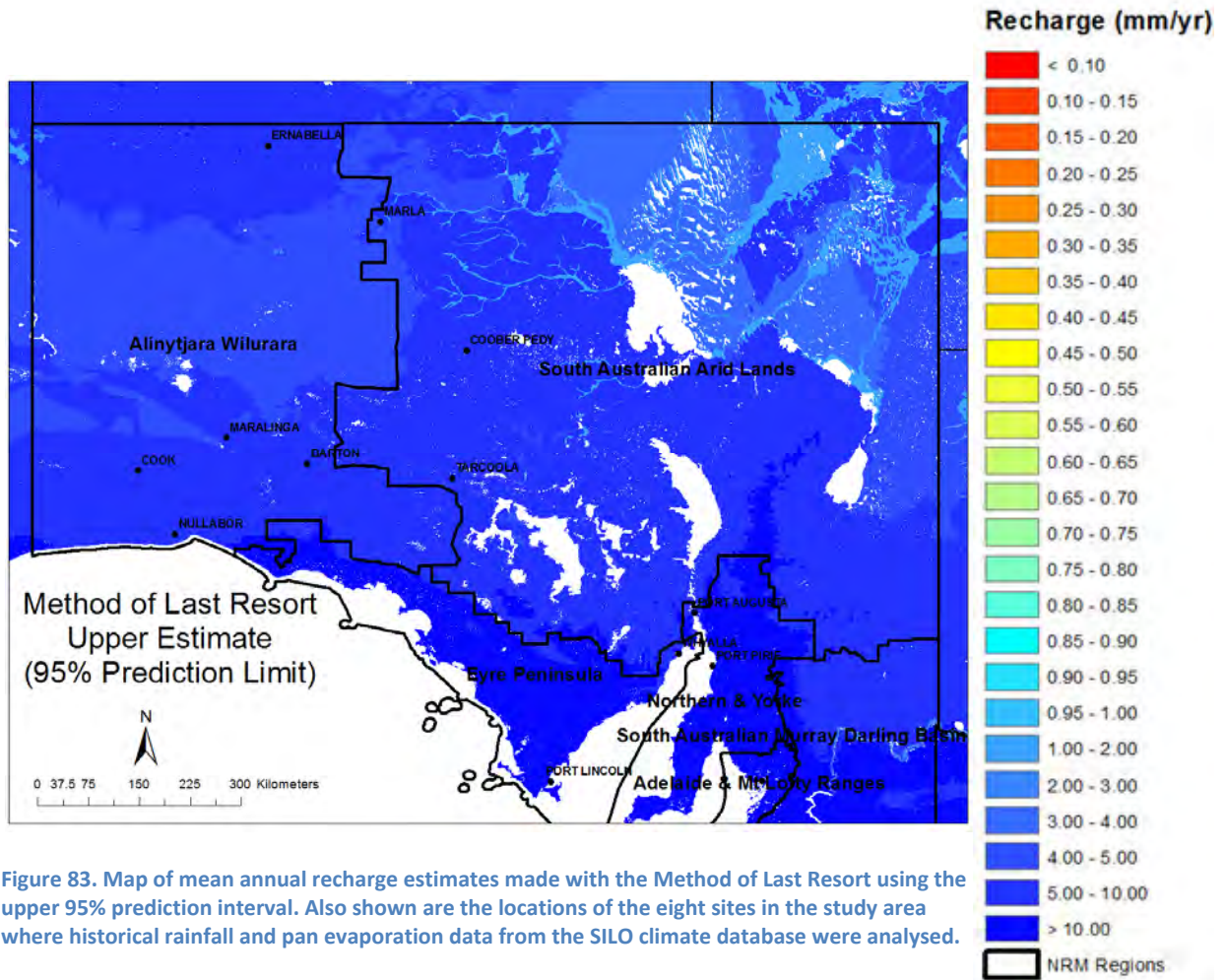


Figure 83. Map of mean annual recharge estimates made with the Method of Last Resort using the upper 95% prediction interval. Also shown are the locations of the eight sites in the study area where historical rainfall and pan evaporation data from the SILO climate database were analysed.

Appendix C - Estimation of recharge using the Groundwater Chloride Mass Balance method

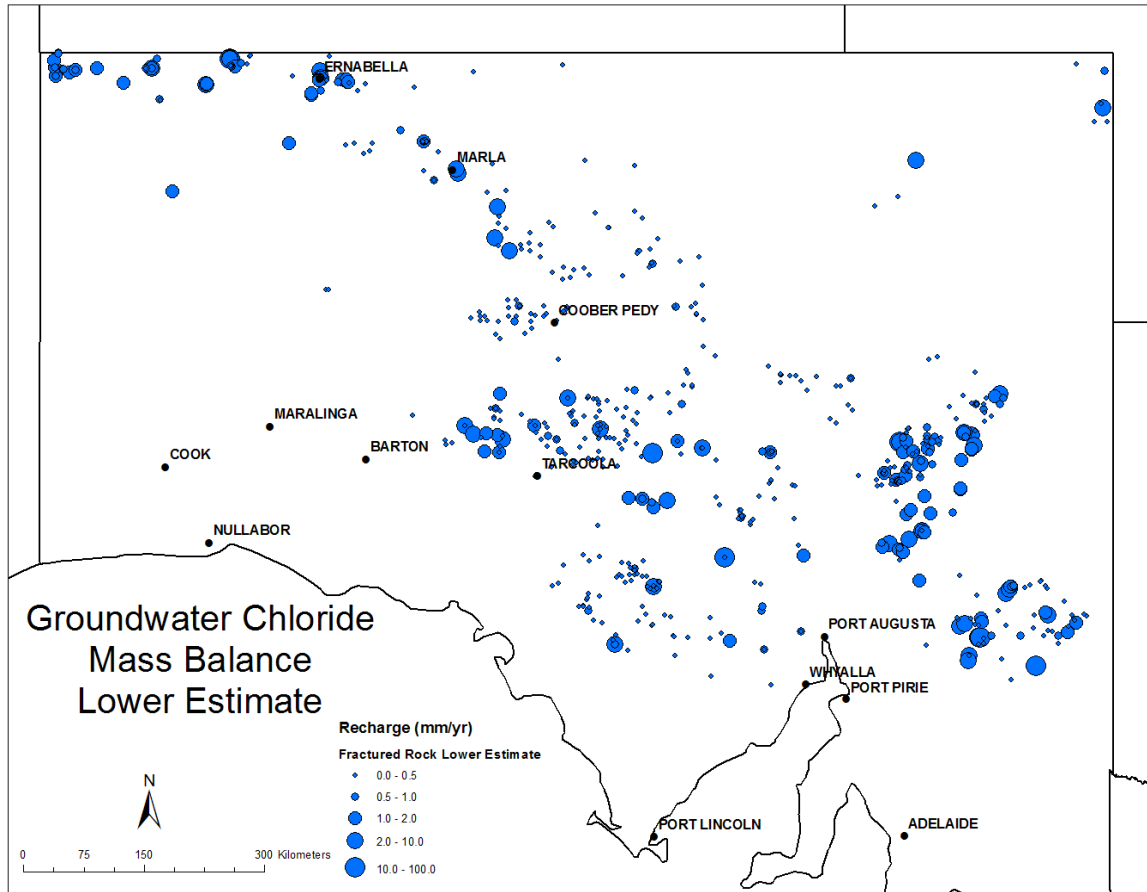


Figure 84. Map of mean annual recharge estimates for fractured rock wells made with the Groundwater Chloride Mass Balance method using the lower 95% prediction interval for the rainfall chloride deposition rate. Also shown are the locations of the eight sites in the study area where historical rainfall and pan evaporation data from the SILO climate database were analysed.

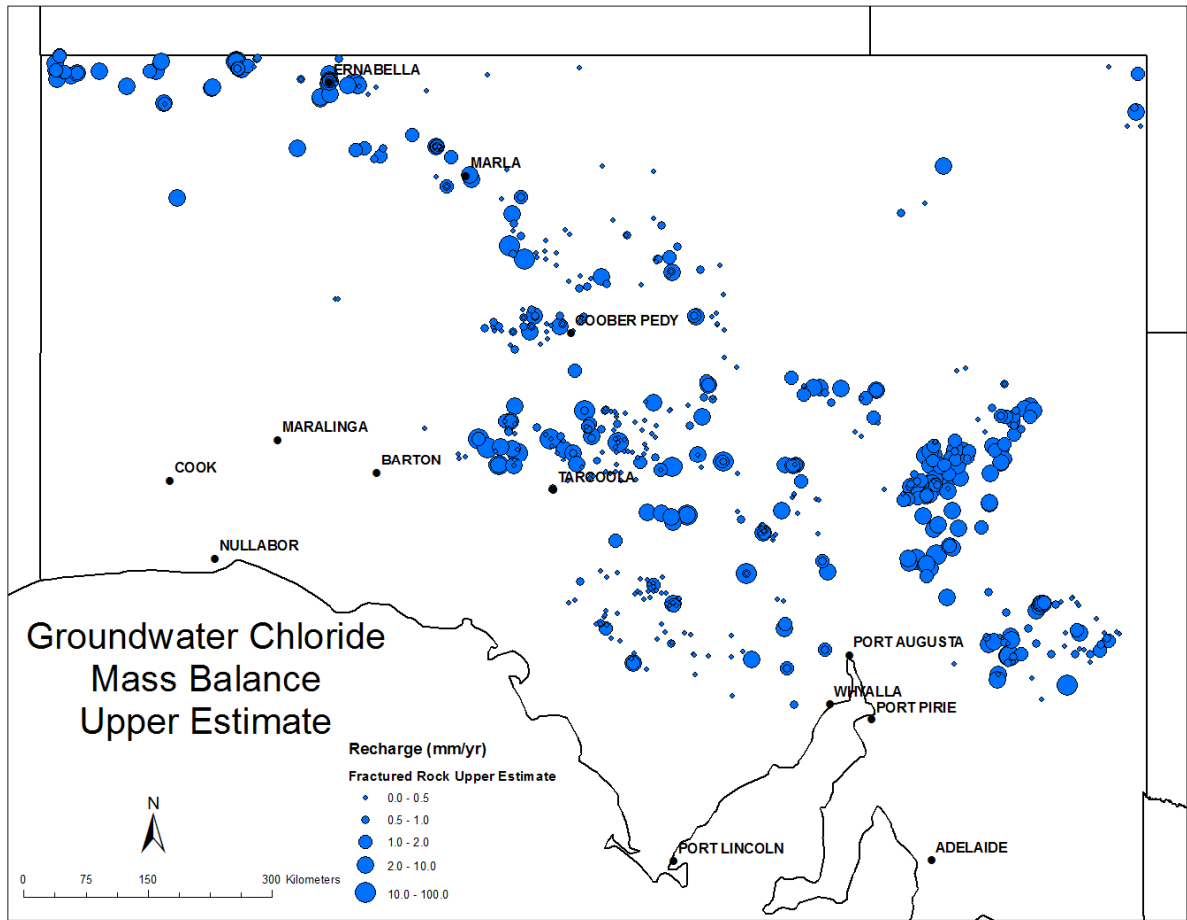


Figure 85. Map of mean annual recharge estimates for fractured rock wells made with the Groundwater Chloride Mass Balance method using the upper 95% prediction interval for the rainfall chloride deposition rate. Also shown are the locations of the eight sites in the study area where historical rainfall and pan evaporation data from the SILO climate database were analysed.

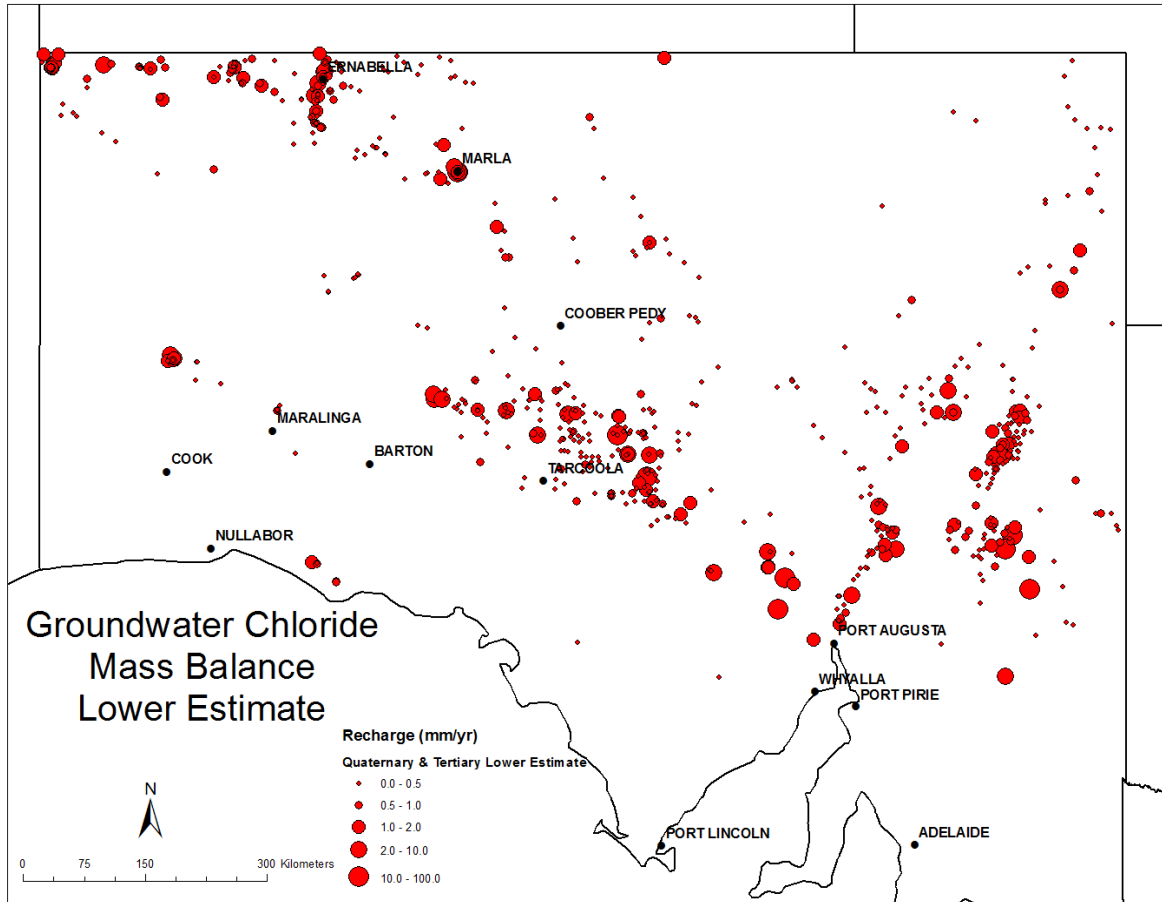


Figure 86. Map of mean annual recharge estimates for Quaternary and Tertiary wells made with the Groundwater Chloride Mass Balance method using the lower 95% prediction interval for the rainfall chloride deposition rate. Also shown are the locations of the eight sites in the study area where historical rainfall and pan evaporation data from the SILO climate database were analysed.

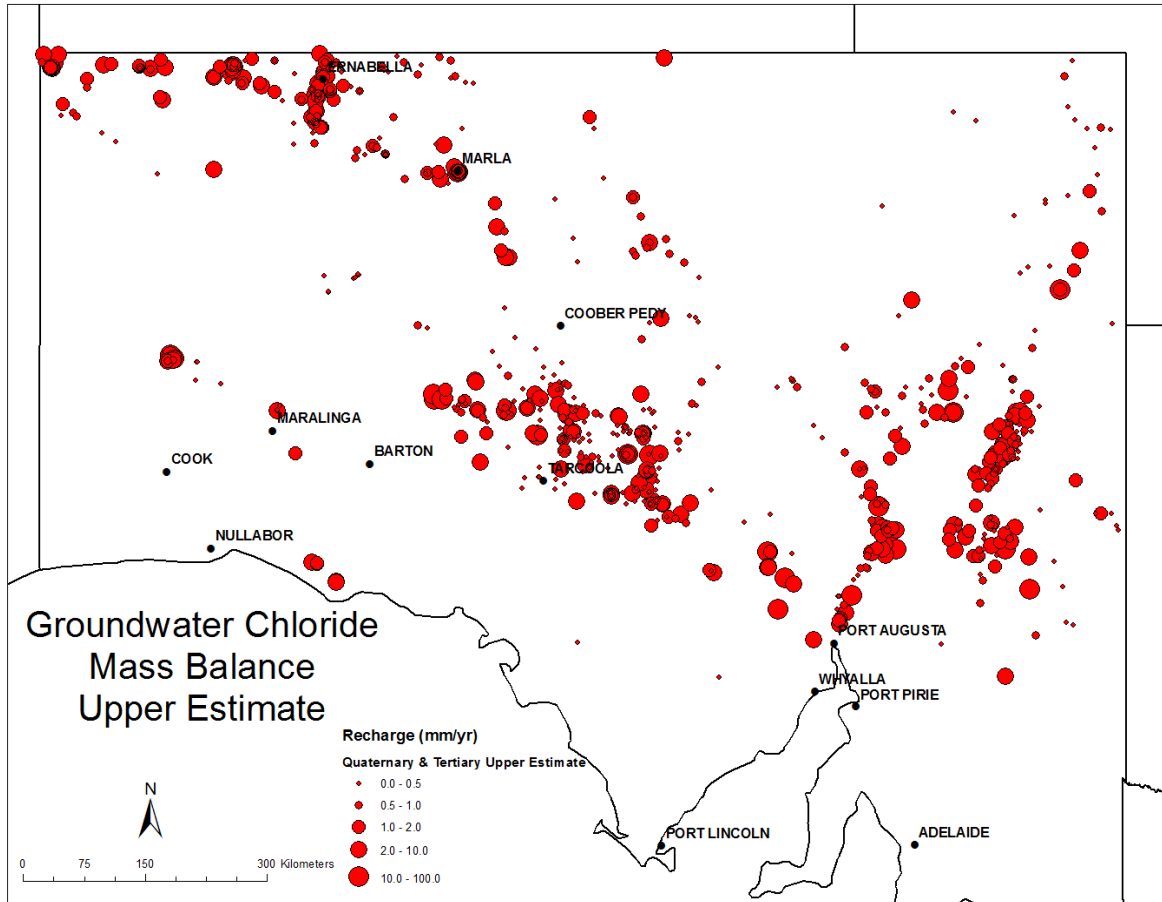


Figure 87. Map of mean annual recharge estimates for Quaternary and Tertiary wells made with the Groundwater Chloride Mass Balance method using the upper 95% prediction interval for the rainfall chloride deposition rate. Also shown are the locations of the eight sites in the study area where historical rainfall and pan evaporation data from the SILO climate database were analysed.



Government
of South Australia

Department of Environment,
Water and Natural Resources



THE UNIVERSITY
of ADELAIDE



University of
South Australia



Flinders
UNIVERSITY
ADELAIDE • AUSTRALIA

The Goyder Institute for Water Research is a partnership between the South Australian Government through the Department for Environment, Water and Natural Resources, CSIRO, Flinders University, the University of Adelaide and the University of South Australia.